LA-5398-MS

INFORMAL REPORT

c.3

Performance of (U, Zr)C-Graphite (Composite) and of (U,Zr)C (Carbide) Fuel Elements in the Nuclear Furnace 1 Test Reactor

los alamos
scientific laboratory
of the University of California
LOS ALAMOS, NEW MEXICO 87544

UNITED STATES
ATOMIC ENERGY COMMISSION
CONTRACT W-7405-ENG. 36

In the interest of prompt distribution, this LAMS report was not edited by the Technical Information staff.

Printed in the United States of America. Available from
National Technical Information Service
U. S. Department of Commerce
5285 Port Royal Road
Springfield, Virginia 22151
Price: Printed Copy $5.45; Microfiche $0.95

LA-5398-MS
Informal Report
UC-33
ISSUED: September 1973

los alamos
scientific laboratory
of the University of California
LOS ALAMOS, NEW MEXICO 87544

Performance of (U,Zr)C-Graphite (Composite) and of (U,Zr)C (Carbide) Fuel Elements in the Nuclear Furnace 1 Test Reactor

by

Luther L. Lyon

This work was done for the Space Nuclear Systems Office, a joint office of the U.S. Atomic Energy Commission and the National Aeronautics and Space Administration.

CONTENTS

PERFORMANCE OF (U,Zr)C-GRAPHITE (COMPOSITE) AND OF (U,Zr)C (CARBIDE) FUEL ELEMENTS IN THE NUCLEAR FURNACE 1 TEST REACTOR

by

Luther L. Lyon

ABSTRACT

The properties of and reactor test results for two types of nuclear-propulsion-reactor fuel elements containing uranium-zirconium carbide, (U,Zr)C, are reported. Composite fuel elements containing graphite and ∿ 35 vol% carbide, along with fuel elements consisting only of carbide, were tested in Los Alamos Scientific Laboratory's Nuclear Furnace 1 reactor for 109 min at peak power densities of ∿ 4500 MW/m^3 and temperatures up to 2500 K. Fission-fragment damage to the graphite phase of the composite fuel elements increased the room-temperature thermal resistivity of the matrix ninefold, resulting in unexpected high mass losses of carbon. The carbide elements developed both longitudinal and transverse fractures but did not fragment into small-size particles.

I. INTRODUCTION

The usefulness of new types of experimental nuclear-rocket-reactor fuel elements for the Rover* program was evaluated in a specially devised small test reactor, Nuclear Furnace 1. Six separate tests of the reactor were conducted during the summer of 1972 at the Nuclear Rocket Development Station at Jackass Flats, Nevada.[1] This report presents reactor performance data on two types of experimental fuel elements containing uranium-zirconium carbide, (U,Zr)C, which were tested for 109 min at matrix temperatures of up to 2500 K and peak power densities of 4500 to 5000 MW/m^3.

The fuel elements used from 1964 to 1969 in six nuclear propulsion test reactors of the Kiwi, Phoebus, and Pewee design had a graphite matrix containing pyrocarbon-coated UC_2 spheres of ∿ 150 μm maximum diameter. Multiple coolant channels, coated with NbC or ZrC to protect the carbon in the matrix from reaction with the hydrogen propellant, formed flow passages through the 1.32-m-long elements. Successful reactor tests of up to one hour duration with maximum matrix temperatures of 2400 to 2600 K were conducted with these elements. However, mass losses of carbon from the elements at the end of one hour of testing were high enough to adversely affect the neutronic characteristics of the reactor core. The development of new fuel elements, which would be highly resistant to hydrogen attack and could be used at high operating temperatures, was therefore initiated. Two approaches were taken: (1) retain the fuel-element geometry but change the matrix to a composite of carbide and graphite with up to 35 vol% of the

*The Rover program was administered by the Space Nuclear Systems Office, a joint office of the U.S. Atomic Energy Commission and the National Aeronautics and Space Administration. The Los Alamos Scientific Laboratory, a prime contractor for the Rover program from 1956 to 1973, developed and tested the Kiwi, Phoebus, and Pewee series of space nuclear propulsion test reactors. The program was terminated on January 5, 1973.

matrix consisting of a solid-solution (U,Zr)C carbide, and (2) produce a new all-carbide fuel element from (U,Zr)C substoichiometric in carbon. The composite element would still require protective ZrC coatings in the flow passages, but, because of a continuous network of carbide throughout the matrix, would better be able to resist massive erosion conditions than the all-graphite type of fuel element. The carbide element, of course, would suffer very small carbon losses because it could only lose chemically combined carbon. The properties of and the performance in the Nuclear Furnace 1 (NF-1) reactor of these elements are described. -- (The NF-1 reactor was a heterogeneous water-moderated beryllium-reflected reactor containing 49 cells in which fuel elements could be tested.[1] Neutronic control was provided by six rotatable drums in the reflector. During operation, water flowed in a two-pass system between the cell tubes while hydrogen gas flowed through the fuel elements. Thermocouples measured the exit-gas temperature from each cell. The hot hydrogen gas exhausted from the fuel elements was cooled by injecting water directly into the gas stream. The resulting mixture of steam and hydrogen was ducted to an effluent cleanup system. After water injection, the effluent consisted of a mixture of steam, hydrogen, and radioactive contaminants at ∿ 600 K. The effluent was filtered, cooled and water-condensed, dried, passed through a cryogenically cooled charcoal trap, and finally discharged into the atmosphere.)

II. (U,Zr)C-GRAPHITE (COMPOSITE) FUEL ELEMENTS

A. Fabrication

The composite elements were extruded from a mix consisting of graphite flour, carbon black, ZrC, UO_2, and liquid thermosetting binder.[2] Solid-solution (U,Zr)C was formed in the elements during final heat treatment. A protective ZrC coating was applied to the flow passages and exterior surfaces by a chemical vapor-deposition process. The composite fuel elements, Fig. 1, were fabricated to a constant volume content of total carbide, regardless of the amount of uranium in each element. By keeping the volume content of carbide constant, a uniform coefficient of thermal expansion was maintained over the uranium loading range of interest in nuclear propulsion reactors, i.e., 200 to 650 kg/m^3. Typical chemical-analysis data* for composite elements of 35 vol% carbide content are given in Table I. One objective was the production of elements of acceptable thermal-stress resistance whose ZrC coatings would have a minimum of physical defects affecting mass loss rates.

B. Thermal-Stress Resistance

The thermal-stress resistance was improved by increasing the thermal conductivity through a carefully controlled heat-treatment process at temperatures at which 10 to 20% of the carbide was liquid. During this heat-treatment the carbide particles coalesced into a strong interconnected carbide network. The three photomicrographs in Fig. 2 illustrate some of the matrix microstructures that were obtained by varying the heat-treatment temperatures. These temperatures are shown on the pseudobinary phase diagram of the U-Zr-C system, Fig. 3. Matrices with Microstructure 1, representative of a heat-treatment temperature below the solidus line, had a thermal conductivity of ∿ 50 W/m·K at 300 K, with individual carbide particles dispersed around the unmodified particles of graphite filler flour. Matrices with Microstructure 2, representative of heat-treatment conditions at which 10 to 20% of the carbide phase was

*SI units are used in this report. Because in this system no multipliers are used in the denominator, uranium loading is expressed as kg/m^3 instead of mg/cm^3, and density as Mg/m^3 instead of g/cm^3. Pressure is expressed in pascals (Pa);--multiply psi by 0.006894 to obtain MPa, e.g., 1000 psi = ∿ 7 MPa.

liquid, had a thermal conductivity of ∿ 80 W/m·K, the carbide had formed a continuous-network type of structure, and the graphite particles had undergone modification. Matrices with Microstructure 3, representative of heat-treatment conditions where most of the carbide phase was liquid, had a thermal conductivity of over 140 W/m·K at 300 K, the carbide had largely coalesced, and most of the graphite was in a highly ordered proeutectic form. The increase in thermal conductivity is attributed to the ordering of the crystallites in the graphite flour particles and in the binder carbon aided by the presence of liquid carbide. Matrices with Microstructure 2 were preferred because their thermal conductivities were relatively high and their mechanical properties were satisfactory; matrices with Microstructure 3 had about one-tenth the flexural strength of those with Microstructure 2. Figure 4 is a scanning-electron photomicrograph of the (U,Zr)C network in a composite element. All the graphite phase had been removed by leaching with hydrogen at ∿ 2000 K. Note the continuous three-dimensional structure of the carbide. Removal of the graphite did not alter the dimensions of the element. However, the room-temperature compressive strength of the leached element was ∿ 10 MPa as compared to ∿ 110 MPa for the unleached element.

C. Properties of Composite Elements

The factors that controlled the formation of defect-free ZrC protective coatings were: (1) the temperature of ZrC deposition, (2) the thickness of the ZrC coating, and (3) the thermal expansion properties of both the ZrC and the fuel-element matrix. The coefficient of thermal expansion (CTE) of vapor-deposited ZrC was ∿ 7.7 μm/m·K for the 293- to 2300-K temperature range. The matrix longitudinal CTE had to be ≳ 6.6 μm/m·K or the very adherent ZrC coating would form microcracks upon cooling from the deposition temperature (∿ 1500 K). In a series of experiments with 50- to 150-μm-thick ZrC coatings on matrices of varying CTE the coatings formed cracks at strains ≳ 1000 μm/m. To minimize this mismatch in CTE between the matrix and the coating, the thermal expansion of the matrices was increased by using high-CTE graphite filler flours and by increasing the volume content of the carbide phase. However, matrices of ≳ 40 vol% carbide had poor thermal-stress resistance, and, if the carbide content was lower than 30 vol%, their maximum uranium loading had to be decreased to avoid conditions at which UC_2

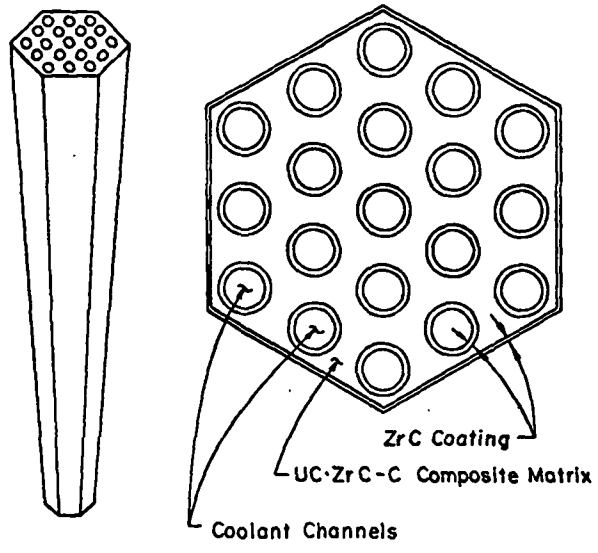

Fig. 1. Full-length and cross-section views of composite fuel element. Length, 1.32 m; across-flats, 19 mm; coolant-channel diameter, 2.3 mm; mass, ∿ 1.1 kg; and volume, 284 x 10^{-6} m^3.

TABLE I

CHEMICAL ANALYSIS DATA FOR COMPOSITE FUEL ELEMENT MATRICES

	Uranium Loading, kg/m^3		
Parameter	180	399	598
U, wt%	5.2	11.1	16.4
Zr, wt%	56.0	52.5	49.6
C, wt% (total)	38.8	36.0	33.6
Density, Mg/m^3	3.49	3.61	3.64
Carbide content, vol%	34.9	35.5	35.6
U, at.% on a metal basis	3.5	7.6	11.4

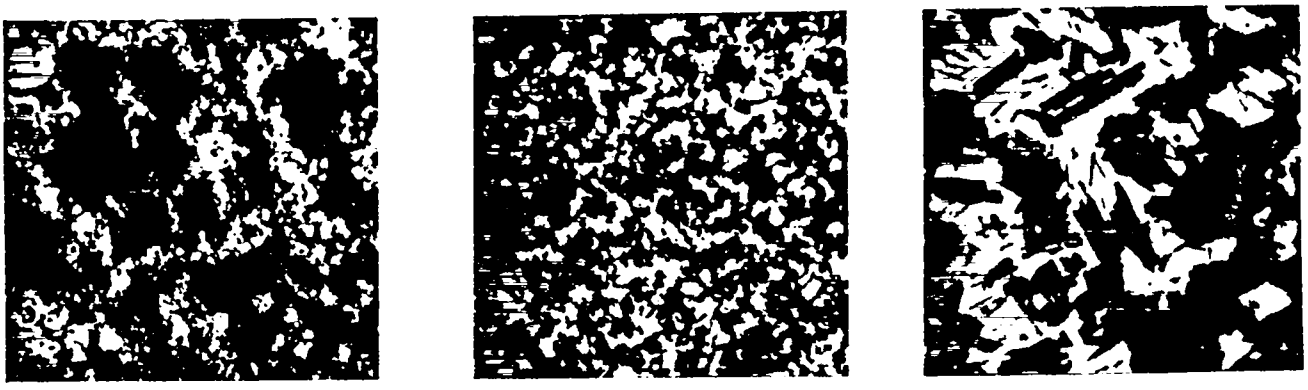

Fig. 2. Photomicrographs of (U,Zr)C-graphite matrices containing 35 vol% carbide and ∿ 400 kg/m^3 of 93%-enriched uranium. The white areas are carbide, the gray areas are graphite, and the black areas are void. Heat treatment at (1) ∿ 2800 K; (2) ∿ 3050 K; (3) ∿ 3120 K.

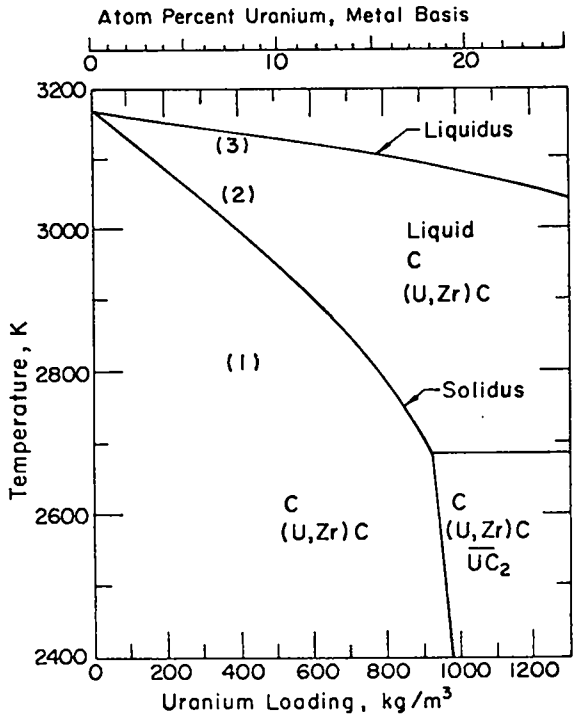

Fig. 3. Portion of pseudobinary phase diagram for U-Zr-C system for composite elements containing 35 vol% carbide. (1), (2), and (3) refer to heat-treatment temperatures in Fig. 2.

Fig. 4. Scanning-electron photomicrograph of the (U,Zr)C network structure in a composite element.

would form (see lower right-hand corner of phase diagram, Fig. 3).

Some properties of (U,Zr)C-graphite (composite) fuel elements are given in Table II. The thermal-stress resistance was evaluated by measuring the electrical power density required to fracture a fuel-element specimen. The test conditions of pressure and hydrogen flow rate simulated those encountered in a nuclear propulsion reactor.

TABLE II

GENERAL CHARACTERISTICS OF (U,Zr)C-GRAPHITE (COMPOSITE) FUEL ELEMENTS

Parameter	Value
Carbide content, vol%	30 - 35
Useful U-loading range, kg/m^3	50 - 650
Thermal conductivity (300 K), W/m·K	50 - 90
Coeff. of thermal expansion (293 to 2300 K), μm/m·K	6 - 7
Flexural strength (300 K), MPa	∿ 50
Compressive strength (300 K), MPa	∿ 110
Strain to fracture (300 K), μm/m	2000 - 3000
Stress at fracture (300 K), MPa	35 - 50
Elastic modulus (300 K), GPa	∿ 50
Compressive deformation at 2800 K (3.5 MPa for 1 h),%	0.5 - 1.0
Thermal stress resistance at ∿ 1700 K (power density at fracture), MW/m^3	4500 - 6000

Forty-seven composite fuel elements* were used in the NF-1 reactor. These elements were divided into three broad experiments: (1) a carbide-content experiment of 30 vs 35 vol%, (2) a matrix CTE experiment of 6.1 vs ∿ 6.7 μm/m·K, and (3) a matrix thermal-stress-resistance experiment with fracture power densities of 4700 to 6200 MW/m^3. Table III summarizes the range of properties of these elements in the reactor. The CTE experiment was, in reality, a ZrC coating-crack experiment. The coatings on matrices with a CTE of 6.1 μm/m·K formed ∿ 600 circumferential cracks/meter of coolant-channel length on cooldown from the temperature (1500 K) at which the coatings were applied; but the coatings on matrices with a CTE $\geq$ 6.5 μm/m·K were essentially crack-free as fabricated and

*Five of the 30-vol% composite elements were fabricated by the Westinghouse Astronuclear Laboratory (WANL) as part of the Nuclear Engine for Rocket Vehicle Application Program (NERVA).

TABLE III

RANGE OF MATRIX PROPERTIES OF COMPOSITE ELEMENTS IN THE NF-1 REACTOR

Carbide Content, vol%	Thermal[a] Expansion, μm/m·K	Thermal Conductivity,[b] W/m·K	Fracture Power Density, MW/m^3
35	6.7	75	4700
35	6.7	74	4900
35	6.6	71	5000
35	6.6	84	5200
35	6.8	80	5400
35	6.8	87	6100
30	6.5	83	5500
30	6.5	77	5800
30	6.6	75	6200
30	6.1	40-50	4700 to 5500

[a] 293 to 2300 K range.

[b] at ∿ 300 K.

installed in the reactor. Based on the results obtained from component tests, very low carbon mass losses were predicted for those elements in the NF-1 reactor with crack-free ZrC coatings.

The details of a standard NF-1 reactor cell in which a composite element was housed is shown in Fig. 5. The NF-1 reactor full-power conditions that affected the composite fuel elements are listed in Table IV.

III. REACTOR PERFORMANCE OF COMPOSITE ELEMENTS

Postmortem examinations comprised rather sophisticated nondestructive and destructive examinations as a function of fuel-element length. A position along the 1.32-m-long element was designated a Station, measured in millimeters from the cold end of the element where the hydrogen propellant entered.

The mass losses ranged from 8 to over 50 g/element. The 24 elements with a CTE of 6.1 μm/m·K had an average loss of 37.6 g/element as compared to 13.7 g for the 23

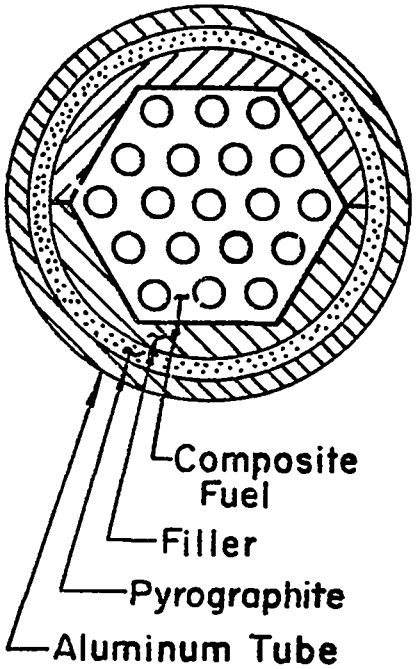

Fig. 5. NF-1 reactor cell containing (U,Zr)C-graphite (composite) fuel element. The filler material was an extruded composite of 30-vol% ZrC and the remainder graphite.

elements with a CTE $\geq$ 6.5 μm/m·K. Two-thirds of the mass loss* occurred in the midrange region, between Stations 300 and 600 (Figs. 6 and 7). Large losses in the midrange region were unexpected, and very little loss had been predicted in this region for the high-CTE elements. However, the mass loss rates for the hot-end region, Station 1000 to 1300, were within the range of loss rates determined by laboratory component tests (Fig. 8).

Mass losses associated with matrix cracks were observed in several composite elements. The small peak in the mass-loss curve at Station 1300, Fig. 6, and the peaks from Station 800 to 1300 in Fig. 7 were the result of matrix cracking and of associated cracks in the ZrC protective coating. Matrix cracking was readily detected by high-resolution eddy current

*Mass-per-unit length evaluation (MULE) was performed nondestructively by using gamma-ray absorptometry.[3]

TABLE IV

NF-1 REACTOR FULL-POWER CONDITIONS

Parameter	Value
Reactor thermal power, MW	44
Power/composite element, MW	∿ 0.90
Hydrogen flow/element, kg/s	0.022
Hydrogen-inlet pressure, MPa	4.7
outlet pressure, MPa	3.2
inlet temp., K	340
outlet temp., K	2450
Maximum matrix temp., K	∿ 2500
Peak power density, MW/m^3	∿ 4500
Run time at full power, min	109

examination of each coolant channel. Most matrix cracks were found at the higher stations and not too many were observed in the vicinity of Station 700, the peak of power generation. The matrix cracks at the higher stations were believed to have occurred during two automatic emergency shutdowns from full power when the control temperatures during the first 5 sec of the shutdown changed at an average rate of ∿ 300 K/sec.

The high-CTE elements were examined for type and number of coating cracks as a function of station. Surprisingly, numerous coating cracks occurred at the cold end of the element (Figs. 9 and 10). These coating cracks were the cause of the unexpected mass loss in the midrange region, i.e., the loss was due to the transport of hydrogen and of its products of reaction with the matrix (methane and acetylene) in and out of open coating cracks. The peak in the mass-loss curve was caused by the increased reaction rate of hydrogen with carbon at temperatures above 1000 K (Station 250); however, the coating cracks were closing as the temperature increased and they were essentially closed at 1600 K (Station 500)--a temperature slightly above that used in depositing the ZrC (see Fig. 11 for matrix temperature vs station). The coating cracks could have been caused by the large temperature gradient

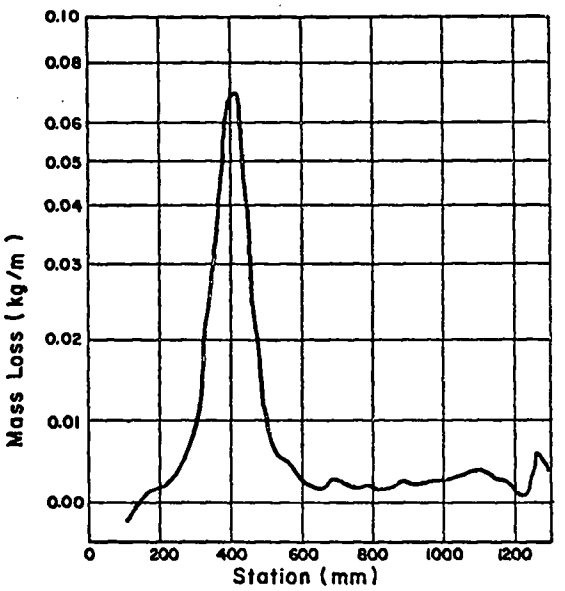

Fig. 6. Mass loss vs length for a (U,Zr)C-graphite element with a thermal expansion > 6.5 μm/m·K.

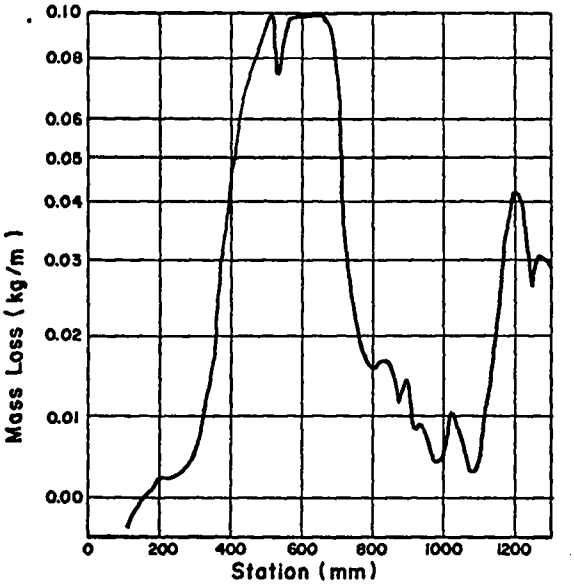

Fig. 7. Mass loss vs length for a (U,Zr)C-graphite element with a thermal expansion of 6.1 μm/m·K.

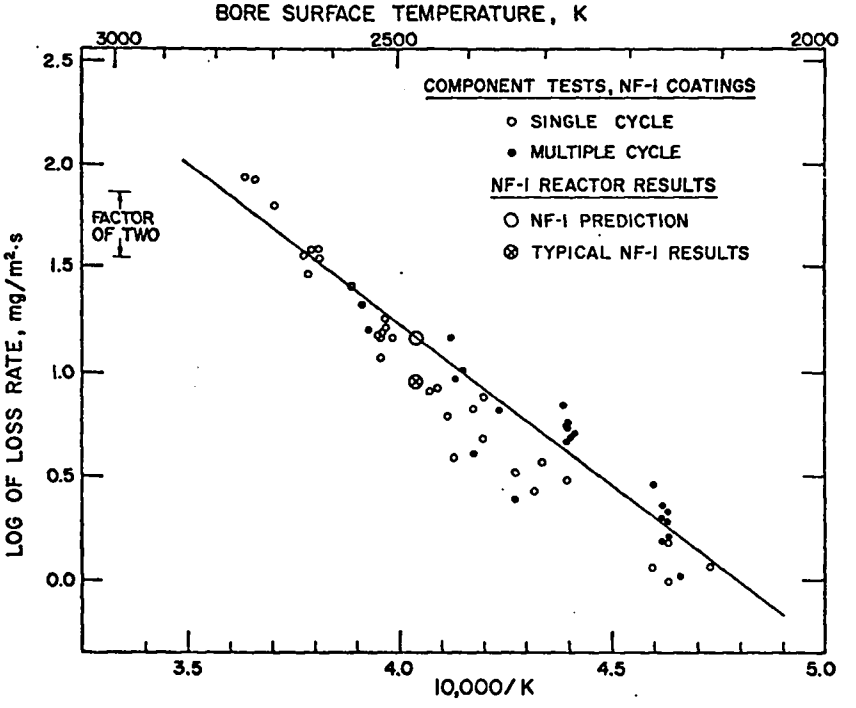

Fig. 8. Component and NF-1 reactor test results for hot-end mass-loss rates of composite elements. Loss rates per second are given in milligrams of loss per square meter of coolant channel surface area.

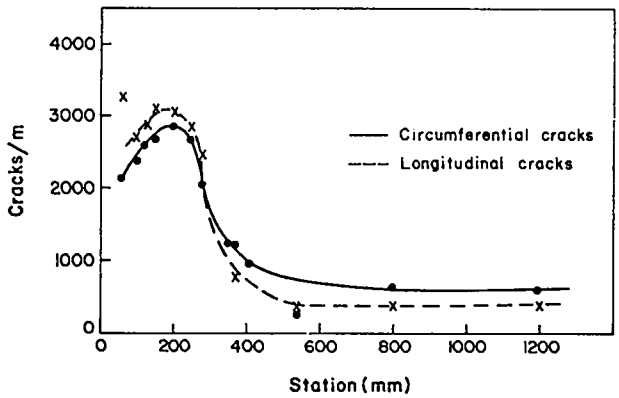

Fig. 9. Number of cracks in ZrC coolant-channel coating as a function of length for a NF-1 composite fuel element.

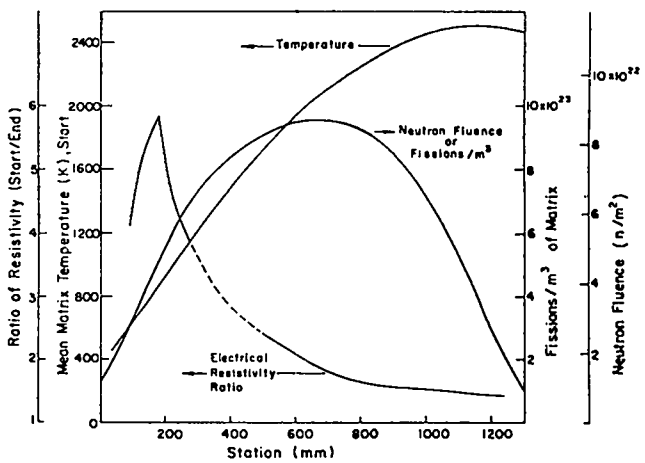

Fig. 11. Fuel-element environment vs length: temperature, fissions, and fast-neutron fluence (>0.18 MeV). Also plotted is the change in room-temperature electrical-resistivity ratio for a composite fuel element, start to end, of the NF-1 reactor run.

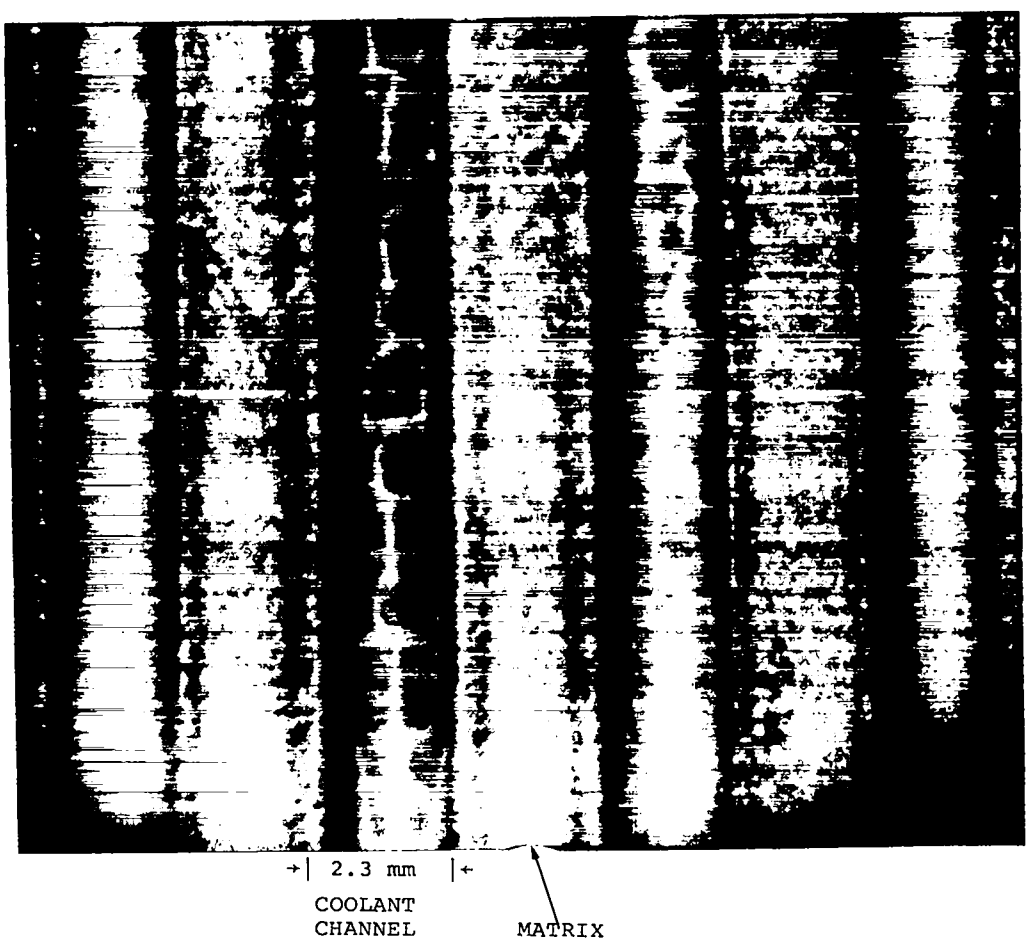

Fig. 10. Split composite fuel element from the NF-1 reactor showing cracks in the ZrC coolant-channel coating.

generated during the two emergency shutdowns from full power, or by the changes that could have taken place due to exposure to the radiation field. Plotted among other data in Fig. 11 is the change of room-temperature electrical resistivity vs station of the composite elements at the start as compared to the end of the NF-1 test. At Station 200 the electrical resistivity increased by a factor of six, indicating radiation damage. The dotted portion of the resistivity curve has been sketched in, disregarding resistivity effects of mid-range corrosion. The coating-crack curves of Fig. 9 were similar to the electrical resistivity curve, which suggested that the formation of coating cracks might be related to radiation damage.

Changes in room-temperature thermal conductivity of whole element cross sections from Station 200 were determined by a flash-diffusivity method. The average room-temperature thermal resistivity of five elements increased by a factor of 9.3. However, a sample from hot-end Station 1110 had a thermal resistivity ratio (start/end) of only 1.5. Subsequent annealing studies on samples from Station ∿ 200 indicated that after one hour at 1500 to 1600 K most of the damage was removed, i.e., both the room-temperature electrical and thermal-resistivity ratios (start/end) decreased from 9.0 to 1.2. Because these annealing results were very similar to those obtained on fast-neutron-irradiated graphite by Taylor, Kelly, and Gilchrist[4] the radiation damage in the composite elements was assumed to be associated primarily with the graphite phase. At room temperature ∿ 10% of the thermal conductivity of a composite element can be attributed to the carbide phase.

The thermal conductivity of the matrix as a function of temperature was determined by a laser flash-diffusivity technique. Disks, 12 mm in diameter and 1 mm thick, were obtained at Station ∿ 160 from two similar elements, only one of which had been in the reactor. As shown in Fig. 12, the thermal conductivity of the irradiated matrix at the operating temperature (800 K) for Station 160 had decreased from 40 W/m·K at the start to 12 W/m·K at the end of the NF-1 test. The thermal conductivity of this disk at temperatures above 800 K (solid curve, Fig. 12) is a function of the amount of annealing that occurred during the time the thermal-conductivity measurements were being taken. The higher thermal conductivity at 2300 K of the irradiated sample than that of the unirradiated sample is not understood.

The changes in thermal conductivity of the matrix caused commensurate changes in the steady state thermal gradients in the matrix. Figure 13 shows the calculated mean differential temperature between the matrix and the ZrC channel coating as a function of station. Note the large changes at the lower stations from the start to the end of the NF-1 test. The corresponding changes in strain, which increased about twofold, were high enough to exceed the 1000-μm/m strain limit of the coating. Thus, even steady state full-power conditions would cause the coatings to crack, let alone the strains developed during emergency shutdowns.

The curves in Fig. 11 outline the relationships among matrix temperature, neutron fluence, and fissions as a function of station. Studies of irradiated graphites[4-6] have indicated that fast-neutron fluences of 10^{25} neutrons/m² (> 0.18 MeV) would be required to change the ratio of thermal resistivity of graphite by a factor of 8 to 10 as in the NF-1 composite elements. However, because the fast-neutron fluence in NF-1 was only 5×10^{22} neutrons/m² at Station 160 (the station with the greatest radiation damage) the possibility of damage by fission-fragment interaction was considered. If the range of fission fragments in (U,Zr)C is assumed to be 5 to 7 μm and the web thickness of the carbide network

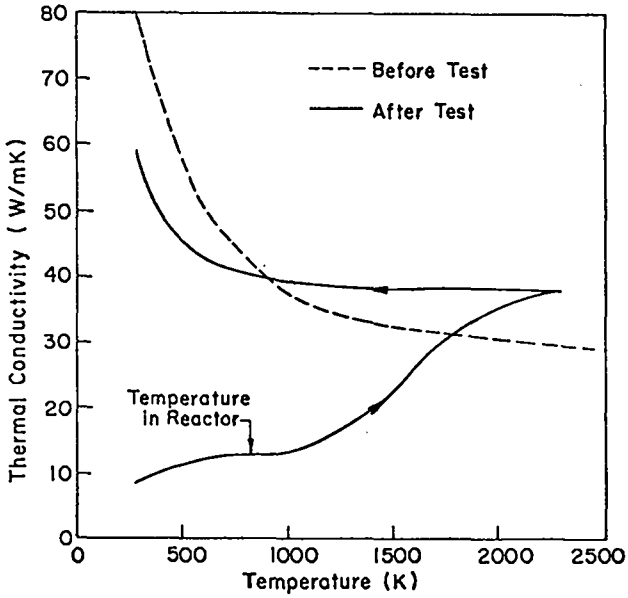

Fig. 12. Comparison of thermal conductivity vs temperature of a composite fuel-element matrix before and after testing in the NF-1 reactor.

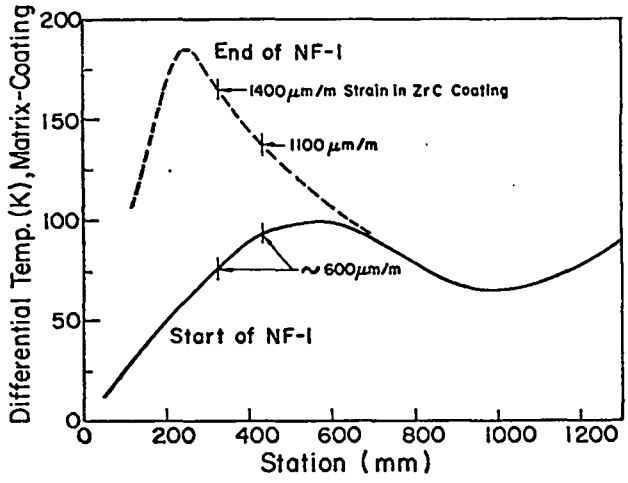

Fig. 13. Temperature differences between composite matrix and ZrC protective coating and resultant coating strains at the start and end of the NF-1 reactor test.

is 5 to 10 μm (Fig. 5), the probability of a fission fragment entering the graphite phase is estimated to be > 0.1. With 5×10^{23} fissions/m³ and double that number of fragments, at least 10^{23} fragments/m³ interacted with the graphite at Station 160.

Table V compares the dosages of fast neutrons, ^{235}U fission fragments, and the α and ^{7}Li particles from the $^{10}B(n,\alpha)^{7}Li$ reaction that produced a room-temperature thermal-resistivity ratio change of ∿ 10 in graphite irradiated at 700 to 900 K. Radiation damage of graphite by fast neutrons has been studied by numerous investigators, and all the results are in agreement that considerable damage is done at fluences of 10^{25} neutrons/m². Radiation damage effects in borated graphite by α and ^{7}Li particles from the $^{10}B(n,\alpha)^{7}Li$ reaction were studied by Davidson, Gates, and Nightingale.[7,8] The boron carbide was dispersed throughout a graphite matrix as particles of 10-to 100-μm diam. About 5% of the reaction products were estimated to be effective in causing displacement of carbon atoms.[9] The effect of ^{235}U fission fragments on the thermal conductivity of

TABLE V

COMPARATIVE STUDIES OF RADIATION INDUCED DAMAGE TO GRAPHITE AT 700 TO 900 K

Dose in Graphite	Temperature of Irradiation, K	Thermal-Resistivity Ratio[a]
4.5×10^{25} neut/m² (> 0.18 MeV)[b]	725	9.7
	925	7.0
∿ 10^{25} combined α and ^{7}Li particles/m³ from $^{10}B(n,\alpha)^{7}Li$ reaction[c]	775	10 to 14
10^{24} fission fragments/m from ^{235}U fission[d]	900	10
10^{23} fission fragments/m from ^{235}U fission, data from this report	800	9

[a] Room-temperature thermal-resistivity ratio before and after irradiation.

[b] PGA, a pile grade graphite.[5]

[c] Borated graphite.[7] Burnout was 5 to 15 x 10^{26} atoms $^{10}B/m^3$ with ∿5% of the reaction products effectively entering the graphite from B_4C particles of 10-to 100-μm diam.

[d] National Carbon Co. B-1508-A graphite containing 2- to 5-μm-diam U_3O_8 particles.[10] Dose was 3×10^{24} fissions/m³.

graphite was studied by Hunter,[10] using a graphite containing 2- to 5-μm-diam U_3O_8 particles. The probability of fission fragments leaving these small particles and entering the graphite phase was high. Considering all the imponderable differences between Hunter's experiment and the NF-1 experiment, the agreement within a factor of 10 of the influence of fission fragments on graphite is considered good.

IV. (U,Zr)C (CARBIDE) FUEL ELEMENTS

Two of the 49 cells in the NF-1 reactor contained (U,Zr)C solid-solution carbide elements, Fig. 14. Each cell contained seven elements, bundled together, as shown in Fig. 15, with another seven elements stacked on top to complete the length of the cell. The 28 carbide elements in the two cells represented three types of matrix experiments.

The carbide elements were extruded from a mix consisting of ZrC powder, enriched UO_2 powder, ZrO_2 powder, graphite flour, and a thermosetting binder. Solid-solution (U,Zr)C was formed in the elements during a high-temperature heat treatment. The elements contained ∿ 3% excess carbon to facilitate densification during heat treatment, to prevent sticking to graphite fixtures during heat treatment, and to aid in machining the elements to a hexagonal cross section. The excess free carbon was removed by leaching with hot hydrogen gas. After leaching, the elements were impregnated with various amounts of zirconium by a chemical vapor-deposition process to adjust the carbon stoichiometry. A final heat treatment at $\geq$ 2800 K was applied in an attempt to obtain uniform chemical composition. Matrices that gained 0, 3, and 8% mass during the zirconium impregnation process were used in the NF-1 reactor experiment. Table VI presents the chemical analyses and property data for these elements. The carbon-to-metal ratio of the impregnated elements was not as low as had

Fig. 14. Full-length view of (U,Zr)C (carbide) fuel element. Length, 0.64 m; across flats, 5.5 mm; coolant-channel diameter, 3.2 mm; and carbon/metal atom ratio, 0.8 to 0.92.

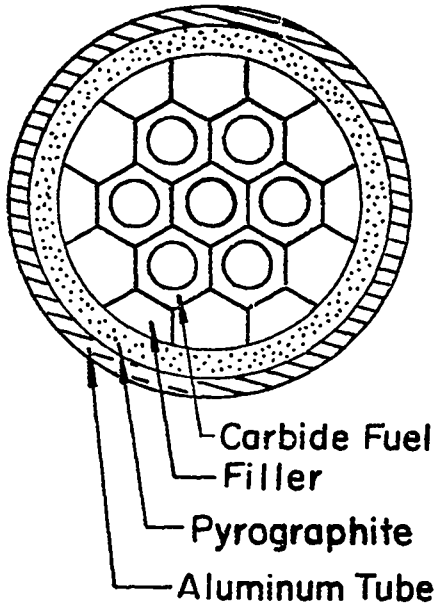

Fig. 15. NF-1 reactor cell containing (U, Zr)C (carbide) fuel elements. The filler was ZrC-graphite (composite) coated with ZrC.

TABLE VI

GENERAL CHARACTERISTICS FOR
(U,Zr)C (CARBIDE) FUEL ELEMENTS

Parameter	Impregnation Mass Gain, %		
	0	3	8
Uranium loading, kg/m^3	∿ 300	∿ 300	∿ 300
U, %	5.88	5.64	5.42
Zr, %	82.9	83.1	83.5
C, % total	11.0	11.0	10.8
C, % free	<0.05	<0.05	<0.05
O, %	0.05	0.07	0.04
N, %	0.14	0.22	0.29
Carbon/metal atom ratio	0.981	0.980	0.958
Density, Mg/m^3	5.48	5.46	5.71
Porosity, %	23	21	18
Thermal conductivity,[a] W/m·K	10.0	8.6	8.2
Long./Trans. properties[a]			
Failure strain, μm/m	540/460	470/460	300/450
Failure stress, MPa	140/75	140/90	100/95
Modulus, GPa	250/160	290/200	330/210
CTE,[b] μm/m·K	7.8	7.8	7.8
Compressive deformation,[c] %			
at 2770 K	--	4	2
at 2870 K	--	-	5
at 2970 K	26	20	7

[a]Room temperature longitudinal and transverse properties.
[b]Coefficient of thermal expansion, 293 to 2300 K.
[c]6.9 MPa for one hour.

been expected because of carbon pickup from the atmosphere of the heat-treatment furnaces.

The temperatures at which liquid is formed in $(U_{0.1}Zr_{0.9})C_x$ as a function of carbon stoichiometry are shown in Fig. 16.

A proposed maximum operating temperature of 3200 K is equivalent to a specific impulse of ∿ 950 sec in a nuclear propulsion engine using hydrogen as a propellant and, as indicated in Fig. 16, would require careful control of the carbon stoichiometry.

V. REACTOR PERFORMANCE OF CARBIDE ELEMENTS

The NF-1 full-power conditions affecting the carbide elements were essentially those listed in Table IV. The primary purpose of the carbide fuel-element experiment in the NF-1 reactor was to determine the fracture mode of the carbide elements at peak power densities up to ∿ 4500 MW/m^3. Considerable transverse fracturing could be tolerated, but extensive longitudinal fracturing or fragmentation would cause operational difficulties, i.e., plugged flow passages and hot spots.

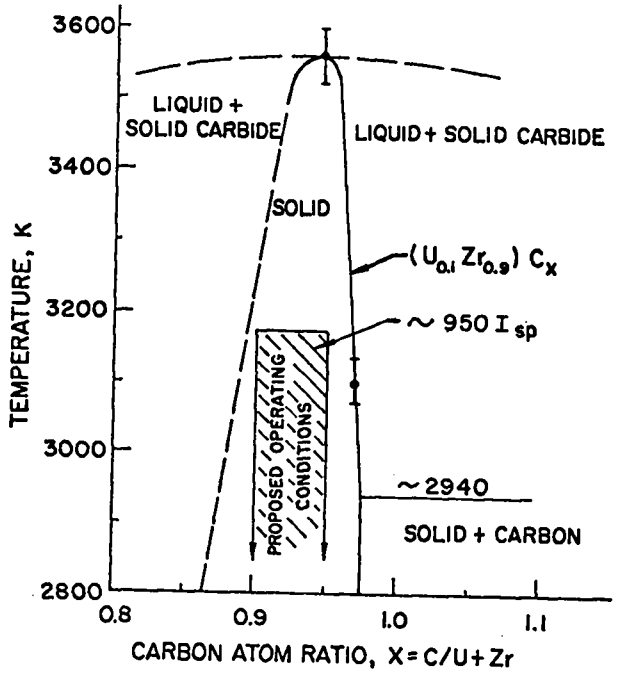

Fig. 16. Pseudobinary phase diagram for $(U_{0.1}Zr_{0.9})C_x$.

The two thermocouple channels, which measured the exit-gas temperature from the two cells of carbide elements, behaved considerably different than the other channels. First, their temperatures were ∿ 100 K lower than the core average of 2450 K, either due to improper orificing or because of incorrectly predicted carbide-element power. Secondly, the two channels showed a greater variability with time than any other channel, exhibiting both long-term drifts and short-term fluctuations. The fluctuations may have been due to impedance variations, such as might be caused by fractured elements.

Before disassembling the two cells, steel skewers were inserted in the coolant-channel passages of the elements. The metal walls of the cells were split longitudinally and the elements were exposed to view. There were many transverse fractures, but no fragmentation into small-size particles.

The nonimpregnated elements, installed only in the cold-end section of the core (from Station 0 to 650), had transverse fractures at 5- to 15-mm intervals [one to three fuel-element diameters, Fig. 17, (A) and (B)]. Microscopic examination of polished samples showed up to two longitudinal cracks per cross section from Station 200 to Station 650. There was considerable longitudinal and transverse fracturing -- typically shown in Fig. 17, (C) -- from Station ∿ 500 to 650.

The 3%-impregnated elements, in both the cold- and hot-end sections, had a similar fracture pattern, except that the highly fractured region extended from Station ∿ 500 to Station ∿ 800. As many as four longitudinal cracks per cross section were counted in this region. At higher stations, 1000 to 1300, the transverse fractures occurred at 25- to 50-mm intervals, with one longitudinal crack per cross section occasionally.

The 8%-impregnated elements, installed only in the hot-end section (from Station 650 to 1300), did not undergo as much fracturing as the other two types. At Station 700, where the peak power density was ∿ 4500 MW/m , the characteristic transverse fracture interval was ∿ 25 mm, and at higher stations fractures occurred sometimes only at 100-mm intervals. Typical fractures are shown in Fig. 17,(D). Microscopic examination of polished sections indicated that some samples had no longitudinal cracks, even at Station 700, and at the most only one crack per cross section.

Although the extent of longitudinal cracking in the carbide elements was disappointing, their performance in retrospect was not unreasonable considering the low strain-to-fracture characteristics of the matrices, the high power density, and the thermal gradients developed during the two emergency shutdowns. New matrix development experiments have indicated that the strain-to-fracture characteristics of the carbide elements probably can be increased

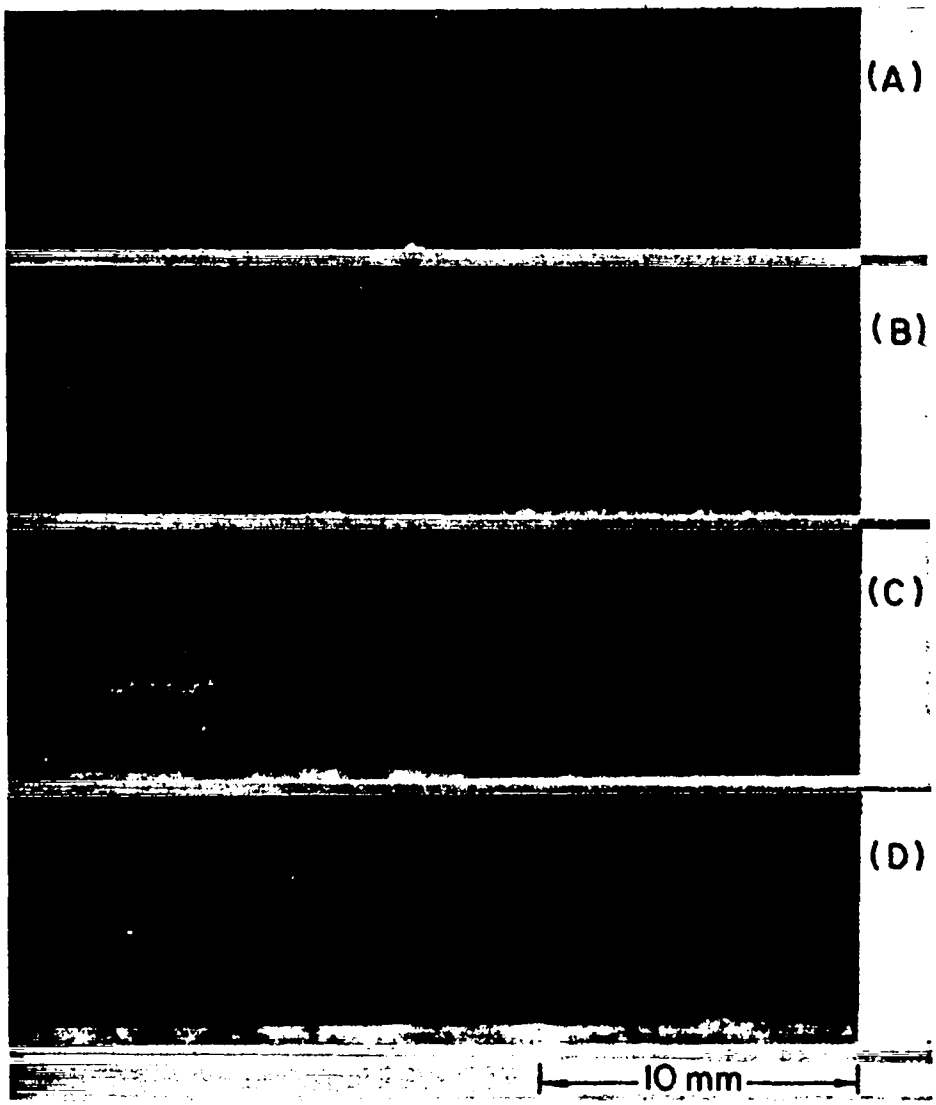

Fig. 17. Fracture patterns in NF-1 carbide elements: (A) and (B) show transverse fractures at low Stations 0 to 600; (C) shows both longitudinal and transverse fractures with a piece removed, and (D) shows a transverse fracture at high Stations 700 to 1300.

by a factor of two, i.e., to about 800 to 1000 μm/m versus 300 to 500 μm/m of the NF-1 carbide elements. Reducing the cross section and web thickness of the elements by 25% would substantially decrease the steady state temperature gradients. An improved matrix coupled with a modified design would significantly increase the fracture resistance of carbide elements over that of those used in the NF-1 reactor. Component tests have indicated that carbide elements would perform for many hours at temperatures of 2800 to 3100 K without serious losses of C, U, or Zr.

VI. CONCLUSIONS

A. Composite Elements

The mass losses of composite elements, because of the reaction of hydrogen with graphite, were very dependent on the formation of cracks in the protective ZrC coating. Minimizing the thermal-expansion mismatch between the ZrC coating and the composite

matrix reduced both the tendency to form coating cracks and the mass loss. Mass losses were unexpectedly high in those portions of the elements which had been damaged by radiation. This damage--apparently due to interaction of fission fragments with the graphite--degraded the thermal transport properties of the matrix, and the resulting temperature gradients caused extensive cracking of the coating. The composite elements withstood peak power densities of 4500 to 5000 MW/m^3 without major difficulties. In general, the NF-1 experiments indicate that composite elements (even those suffering the highest carbon loss) would perform satisfactorily for at least two hours in a nuclear propulsion reactor which heated hydrogen to the temperature region of 2500 to 2800 K. The basic information leading to this conclusion is the constancy of the individual exit-gas thermocouple readings for each fuel element during the course of the NF-1 reactor operation. These readings were essentially constant for all composite elements; consequently, it could be concluded that even the highest carbon losses had not interfered with the proper functioning of the elements concerned. An extrapolation of these results to longer reactor run times--ten hours for example-- is difficult. Massive nonlinear and catastrophic carbon losses such as those previously observed for carbide-coated graphite elements would not be expected. What might occur in a nuclear propulsion reactor (in which, unlike the conditions in NF-1, element-to-element interactions could be of importance) is transverse fracturing of some elements, due to repeated temperature cycling, in the region from which the most carbon had been removed and thereby weakened; (Fig. 18 shows the change in flexure strength due to midrange mass losses). Such fractures could cause radial cross-flow of hydrogen among coolant channels, particularly for those elements which had a large variation in inlet orifice sizes. Therefore, matrix

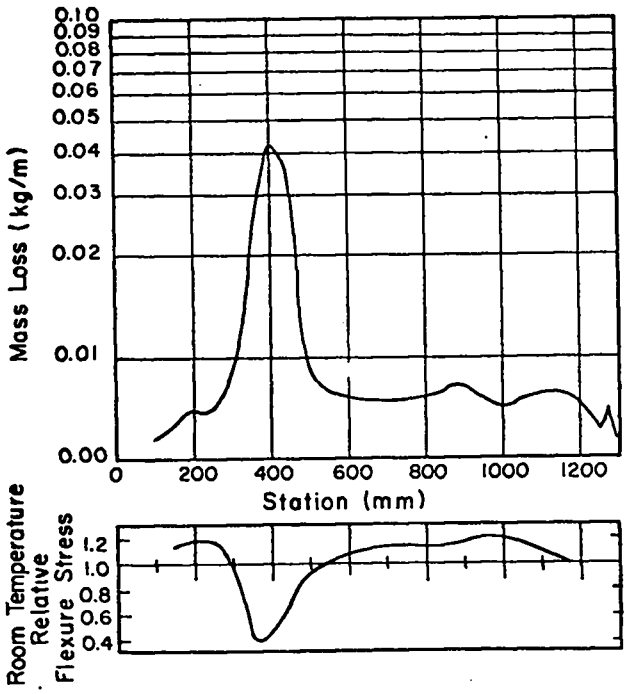

Fig. 18. Changes in room-temperature flexure stress-to-fracture of NF-1 composite elements relative to the fracture strength before the NF-1 test.

temperatures might increase locally. The consequences of such local temperature increases are not easily determined. The useful life of composite elements, of the high-CTE matrix type with the lowest mass losses in the NF-1 reactor, is certainly longer than two hours, probably two to three times as long.

B. Carbide Elements

The carbide elements in NF-1 cracked extensively, particularly near the center of the reactor where the peak power densities were ∿ 4500 MW/m^3 and the temperature was 1500 to 1800 K. No evidence of fragmentation into millimeter-size particles was seen. Improvements in strain-to-fracture properties of the matrix, and design changes to minimize temperature gradients, would make these elements useful at power densities of 3000 to 4000 MW/m^3.

C. Reactor Performance of Composite vs Graphite Elements

The mass-loss behavior of composite elements cannot be compared directly with that of graphite elements because the two types of elements were never tested in the same reactor. However, the performance of graphite elements tested in the Pewee 1 reactor can be compared with that of composite elements in the NF-1 test. The run time of the Pewee 1 reactor was 40 min versus 109 min for the NF-1 reactor. The time-average coolant-channel surface temperature at Station 1000 was 2575 and 2475 K for the two reactors, i.e., the test temperature in the Pewee 1 reactor was ∿ 100 K higher than in the NF-1 reactor. The average fuel-element power density was 1.2 and 0.9 MW/element for the Pewee 1 and NF-1 tests, respectively. The coolant channels from Station 800 to 1300 of the graphite elements in the Pewee 1 reactor were coated with either a NbC or a ZrC coating of ∿ 75 μm thickness, whereas the coolant channels at these stations of composite elements in NF-1 were coated with a ZrC coating of 100 to 150 μm thickness.

Figure 19 presents the average mass loss rates per unit surface area of coolant channel as a function of station for Pewee-1 and NF-1 elements. The average losses in the midrange section were similar for all types of elements; however, these losses were quite variable for individual elements. The CTE of the graphite fuel-element matrix, containing pyrocarbon-coated UC_2 spheres, was ∿ 5 μm/m·K as compared to ∿ 6.6 μm/m·K (293-2300 K range) for the high-CTE type composite matrix. The strain capability of the coatings on the graphite elements was exceeded on cooldown from the temperature used in the coating deposition process, and the coolant-channel coatings of these elements therefore cracked extensively. Apparently, the mass-loss rates in the midrange section of both types of elements were due to the presence of coolant-channel

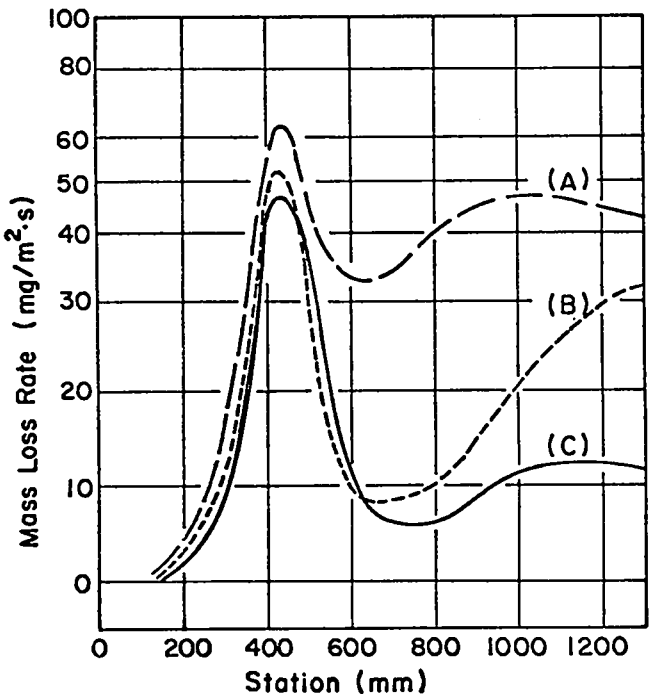

Fig. 19. Mass loss rates per unit surface area of coolant channel vs station for graphite and composite elements: (A) average for 102 Pewee-1 graphite fuel elements coated with NbC, (B) average for 12 Pewee-1 graphite fuel elements coated with ZrC, (C) average for 23 NF-1 high-CTE composite fuel elements coated with ZrC, adjusted to the Pewee-1 test temperature.

coating cracks regardless of the mechanism by which these cracks had been formed (mismatch of matrix and carbide coating CTE, effects of emergency shutdowns, or radiation damage to the matrix).

The hot-end mass loss rates of the NbC-coated graphite elements in Pewee 1 were considerably higher than those of comparable ZrC-coated graphite elements. This difference was expected because of the higher diffusion coefficient of carbon through NbC than through ZrC. The hot-end mass loss rates of ZrC-coated high-CTE type composite fuel elements in NF-1 were lower than those of the graphite elements even after adjustment for the difference in operating temperatures between the two reactors (based on the data of Fig. 8: - the 100-K difference in bore

surface temperature between the two reactors results in a hot-end mass loss rate which, for the Pewee 1 reactor, is 1.5 times higher than for the NF-1 reactor). These lower hot-end mass loss rates of the NF-1 elements undoubtedly were due, in part, to the increased thickness of the ZrC coatings in the NF-1 elements.

The assumption used in this comparison of graphite vs composite elements is that the mass loss rates are linear with respect to time and amount of mass loss. Previous reactor tests with graphite elements indicate a high incidence of catastrophic erosion if mass losses were high. However, the presence of a continuous carbide network in composite elements has prevented erosion both in component tests and in the NF-1 test. In component tests, these elements have not shown any substantial change in mass loss rate as a function of test time.

The graphite fuel elements would not have undergone degradation of properties by interaction of fission fragments with the matrix because the range of the fission fragments would not have exceeded the dimensions of the pyrocarbon-coated UC_2 particles. In addition, radiation damage to the graphite fuel element by fast-neutron fluence is considered to become important only after several hundred hours of operation in a nuclear propulsion reactor. To reduce the losses in the midrange section of graphite elements, the CTE of the matrix should be increased to $\sim$ 7 $\mu m/m \cdot K$. Recent developments at Union Carbide's Y-12 plant at Oak Ridge may eventually have resulted in a much improved high-CTE element.[11]

The usefulness of composite elements is limited by their high susceptibility to radiation damage. However, wherever resistance to erosion is a requirement, their performance is highly superior to that of graphite-matrix fuel elements.

VII. APPENDIXES

Attached are Appendixes A through E, which summarize the development history of the (U,Zr)C-graphite and carbide fuel elements. The results of detailed evaluation studies of composite elements are also included.

ACKNOWLEDGMENTS

This work was sponsored by the U.S. Atomic Energy Commission under Contract W-7405-Eng-36. The author wishes to thank the numerous individuals who contributed to this work: C. Bankston, R. Bard, A. Driesner, K. Davidson, J. Rowley,and T. Wallace of the Rover Fuel Element Committee; F. Criss, A. Driesner, D. MacMillan, W. Martin, D. Schell and A. Zerwas for development and fabrication of the elements; J. Fullbright, D. Garrett, T. Gregory, R. Strong,and M. Winkler for nondestructive evaluation; H. Filip, C. Hoffman, R. Lawton, H. Murphy, B. Morrison, W. Prince,and L. Wahman for property and component testing; I. Leffler, A. Pereira, and D. Rose for reactor postmortem operations; B. Fisher, R. Malenfant,and R. McFarland for analytical calculations; and the members of Group CMB-1 for chemical analyses.

REFERENCES

1. W. L. Kirk, "Nuclear Furnace-1 Test Report," Los Alamos Scientific Laboratory Report LA-5189-MS (1973).

2. K. V. Davidson, W. W. Martin, D. H. Schell, J. M. Taub, and J. W. Taylor, "Development of Carbide-Carbon Composite Fuel Elements for Rover Reactors," Los Alamos Scientific Laboratory Report LA-5005 (1972).

3. M. A. Winkler and H. J. Fullbright, "Improved Method of Fuel Element Incremental Mass Measurement," Los Alamos Scientific Laboratory Report LA-4105 (1969).

4. R. Taylor, B. T. Kelly, and K. E. Gilchrist, "The Thermal Conductivity of Fast Neutron Irradiated Graphite," Phys. Chem. Solids 30, 2251 (1969).

5. W. H. Martin and A. M. Price, "Determination of Dose Temperature in Graphite Irradiation Experiments in the Dounreay Fast Reactor," J. Nuclear Energy 21, 359 (1967).

6. G. B. Engle and K. Koyama, "Thermal Conductivity Changes in Nuclear Graphites at High Temperatures and High Fluences," Gulf General Atomic Co. Report Gulf-GA-A12137 (1972).

7. J. M. Davidson, L. O. Gates, and R. E. Nightingale, "Radiation-Damage Effects in Borated Graphite," Nucl. Sci. Eng. 26, 90(1966).

8. J. M. Davidson and L. O. Gates, "Boronated-Graphite Irradiation Studies--Final Report of Irradiation Experiments Conducted in a Hanford Reactor," Battelle-Northwest Report BNWL-96 (1965).

9. R. E. Dahl, "Correlation of Radiation Damage in Boronated Graphite," Battelle-Northwest Report BNWL-199 (1966).

10. L. P. Hunter, "Effect of Fission Recoil Fragments on the Thermal Conductivity of Graphite," J. Appl. Phys. 30, 1969 (1959).

11. J. M. Napier, "NERVA Fuel Element Development Program Summary Report - July 1966 through June 1972: Extrusion Studies," Union Carbide Oak Ridge Y-12 Plant Report Y-1852, Part I (1973).

APPENDIX A

HISTORY OF LASL DEVELOPMENT OF CARBIDE-GRAPHITE COMPOSITE STRUCTURAL MATERIALS; (U,Zr)C-GRAPHITE (COMPOSITE)FUEL ELEMENTS; AND (U,Zr)C FUEL ELEMENTS

I. INTRODUCTION

The need for structural materials that would withstand the Rover reactor core environment better than NbC-coated graphite was recognized early in 1962. Niobium-carbide coated graphite was used as part of the structural support of the core but was subjected to attack by flowing hydrogen gas at temperatures up to 2800 K. The NbC-coated graphite lost mass by the carbon-hydrogen reaction and, at times, experienced considerable erosion. The main difficulties with this material were attributed to the poor adherence of the NbC to the graphite and to the presence of numerous cracks in the coating.

Composites of carbide and graphite were developed to replace NbC-coated graphite and were used as fuel-element tips, support pedestals, support cups, support elements, and peripheral filler elements. Where neutronic considerations were not important, e.g., at the end of the reactor core, composites containing TaC, NbC, or mixtures thereof were used. Zirconium-carbide graphite composites were used at all locations where neutronic considerations were important. The structural composites were coated with a TaC, NbC, or ZrC protective coating of 50 to 100 μm thickness. These coatings, when deposited on the composites, were very adherent and afforded much better protection to hydrogen attack than on graphite.

The success of structural components made from carbide-graphite composites led to the development of both the (U,Zr)C-graphite (composite) and all-carbide types of fuel elements. The main objective was the development of fuel elements which would be highly resistant to hydrogen attack and could be used at high operating temperatures. The composite fuel element retained the geometry of the old graphite element, but the all-carbide fuel element, which consisted of (U,Zr)C substoichiometric in carbon had to be redesigned. The all-carbide element was expected to have excellent resistance to hydrogen attack, but would have low thermal-stress resistance. Achieving a balance among thermal-stress resistance, high-temperature performance, and resistance to hydrogen attack was one of the goals throughout the entire development of structural composites, composite fuel elements, and all-carbide fuel elements. However, in the case of all-carbide elements, it was recognized from the start that its resistance to thermal stress would be s low that cracking and breaking during reactor operation could not be avoided, but it was thought possible to restrict thermal-stress cracking to tolerable levels by changing the geometry to a thinner element with only one coolant channel.

II. CARBIDE-GRAPHITE COMPOSITE STRUCTURAL MATERIALS

In November 1962, Union Carbide Nuclear Corp. (Y-12) made some experimental nozzles for NASA from composite containing carbide and graphite. The nozzles were made by a cold press-sinter technique using graphite filler flour, Varcum binder, and either TaC or NbC carbide powder. The carbide content ranged from 0 to 100%. Samples of these materials were submitted in January 1963 to LASL for possible use in the Rover program.

In late 1963 and all through 1964, small-scale cooperative experiments were conducted by Y-12 and LASL on the usefulness of carbide-graphite composites as fuel-element tips. NbC- and TaC-graphite composites were made by cold press-sintering and extrusion techniques at Y-12 from June 1963 through 1965, whereas during this time LASL was fabricating carbide-graphite composite materials by hot-pressing[A1] and by extrusion[A2] techniques. Also, in early 1964, Illinois Institute of Technology and Research (IITR) began an independent study of the fabrication process and of the properties of hot-pressed carbide-graphite composites. In February 1965, LASL formed a committee to guide the development activities relating to carbide-graphite composites.

During this exploratory work, the advantages of composite materials containing 50 to 80 vol% carbide (e.g., their adequate structural strength at temperatures up to 2800 K, excellent adherence of vapor-deposited carbide protective coatings, and retention of some structural integrity upon loss of carbon due to diffusion through the coating or through coating defects) were recognized for possible use in Rover reactors. Acceptable thermal-stress resistance was obtained in structural applications by adjusting the amount of carbide and by designing the parts so that only low-temperature gradients would arise in either steady state or transient conditions. The first reactor use of these carbide-graphite composite support materials was planned as a LASL experiment in the NERVA program's NRXA-6 reactor in the form of support pedestals, fuel-element tips, and special cups for use with graphite support blocks. Due to reasons not connected with these plans, only the cups were used in the NRXA-6 reactor. The reactor was run on December 15, 1967, and the composite cups performed satisfactorily. Later, complete dependence on composites was initiated for the hot-end support hardware in the Pewee 1 reactor including pedestals, fuel-element tips, support-element tips, and cups. The LASL and WANL designs of these units were slightly different, but in all cases the composite support hardware performed quite well in the December 1968 Pewee 1 test.[A3] Composite support hardware was also fabricated for the Pewee 2 and NF-1 reactors.

III. (U,Zr)C-GRAPHITE (COMPOSITE) FUEL ELEMENTS

The use of uranium carbides as a component of fuel elements for nuclear propulsion reactors was discussed from the very beginning of the Rover program. On May 15, 1956, the fabrication of parts for the first Rover reactor was discussed in a LASL conference. At that time the reactor design had advanced far enough to specify the use of flat plates of graphite as fuel elements. Much of the discussion, however, centered on the problem of incorporating UC_2 into these plates and on the expressed doubt that the UC_2-graphite system might not be satisfactory at temperatures of $\geq$ 2770 K because of the formation of a eutectic melt at 2725 K. The possible use of (U,Zr)C solid-solution carbide as a replacement for UC_2 was therefore also discussed at that meeting. The melting point of 80 wt% ZrC mixed with 20 wt% UC ($\sim$ 10 mol% UC) in the presence of excess carbon was thought to be in excess of 2970 K, and such a material was expected to be better suited for use in graphite elements than UC_2. However, the first fuel elements were made by impregnating graphite plates with a solution of uranyl nitrate and subsequent heat treatment formed UC_2 particles. Solid-solution carbide dispersed throughout the graphite was not used.

The first Rover reactor tests were primarily engineering feasibility tests, and extruded graphite fuel elements containing dispersed UC_2 continued to be used for these early test reactors.

In April 1962 the use of graphite fuel elements containing finely divided UC_2 was discontinued, primarily because of the

problems associated with hydrolysis of the UC_2 with the moisture in air. The fuel elements used thereafter until 1969 in six nuclear propulsion test reactors of the Kiwi, Phoebus, and Pewee design had a graphite matrix containing pyrocarbon-coated UC_2 spheres of $\sim$ 150 μm maximum diameter. Not only did the coated spheres solve the hydrolysis problem, but their use allowed the application of NbC or ZrC coatings, by a chemical vapor-deposition process, to the coolant channels. However, mass losses of carbon from the elements at the end of one hour of component or reactor testing were high enough to cause doubts as to whether graphite elements could be used for longer periods of time. As outlined below, the search for fuel elements that had more resistance to carbon mass losses than graphite elements began in 1965.

From 1964 to 1966, extruded 19-hole hexagonal 50-vol% composite elements were made, both at Y-12 and LASL, by using NbC or TaC carbides. These elements were fabricated primarily as an experiment to evaluate the usefulness of extruded material for fuel-element tips as compared to hot-pressed material. In the course of this evaluation, an attempt was made to run 50-vol%-carbide elements in normal hydrogen corrosion tests. On rampup to full-power conditions of 0.9 MW these elements developed longitudinal cracks terminating in several transverse cracks. The formation of these cracks was interpreted as being due to the relatively low thermal-stress resistance of the composites as compared to that of graphite fuel elements. Exploratory extrusions were made at LASL in the last half of 1965 beginning the development of (U,Zr)C-graphite elements. In 1967, a laboratory component test was perfected which evaluated the thermal-stress resistance[A4] of Rover fuel elements. In August 1967, a program of evaluating the thermal-stress resistance of composite elements as a function of carbide content was started. Early in 1968, the results from the Laboratory thermal-stress study indicated that 20- and 30-vol%-NbC composite elements and the standard graphite elements had comparable thermal-stress resistances. These encouraging results, along with the excellent adherence of protective coatings on composites and the resistance of composites to disastrous corrosion and erosion attack by hydrogen, led to a decision in early 1968 to accelerate the development work on composite elements. The carbide chosen for use in composite fuel elements was (U,Zr)C because of its advantageous neutronic and high-temperature properties. Simultaneously, work was started on the chemical-vapor-deposition techniques of applying ZrC coatings both to the standard graphite and to the (U,Zr)C-graphite elements, and in June 1968, the efforts of the Rover materials program at LASL were concentrated on the development of the (U,Zr)C-graphite fuel elements.

Considerable work[A5-A7] was done by General Electric (Evandale) in 1963-1965 investigating the usefulness of loading graphite Rover elements with (U,Zr)C solid solutions. Most of their work consisted of extrusions starting with (U,Zr)C solid solutions rather than forming the solid solution <u>in situ</u>. Due to oxidation problems during the early stages of fabrication, the mechanical properties of the final elements were relatively poor. In addition, disproportionation of the (U,Zr)C solid solution into UC_2 developed during the final high-temperature heat treatment with subsequent hydrolysis problems due to reaction of the UC_2 with moisture in air. This disproportionation was attributed to the use of 30- to 50-mol% UC in the solid solution. In their final work with (U,Zr)C solid solutions of < 20 mol% UC, General Electric experienced very little disproportionation into UC_2 and very little hydrolysis. In the type of composite elements fabricated at LASL, the concentration of UC in the final solid solution formed was $\lesssim$ 14 mol%.

As mentioned earlier, the Pewee 1 reactor tested in December 1968 contained

experimental composite support materials; however, the fuel elements were of the old graphite type loaded with pyrolytic-carbon-coated UC_2 spheres. The next reactor, Pewee 2, was planned to test new types of fuel elements and many forms of composite support materials. The Pewee 2 reactor was never tested because of funding and environmental-impact difficulties. However, the following list of core components, fabricated and assembled into the Pewee 2 reactor, indicates the number of composite experiments in the reactor.

Number	Description
∿ 175	(U,Zr)C-C, 30-vol% carbide, extruded composite fuel elements.
∿ 225	High-CTE graphite-matrix fuel elements containing coated UC_2 particles from WANL and Y-12.
∿ 100	ZrC-C, 36-vol% carbide, extruded composite support elements.
∿ 25	ZrC-C containing ∿ 300 kg/m^3 TaC, 36-vol% carbide, extruded composite support elements used as neutronic shims.
∿ 127	TaC/NbC-C, 46-vol% carbide, hot-pressed composite pedestal-cup assemblies.
∿ 80	ZrC-C, 30-vol% carbide, extruded filler elements for the core periphery.

All composite materials were fabricated at LASL. The composite fuel, support, and filler elements were coated with ZrC and the pedestal-cup assemblies were coated with TaC. The fabrication and assembly of Pewee 2 was completed by the summer of 1971.

During 1970 the design of a small reactor (NF-1) for use as a materials test vehicle was completed. Forty-seven composite elements, 28 all-carbide elements, and several composite support materials experiments were fabricated for use in this reactor. The NF-1 reactor was tested in the summer of 1972 and the results of this test are a part of this report.

IV. (U,Zr)C, ALL-CARBIDE FUEL ELEMENTS

Throughout 1965 the possibility of using an all-carbide fuel element as a means to reduce and perhaps eliminate carbon mass losses began to be considered seriously. Attempts were made to extrude small single-hole carbide-graphite composites containing large amounts of carbide. In December 1965, tubes of ∿ 7 mm diameter were extruded, using UO_2 and ZrC as starting materials in an attempt to produce an all-carbide fuel element. Throughout 1966 parametric studies were conducted to develop information concerning the effect of starting materials and extrusion conditions on the properties of the elements, i.e., strength, shrinkage during processing, density, etc. At the end of these studies the advantages of retaining ∿ 3 wt% free carbon in the fuel element after the final high-temperature heat treatment became evident. This quantity of carbon aided in the extrusion process, controlled shrinkage and matrix microstructure, prevented sticking of the elements in the graphite fixtures used during heat treatment, and improved the machining characteristics of the elements.

In 1967 and 1968 carbide elements were made by using ZrO_2 and UO_2 rather than ZrC and UO_2 mixtures. The elements made with ZrO_2 had very excellent strength properties and high densities. However, the shrinkage and strength of these extrusions was so unpredictable, depending on the source of the ZrO_2, that this approach was dropped. Elements made from ZrC, UO_2, and small amounts of ZrO_2 were then developed, and their shrinkage and final density properties were reproducible. These elements contained ∿ 3 wt% free carbon, and the carbon and void space occupied ∿ 25 vol% of the matrix gross volume.

In 1969 attempts were started to develop processes to remove the free carbon from the elements and to achieve matrices substoichiometric in carbon. Impregnation of the matrices with zirconium, by using a modification of the techniques developed for chemical vapor deposition of ZrC protective coatings, was started. Eventually a process was developed where a combination of leaching out the free carbon with hydrogen and then impregnating the matrix with zirconium resulted in matrices substoichiometric in carbon.

In June 1970, a series of carbide elements was made by using ^{235}U of 93% enrichment, with uranium loadings from 200 to 1300 kg/m^3. This series of elements was used to detect and identify any fabrication problems as a function of uranium loading. Following this work, ∿ 4000 carbide elements, containing ∿ 3 wt% free carbon, were fabricated in late 1970 for use in neutronic experiments pertaining to reactors of the Pewee design (critical mass of ∿ 40 kg of 93% enriched ^{235}U).

Throughout 1971 and in early 1972 carbide elements were fabricated for use in the NF-1 reactor with results as described in the main body of this report.

REFERENCES

A1. K. V. Davidson, R. E. Riley, and J. M. Taub, "Carbide-Graphite Composites," Los Alamos Scientific Laboratory Report LA-3659-MS (October 1966).

A2. R. E. Riley, N. K. Richerson, and D. H. Schell, "Extruded Carbide-Graphite Composites," Los Alamos Scientific Laboratory Report LA-4077 (1969).

A3. "Pewee 1 Reactor Test Report," Los Alamos Scientific Laboratory Report LA-4217-MS (August 1969).

A4. R. G. Lawton and W. R. Prince, "Rover Graphite Fuel Element Thermal Stress Experiments and Analyses," Los Alamos Scientific Laboratory Report LA-3849-MS (July 1968).

A5. "2nd Annual Report of High Temperature Materials and Reactor Components Development Program," General Electric Co., Evandale, Ohio, Report GEMP-177B, Vol. II, pp. 299-232 (February 1963).

A6. "3rd Annual Report of High Temperature Materials and Reactor Components Development Program," General Electric Co., Evandale, Ohio, Report GEMP-270B, Vol. II, pp. 124-143 (February 1964).

A7. "4th Annual Report of High Temperature Materials and Reactor Components Development Program," General Electric Co., Evandale, Ohio, Report GEMP-334B, Vol. II, pp. 183-189 (February 1965).

APPENDIX B

A COMPREHENSIVE STUDY OF COMPOSITE FUEL ELEMENT MATRICES: THE NF-1 EXPERIMENT

I. INTRODUCTION

Extensive effort was devoted at LASL toward the development of a (U,Zr)C-graphite (composite) matrix, with the goal of producing fuel elements of acceptable thermal stress resistance whose ZrC coatings would remain crack-free even after simulated or actual reactor testing. The general approach was (1) to improve the thermal-stress resistance of elements by heat-treating the matrix to increase the thermal conductivity and to develop a strong interconnected carbide network, and (2) to increase the matrix longitudinal coefficient of thermal expansion (CTE) to at least 7 μm/m·K (293 to 2300 K range) by increasing the volume content (vol%) of carbide and by the use of high-CTE filler flours, both of which should minimize the mismatch between the matrix and the ZrC coating (whose CTE is ∿ 7.7 μm/m·K).

The goal was attained only occasionally because of difficulties in obtaining proper heat-treatment conditions. These difficulties were due to the sensitivity of composite matrix properties to heat-treatment temperature and to difficulties of controlling the temperature of the heat-treatment furnace. Nevertheless, 35-vol% carbide composite matrices were manufactured successfully with a CTE of ∿ 6.8 μm/m·K and with thermal-stress resistances greater than those required for elements in a typical nuclear propulsion reactor of the Pewee and Phoebus designs.

The high-CTE filler flours used in this study [KX-88, JM-15, GL-1076, and POCO (L.F.)] are described in detail; and the effects of the various fabrication steps, particularly of the final heat-treatment, are described in terms of metallography, resistance, density, x-ray diffraction, permeability, and chemical analysis. Properties of the composite matrices -- of importance in reactor use -- are presented and are correlated with fabrication conditions. The microstructure, carbide-cage structure, CTE, thermal conductivity, thermal-shock resistance (ZAP test), and thermal-stress resistance (peak power-density test) of the matrices are discussed.

II. SUMMARY

A. Microstructure

The best microstructure was obtained by heating the composite matrix substantially above the solidus temperature. Although heat-treatment temperatures were not known accurately, it is suspected that 15 to 25% of the carbide in these matrices was in liquid form for at least a short time during final heat-treatment. The microstructure had the following characteristics,as revealed by optical and electron microscopy: (1) the carbide was coarsened and coalesced into a continuous network, with the coalesced carbide having a cross-sectional width ranging from 5 to 20 μm; (2) the large filler-flour particles were reorganized, i.e., polygonized, into blocky domains of graphite and contained angular voids; and (3) interparticle voids were often relatively equiaxed, with scalloped edges generally bounded by Type-I reorganized graphite. -- [A common feature in the microstructures of (U,Zr)C-C (composites) heat-treated to graphitizing temperatures is

the presence of reorganized graphite, three forms of which have been recognized. Type I appears at relatively low graphitizing temperatures, principally at the expense of binder carbon and carbon black, and occurs largely as shells on carbide particles. Type II forms at higher temperatures, involves all the carbon in the matrix of the composite, and appears as large, blocky particles of extremely well-ordered material. It has often been described as proeutectic graphite. A third, polygonal, type develops from an internal reorganization of filler particles and appears as a progressive ordering of the filler-particle structure with no apparent change in size or shape of the particles. Further reorganization results in the formation of Type II graphite.]

B. Carbide Network

The best composite matrix had a strong, interconnected three-dimensional network of coarse carbide. Scanning-electron microscopy of a piece of a fuel element from which all free carbon had been leached with 1-atm hydrogen at ∿ 1800 K revealed the network character of the carbide phase and confirmed the metallographic evidence that the carbide filaments were ∿ 5 to 20 μm in cross section. The 25-mm-long leached piece had its original shape and dimensions, and had a room-temperature axial crushing strength of 11.7 MPa.

C. Coefficient of Thermal Expansion (CTE)

Elements with 35 vol% carbide and medium loadings of 298 to 382 kg/m^3 of 93% ^{235}U, containing any of the high-CTE filler flours, did not have values of CTE above 6.8 μm/m·K after heat-treatment at > 2950 K (near or above the solidus temperatures). The matrices containing the high-CTE fillers had substantially higher values of CTE than matrices containing S-97 filler. For matrices containing high-CTE fillers: (1) the CTE increased with carbide content for comparable heat treatment; (2) the CTE of matrices containing KX-88 filler was insensitive to heat-treatment temperature; (3) the CTE of matrices containing JM-15 filler, and perhaps POCO (L.F.) filler, decreased with increasing heat-treatment temperature; and (4) matrices made with high-CTE filler were more isotropic than matrices made with S-97 filler, with the matrix containing POCO (L.F.) filler being isotropic.

Elements with 35 vol% carbide and high loadings of 725 kg/m^3, containing KX-88, JM-15, or GL-1076 filler, had CTE values of 7.0 to 7.2 μm/m·K when heat-treated at ∿ 2620 K for 6 h or subsequently at ∿ 2770 K for 2 h (versus a solidus temperature of 2820 K). These elements had values of CTE that were higher than those of any 35-vol%-carbide composite element made before. However, the KX-88 matrix, the only one tested to date, had poor thermal-stress resistance reflecting a poor microstructure.

D. Thermal Conductivity

Composite matrices heated to temperature near or above the solidus temperature had room-temperature thermal conductivities ranging from 69 to 87 W/m·K. These data were consistent with values predicted on the basis of Bruggeman's model for variable dispersions, unlike the lower values obtained previously on materials containing S-97 filler that had been heat-treated far below the solidus temperatures. One composite matrix (35 vol% carbide, KX-88 flour, 382 kg/m^3 loading, 3010 K solidus temperature) showed an increase in thermal conductivity from 71 to 87 W/m·K when the nominal final heat-treatment temperature was increased from ∿ 3020 to 3070 K, giving the desired microstructure.

Some fuel-element sections had extremely high room-temperature thermal conductivities. The high values were associated with excessive melting at the surfaces of bores, which occurred in portions of 30-vol% carbide elements in two final heat-treatment runs. Substantial axial movement of the carbide took place in these elements.

This movement can be explained only as due to a lowering of the carbide melting point by impurities in the argon sweep gas. The excessively melted porous region next to each bore near the middle of the element showed the presence of massive carbide and of large blocks of Type-II (proeutectic) graphite. Such material had a room-temperature thermal conductivity of 150 W/m·K. Moreover, relatively nonporous regions from near the ends of the same element, in which highly coalesced carbide and very highly reorganized graphite was present, had thermal conductivities of ∿ 120 W/m·K. This indicates that usable composite matrices can be made with thermal conductivities > 100 W/m·K. The CTE of this excessively melted matrix was approximately the same as that of an unmelted matrix.

The room-temperature thermal conductivity of a composite matrix clearly is determined primarily by the thermal conductivity of the carbon phase. The contribution of the carbide network to the conductivity would be expected to be substantially less than the ∿ 25 W/m·K for dense ZrC. The degree of reorganization or polygonization of the filler flour that occurs during heat-treatment at temperatures near and above the solidus temperature of the composite matrix clearly is the important factor because the carbon blacks and the binder residue have earlier been converted to Type-I graphite. The reorganized graphite in the composite element, if fully dense, should have a room-temperature conductivity > 100 W/m·K.

E. Thermal Shock Resistance

Elements that showed excessive melting near the middle of their length showed spectacularly high thermal-shock resistance at that location in most cases. There were indications, however, that the high thermal-shock resistance may have been due to microstructural effects as well as to the exceptionally high thermal conductivity (i.e., 150 W/m·K for one matrix).

The general trend was that 30-vol%-carbide materials were more resistant to thermal shock than 35-vol%-carbide materials. No correlation with flour type was found. Within a given extrusion lot of elements that had medium loadings and did not show excessive melting, thermal-shock test results were essentially independent of final heat-treatment temperature. Thus, for these elements, thermal conductivity did not appear to affect the thermal-shock test results. For elements with high uranium loading, thermal shock resistance increased with final heat-treatment temperature.

F. Thermal Stress Resistance (Peak Power Density Test)

The test results obtained on uncoated fuel elements demonstrated that 35-vol%-carbide composite matrices with thermal-stress resistances greater than those required for elements in a nuclear propulsion reactor can be made by using high-CTE KX-88 or JM-15 filler flour. The best of the KX-88, 35-vol%-carbide elements were almost as resistant to thermal stress as the best 30-vol%-carbide matrix made previously with S-97 filler and were comparable to the GL-1074, 30-vol%-carbide WANL element tested. The KX-88, 35-vol%-carbide elements showed increasing thermal-stress resistance that correlated well with the degree to which the desired microstructure was approached and to which the thermal conductivity increased. Several KX-88, 30-vol-%-carbide elements showed very good thermal-stress resistance, i.e., could not be broken before the test was terminated due to carbon leaching, even though they were not heat-treated to the desired microstructure.

G. Heat-Treatment Conditions

A summary of properties of composite elements as influenced by a slight change in heat-treatment conditions is given in Fig. B1. A change of ∿ 50 K in heat-treatment temperature increased the thermal conductivity by ∿ 20% and the thermal-stress resistance by ∿ 30%.

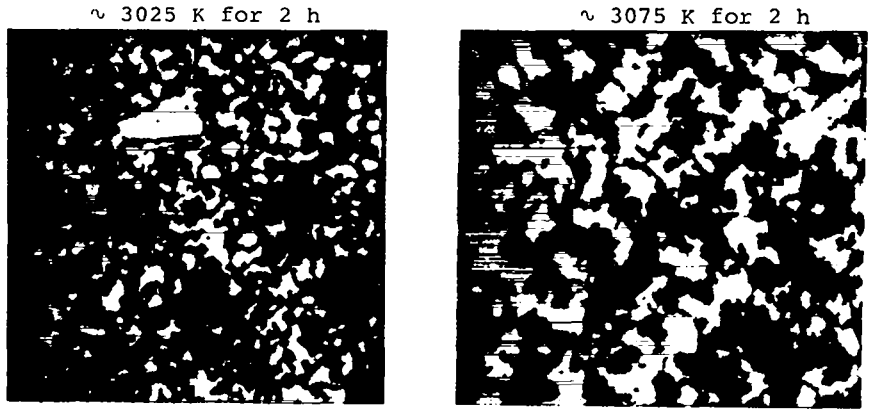

(a)

|← 100 μm →|

Thermal Conductivity	71	87 W/m.K
Thermal Expansion (293-2300 K)	6.6	6.8 μm/m·K
Power to Fracture	4400-5300	5800-6600 MW/m³
Compressive Strength	∿ 110	∿ 110 MPa

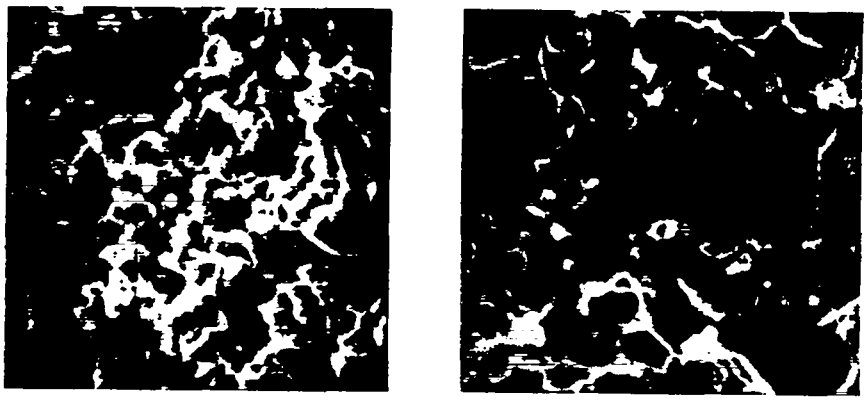

(b)

|←——— 100 μm ———→|

Compressive Strength	5.5	11.7 MPa
Thermal Expansion (293-2300 K)	--	7.6 μm/m·K

Fig. B1. Effect of heat-treatment temperature on selected properties of a composite element. Material: 35-vol% (U,Zr)C at 382 kg U/m³ loading; KX-88 graphite flour; solidus, ∿ 3010 K. (a) microstructure; (b) carbide structure, carbon leached out.

III. COMPOSITE MATRIX PREPARATION

A. Introduction

The goal of the LASL composite fuel-element development program was to produce elements of acceptable thermal-stress resistance whose ZrC coatings will remain crack-free even after electrical corrosion or reactor testing.

A fuel-element matrix with high thermal conductivity will have, under reactor operating conditions, lower temperature gradients in the matrix and thus lower thermal stresses than a matrix with a low thermal conductivity. A strong three-dimensional interconnected network of carbide may be effective in hindering matrix crack propagation, may provide high mechanical strength and, very importantly, may leave a persistent structure should the matrix become subject to hydrogen attack through coating failure or element breakage in a reactor. The smallest attainable CTE mismatch between the matrix and the ZrC coating was desired, to minimize crack formation in the coating and defect corrosion during element use.

Elements were submitted to improved heat-treatment in a vertical coating furnace modified for use up to 3100 K. Attempts were made to increase the CTE of the matrix by using high-expansion fillers and by increasing the carbide content to 35 vol%, the maximum carbide content assumed tolerable from thermal-stress considerations.

The NF-1 composite fuel-element experiment applied these methods toward improving the composite matrix. Some parameters of the experiment are shown in Table BI, namely, four types of filler flour, 30 and 35 vol% carbide content, and medium and high uranium loading. Some elements from this experiment were fabricated to provide improved coated elements for use as elements in the NF-1 reactor.

Composite elements with very desirable properties had been made previously at LASL, i.e., elements made from S-97 flour with 30 vol% carbide and 500 kg/m^3 loading. These elements gave good results in corrosion testing and in thermal-stress testing. Portions of the elements that gave good results in thermal-stress testing had a coarse matrix carbide structure, an unusually high degree of reorganization of the large filler-flour particles, and a thermal conductivity of 76 W/m·K. The three-dimensional interconnected character of the carbide structure from these elements had been demonstrated by scanning-electron-microscope (SEM) examination of pieces from which all the carbon had been leached with flowing hydrogen at 1 atm and 1870 K for more than 300 h. The axial crushing strength of the 25-mm-long leached piece was ∿ 8.6 MPa. The highly reorganized larger filler-flour particles in these elements resembled, in some respects, proeutectic graphite found in composite samples known to have been heated to temperatures above the solidus temperatures. This overall type of carbide and filler-flour microstructure was taken as the target structure (see Fig. B2), and heat-treatment to temperatures above the solidus temperature was presumed to be necessary to attain this target structure.

TABLE BI

DESCRIPTION OF COMPOSITE ELEMENTS IN NF-1 EXPERIMENT

Graphite Filler Flour	Carbide Content, vol%	U Loading, kg/m^3	Extrusion Lot No.	Units in NF-1
KX-88	30	435	52	-
		435	65	-
		324	61	-
	35	382	62	4
		308	50	3
		298	60	1
JM-15	30	424	51	3
	35	308	53	2
KX-88/ JM-15[a]	35	339	56	2
GL-1076	30	382	58	3
POCO (L.F)[b]	30	435	63	-
KX-88	35	725	54	-
JM-15	35	725	55	-
GL-1076	35	725	59	-
GL-1074 (WANL)[c]	30	440	8	5

[a] 50/50 mixture of flours.

[b] Filler flour fired at 1270 K.

[c] Fabricated by Westinghouse Astronuclear Laboratory (WANL).

The overall fabrication and evaluation sequence for composite fuel elements is shown in Fig. B3. The nondestructive tests (NDT) and the evaluation tests conducted were: PERM, permeability of matrix to gas flow; IPDE, resistance of matrix as measured by an incremental potential drop examination; MULE, mass-per-unit length examination by gamma-ray absorptometry; EC (I and E), internal and external eddy current examination of matrix for flaws; GAMMA count examination for nondestructive assay of ^{235}U; RAD, x-ray radiography examination for matrix flaws; HREC, high-resolution eddy current examination for cracks in ZrC

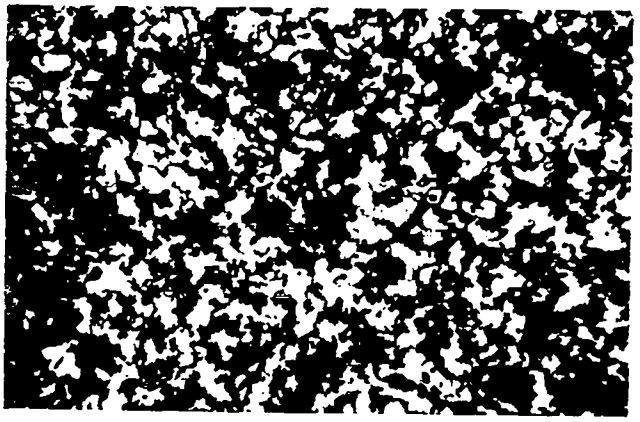

100 μ

TARGET STRUCTURE

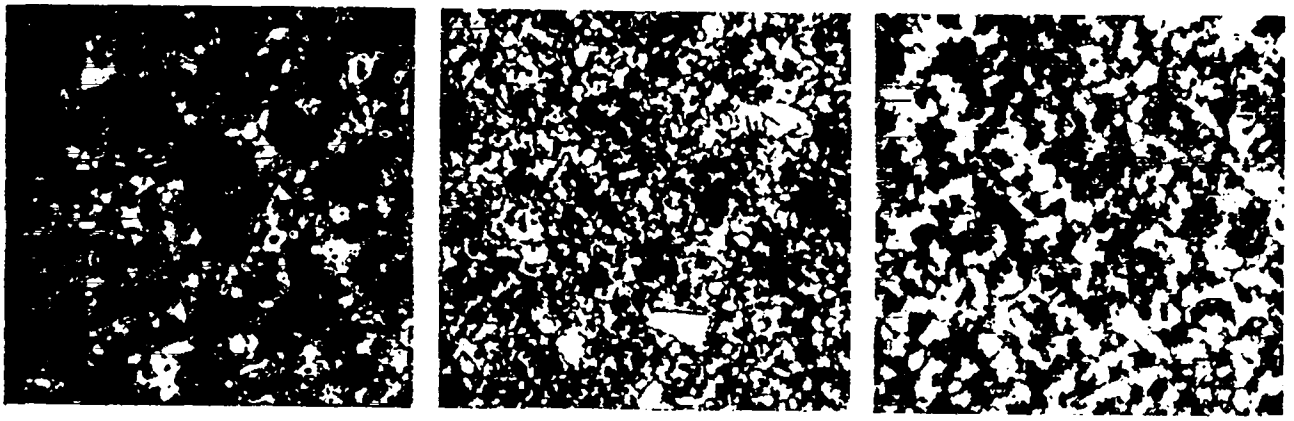

LOW-FIRE 2650 K

HIGH-FIRE 3025 K

HIGH-FIRE 3075 K

ELEMENTS FROM LOT 62 (KX-88, 35 vol%, 382 kg U/cm^3) (STATION 28)

Fig. B2. Microstructure of composite elements as a function of heat-treatment temperature. The gray areas are graphite, the white areas are carbide, and the black areas are void.

coatings; HOLE LOC., examination of a wafer for location of coolant channels; MET, metallographic examination of matrix and coating microstructure; CHEMISTRY, analysis for elemental composition; X-RAY DIFF., x-ray diffraction for composition of (U,Zr)C phase; LEACH, remove carbon from a sample by reaction with hot hydrogen and study carbide network; CTE, coefficient-of-thermal-expansion determination; ZAP, thermal-shock test; THERMAL STRESS, determination of electrical power density required to produce matrix fracture; PHYSICAL PROP., determination of mechanical and thermal properties; and HOT GAS TEST, evaluation of resistance of coated element to reaction with flowing hot hydrogen gas.

The elements were made by an extrusion process from a mixture of powdered ingredients and a thermosetting binder. During the Low-Fire heat-treatment at temperatures up to 2600 K, solid-solution (U,Zr)C carbide was formed in situ. The final High-Fire heat-treatment at temperatures of 2800 to 3100 K produced the structural changes in both the carbide and graphite phases.

B. Materials and Extrusion

The ZrC powder used in the manufacture of fuel elements was reactor-grade (< 200 ppm Hf) and had a Fisher average particle size of 3.5 μm. A typical analysis was 88.3% zirconium and 11.5% total carbon,

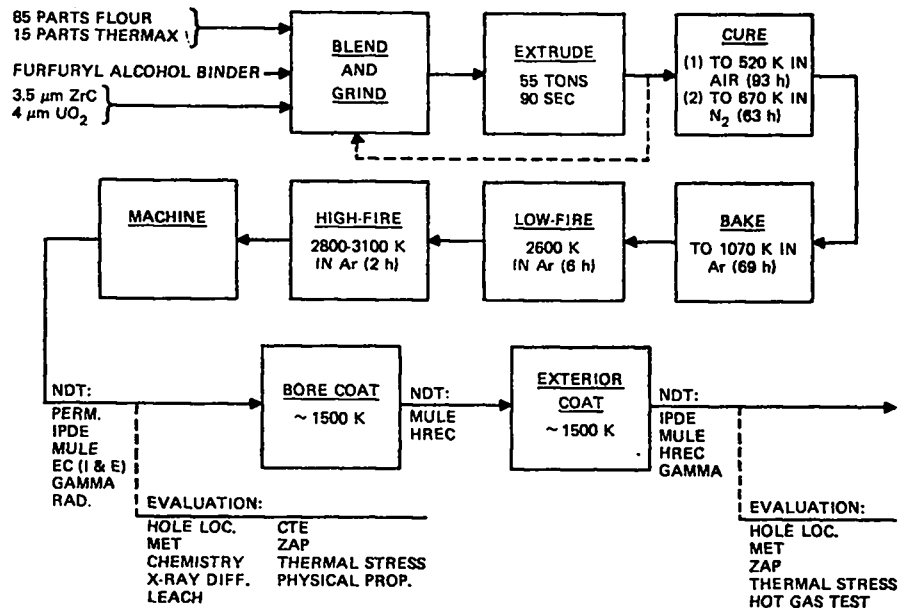

Fig. B3. Preparation and evaluation of composite fuel elements.

∿ 0.2% of which was free carbon. Impurities included 0.2% N_2, 0.2% O_2, and 90 ppm of sulfur. Metallic impurities were low, the major ones being 200 ppm of titanium, 150 ppm of tantalum, and 100 ppm of iron. The carbide particles were of high density and relatively equiaxed.

The enriched UO_2 powder used in the fuel-element extrusion mix was produced at LASL. The powder was -325 mesh and had a Fisher average particle size of ∿ 5 μm. The particles were dense and discrete. Total metallic impurities were limited to 500 ppm with a maximum of 1 ppm of boron and 0.5 ppm of cadmium.

The graphite filler flours used in this program had a particle-size distribution, as determined by sieve analysis, of 2% +200 mesh, 8% -200 +270 mesh, 20% -270 +325 mesh, and 70% -325 mesh. The flours contained ∿ 100 ppm of ash and had a Fisher average particle size of 4.75 μm.

The filler flours used in the NF-1 experiment are to be contrasted with S-97 graphite flour, which was a filler material that had been previously used extensively at LASL to fabricate the first composite elements. The S-97 flour consists of dense, relatively acicular particles which, upon etching, show highly developed lamellar structures and large, elongated, optical domains. Because of their shapes, these particles tend to assume a definite preferred orientation during extrusion, yielding anisotropic graphites which, in the extrusion direction, have low CTE and low electrical resistivity. In general, the thermal conductivity of graphites is inversely proportional to electrical resistivity.

The POCO (L.F.) filler after heating to high temperature consists of particles which, upon suitable etching, were shown to be made up of very fine, nearly equiaxed, randomly oriented optical domains, within each of which the lamellar graphite structure is well developed. Because of the sizes and shapes of these domains, grinding the material to normal particle-size distributions produces principally blocky particles, each of which contains enough randomly oriented domains so that it is essentially isotropic. This randomness also results in high CTE and high electrical resistivity. Typically, therefore, a graphite made from a POCO filler is nearly isotropic and has high CTE

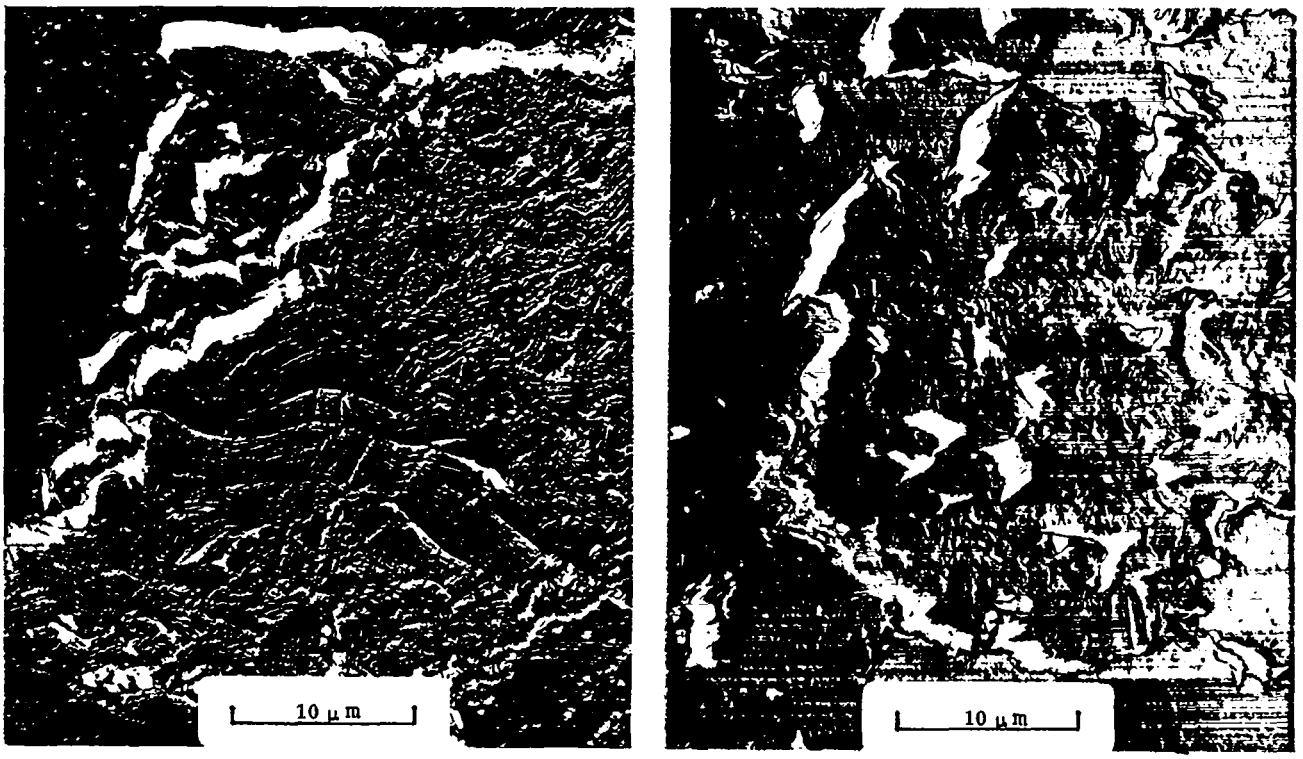

KX-88 POCO

Fig. B4. Electron micrographs of graphite filler flours: KX-88 flour graphitized during fabrication by vendor and POCO (Low-Fire) after heating to 2870 K during fuel-element manufacture.

and high electrical resistivity. POCO fillers also contain a distinctive pattern of fine, quite uniformly distributed voids, which distinguish it from otherwise similar fillers such as Robinson filler.* Figure B4 shows an electron micrograph of a POCO flour particle that had been heated to ∿ 2870 K. One particle is shown in the field of view. Note the fine, nearly equiaxed, randomly oriented optical domains, within which the lamellar graphite structure is well developed.

The KX-88 and JM-15 fillers are very much alike, and would be expected to produce very similar graphites. Both consist principally of quite dense, nearly equiaxed particles which, when etched, are shown to be made of small, elongated optical domains in a variety of sizes and with some order in their arrangements. However, both also contain a significant proportion of acicular particles having highly ordered internal structures, which would be expected to orient during extrusion and result in some degree of anisotropy in the finished graphite. Because they contain particles resembling the POCO filler and also particles resembling the S-97 filler, the KX-88 and JM-15 flours would be expected to produce graphite CTEs and resistivities intermediate between those of matrices made from POCO and S-97 flours. Both flours (KX-88 and JM-15) had desirable particle-size distributions and would be expected to yield

*Robinson filler is made from an experimental airblown coke which was produced by Union Carbide Corp. in a pilot-scale operation. After grinding, the coke consists of dense, blocky particles with extremely fine, random internal structures with an exceptionally high CTE. The Robinson fillers used at LASL have in general been secondary graphite flours, produced by grinding graphites made from Robinson coke and a pitch binder. These fillers contain graphitized binder carbon as well as graphitized coke filler, but have a CTE approaching that of the graphitized coke itself.

dense graphites with good mechanical properties. An electron micrograph of a KX-88 particle is shown in Fig. B4. A relatively large optical domain is shown in the lower portion of the micrograph, whereas the upper-right area contains many small randomly oriented domains. The KX-88 particle was heated during manufacture to a high temperature and shows the structure at the start of the composite fuel-element fabrication process.

GL-1076 filler consists generally of equiaxed particles containing two types of internal structure, one of which is porous and resembles a POCO filler while the other is dense and resembles the Robinson filler. The particle-size distribution of the GL-1076 tends to be bimodal, with many relatively large particles and many very small ones, but few in the intermediate size ranges. Unless an addition (e.g., of carbide) is made of particles which happen to fill this particle-size gap, the GL-1076 filler would be expected to yield a graphite of rather low density with correspondingly low mechanical properties. As is usually true, the very fine particles tend to be somewhat acicular and ordered in internal structure. A graphite matrix made from GL-1076 would therefore be expected to approach the properties of one made from a POCO filler. Thermax carbon black, from Thermatomic Carbon Co., was used because it acted as an extrusion lubricant and aided in increasing the carbon density of the fuel elements. Varcum 8251 thermosetting resin, from Varcum Chemical Div. of Reichhold Chemicals, Inc., was used as the binder. Varcum is a partially polymerized furfuryl alcohol with a room-temperature viscosity of $\sim$ 300 cP. Maleic anhydride was used to catalyze the polymerization (4 g of catalyst to 100 cm^3 of binder).

Calculational procedures were established which allowed a specific volume percent total carbide and uranium loading to be obtained in the finished fuel element. A typical extrusion mixture consisted of: 26.26 wt% graphite flour plus Thermax mixture, 51.62 wt% ZrC powder, 7.46 wt% UO_2 powder, and 14.67 wt% Varcum binder. The weight ratio of graphite flour vs Thermax in the mixture was usually 85:15. Figures B5 and B6 show the extrusion dies used and the air-vein fixture that received the extruded element.

The first of a series of heat treatments required 93 h to reach 520 K (electrically heated circulating-air ovens were used), during which the furfuryl alcohol underwent polymerization. The second heat treatment, using a N_2 atmosphere, required 63 h to heat the elements from 470 to 720 K. The third heat treatment (called the baking cycle) consisted of heating to 1100 K during a 39-h cycle at a pressure of 10 Torr or less using an argon flush.

C. Baked Elements

Differences among the various filler flours show up strikingly in the electrical resistances of baked composite elements, as indicated in Table BII. In the baked condition there is no interconnected carbide network and the resistances of the elements are high, with resistance of the filler-flour particles and binder residue apparently playing the major role in determining the electrical properties of the continuous carbon matrix. These resistance differences have largely disappeared after the elements have been low-fired at $\sim$ 2620 K for $\sim$ 6 h, with only the POCO elements apparently showing slightly higher resistances. However, a portion of this difference may be due to fine matrix cracks that can be seen metallographically in the low-fired POCO elements. These data indicate that in low-fired elements, in which the filler-flour particles are unchanged, the electrical conduction must be mainly through a connected carbide network and through Type-I graphite that is next to the carbide particles. The resistance differences have disappeared

TABLE BII

ELECTRICAL RESISTANCE OF COMPOSITE ELEMENTS AT STATION 635

Graphite Filler Flour	Carbide Content, vol%	U Loading, kg/m	Resistance, Ω/m Baked 1100K	Low-Fired 2620K	High-Fired 3020K
KX-88 & JM-15	30 and 35	298-424	∿0.085	0.020	0.014
GL-1076	35	725	0.15	0.018	---
POCO (L.F.)	30	435	0.20	0.027	0.016

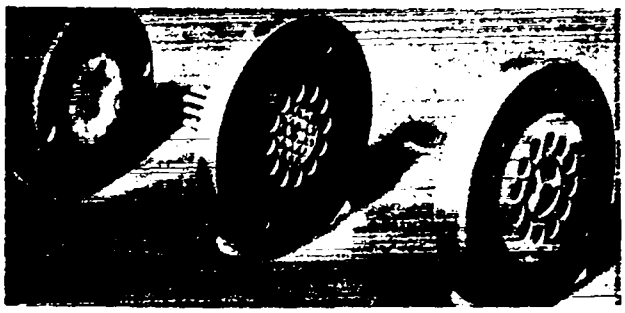

Fig. B5. Extrusion tooling for 19-hole hexagonal (U,Zr)C-graphite (composite) fuel elements.

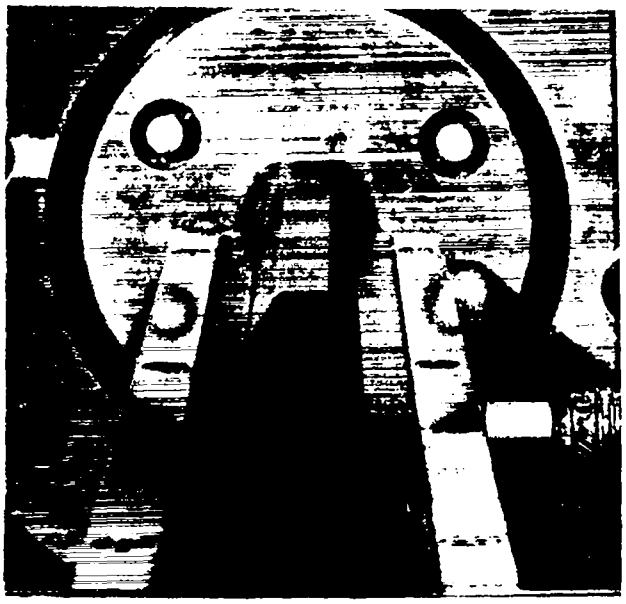

Fig. B6. Extrusion of 19-hole (U,Zr)C-graphite(composite) fuel element onto air-vein fixture.

completely after the elements have been high-fired at 3020 K for 2 h, even for the badly cracked POCO elements. This similarity in resistance may be attributed to coalescence of the interconnected carbide network and possibly to reorganization of the small, but not the large, filler-flour particles. The room-temperature resistivity of stoichiometric ZrC is 20 to 50 x 10^{-6} Ω cm; of polycrystalline fabricated graphite, 500 to 1000 x 10^{-6} Ω cm; and of single-crystalline graphite in the basal plane direction, ∿ 50 x 10^{-6} Ω cm.

D. Low-Fired Elements

Figure B7 shows photomicrographs of matrices from four low-fired elements with medium loadings that were evaluated primarily because of interest in comparing their thermal expansion properties with those of corresponding high-fired elements. The white areas are carbide, the gray areas are graphite, and the black areas are void. The elements containing KX-88 or JM-15 filler flours showed most clearly that the flour particles were surrounded, but not penetrated, by carbide at this stage. Optical and electron microscopy revealed the presence of some Type-I graphite on the surfaces of carbide particles. This type of graphite presumably results from ejection of carbon when UC_2 from carburization of UO_2 reacts with ZrC to form (U,Zr)C solid-solution, as well as from graphitization of carbon black and binder residue in the presence of carbide.

Table BIII gives x-ray diffraction data for low-fired elements with loadings ranging from 0.056 to 0.137 uranium atom

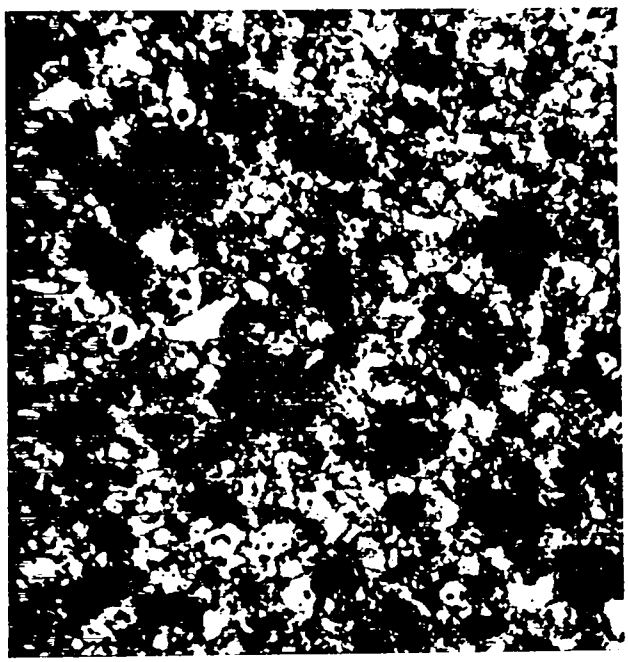

Lot 50 (KX-88, 35 vol%, 308 kg U/m^3)
Low-fire Run 7

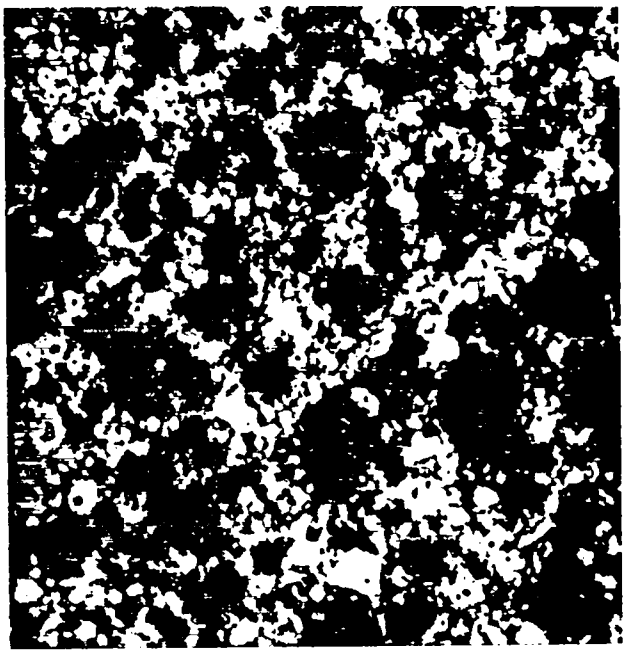

Lot 53 (JM-15, 35 vol%, 308 kg U/m^3)
Low-fire Run 11

100 μm

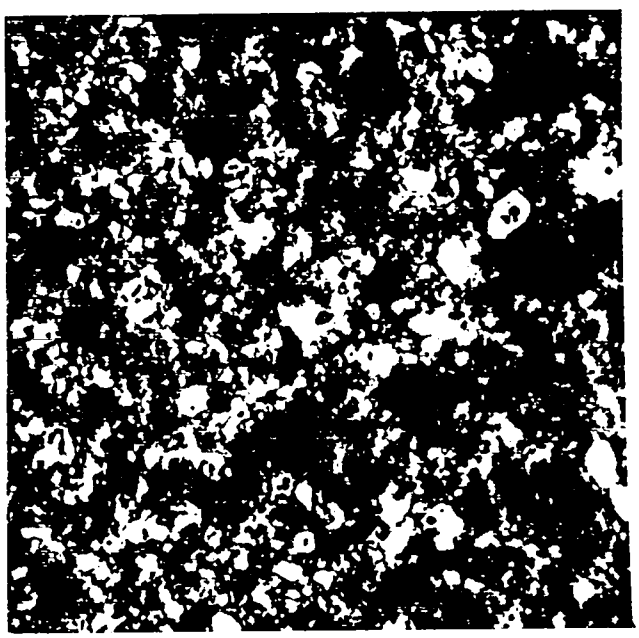

Lot 62 (KX-88, 35 vol%, 382 kg U/m^3)
Low-fire Run 7

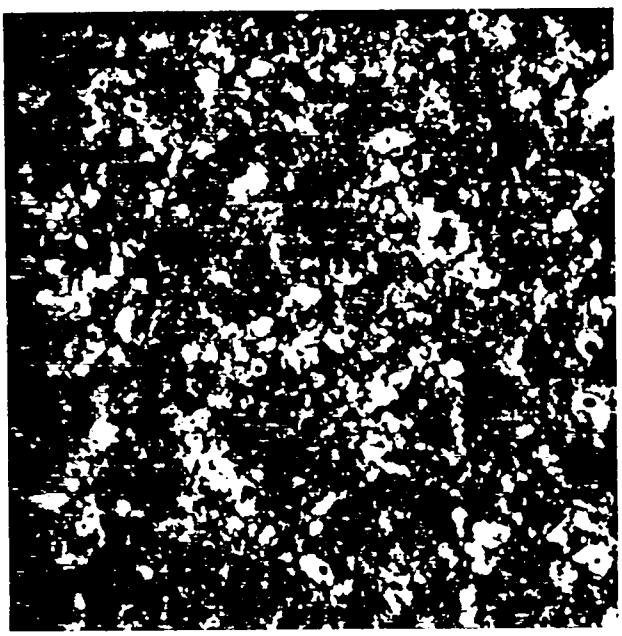

Lot 63 (POCO-L.F., 30 vol%, 435 kg U/m^3)
Low-fire Run 7

Fig. B7. Photomicrographs of low-fired elements (∿ 2620 K for 6 h), sampled at Station 710.

TABLE BIII

X-RAY DIFFRACTION DATA ON LOW-FIRED ELEMENTS FROM NF-1 EXPERIMENT[a]

Low-Fire No.	Element Lot	Load No.	Filler Flour	Carbide Content, vol%	Atom Ratio U/(Zr+U) by Chem.[c]	Lattice Parameter (a_o), Å[b]	Calculated Composition	Comments[e]
7	50-	308-93452	KX-88	35	0.057	4.7303(14)[d]	$U_{0.112}Zr_{0.888}C$	Major phase
						4.7153(2)	$U_{0.059}Zr_{0.941}C$	Minor phase - somewhat diffuse
11	53-	308-93514	JM-15	35	0.056	4.7162(7)	$U_{0.062}Zr_{0.938}C$	Major phase
						4.6952(6)	ZrC	Minor phase
7	62-	382-93701	KX-88	35	0.070	4.7182(2)	$U_{0.069}Zr_{0.931}C$	Single phase - well resolved high angle doublets
7	63-	435-93728	POCO (L.F.)	30	0.093	4.7257(4)	$U_{0.096}Zr_{0.904}C$	Single phase - doublets slightly diffuse
8	54-	725-93529	KX-88	35	0.137	4.7369(3)	$U_{0.135}Zr_{0.865}C$	Single phase - doublets well resolved
8	55-	725-93572	JM-15	35	0.137	4.7363(2)	$U_{0.133}Zr_{0.867}C$	Single phase - doublets well resolved
8	59-	725-93631	GL-1076	35	0.137	4.7361(2)	$U_{0.133}Zr_{0.867}C$	Single phase - sharp, well resolved doublets

[a] Room temperature data.

[b] X-ray diffraction sample taken from Station 635.

[c] Calculated from chemistry data in Table BVII for machined, high-fired elements.

[d] Standard deviation for last place.

[e] If doublets are diffuse, there may be a gradation in composition.

ratio, metal basis. All the elements with uranium atom ratios from 0.07 to 0.137 had single-phase solid solution present and the doublets were sharp and well resolved, indicating that there was little gradation in solid-solution composition. These results suggest that a heat-treatment for 6 h at ∿ 2620 K was sufficient to bring about the homogenization for these loadings. However, the x-ray diffraction data for the two elements with the lower uranium atom ratio of ∿ 0.056 indicated that homogenization had not occurred. Perhaps a slightly higher temperature of heat-treatment is required for homogenization of the lower loadings.

The IPDE (incremental potential drop evaluation) plots of electrical resistance versus station were almost invariably quite flat for the low-fired elements. This indicates that the fabrication process to this stage probably has produced elements of relatively uniform properties along the full length of the element.

E. High-Fired Elements

1. General

A pseudobinary phase diagram for 35-vol%-carbide composite based on recent LASL data is shown in Fig. 3 of the main body of this report. The atom-percent uranium value on a metal basis is shown above the diagram. For a given carbide content, the solidus temperature (temperature at which liquid first appears on heating) drops sharply with uranium loading. The solidus temperature increases with increasing carbide content for a given uranium

loading. Gaseous impurities in the heat-treatment-furnace sweep gases, such as oxygen or water, can lower the effective solidus temperature. For the elements used in the NF-1 experiment, solidus temperatures ranged from 2820 to 3040 K.

Elements that had been previously low-fired at ∿ 2620 K for ∿ 6 h were high-fired for 2 h at temperatures designed to be above the solidus temperatures of the elements in the high-fire batch, in attempts to form the coarse interconnected carbide network and the reorganized large filler-flour particles of the target structure. Obtaining the desired structure in elements in a given run proved to be very difficult, because of the sensitivity of the process to temperature, uncertainties in temperature measurement, and difficulties in controlling temperatures in the furnace as a function of time and position of the elements in the furnace. Nevertheless, some very definitive correlations between matrix structures and properties were obtained.

High-firing and low-firing of the elements was done in a vertical coating furnace modified for this purpose. The graphite fixture to hold the elements was a 30-cm-o.d. by 13-cm-i.d. by 1.57-m long cylindrical annulus with an outer ring of 18 holes and an offset inner ring of 18 holes. The fixture was heated by an inductively heated graphite susceptor. Three banks of induction coils that can be controlled independently were used to control axial uniformity of temperature. The elements were loaded in the fixture so that the G-end* was up. The elements were swept from top to bottom with high-purity argon that flows through the fixture independently of the argon used to flush the furnace shell. The fixture was maintained at a positive pressure relative to the furnace shell. The furnace has five sight ports (SP) in line on the side, through which the outside surface of the susceptor can be observed at positions that correspond from top to bottom to the following stations relative to the final element: -114 (SP2), 254 (SP3), 622 (SP4), 911 (SP5), and 1359 (SP6). The furnace was calibrated periodically by comparing temperatures observed through the sight ports with temperatures measured (through a viewing port in the furnace lid) on stepped graphite elements placed in four adjacent holes in the fixture. The calibration elements were placed at the back of the fixture, opposite the sight ports, i.e., at the hottest part. The calibration steps were arranged to be at levels corresponding to the sight ports.

The calibration data for each sight port were best correlated by the expression $T_a = A + BT_o$, where T_a is the true temperature within the fixture and T_o is the observed temperature through the sight port. Based on several calibration runs, the 2-σ variation of T_a corresponding to T_o was $\pm$ 60 K for SP2; $\pm$ 50 K for SP3; and $\pm$ 40 K each for SPs 4, 5, and 6. These uncertainties in temperature were too large to guarantee that the target structure would be obtained in each high-fire run.

Following high-firing, the flats of all elements were machined to dimension, and the machined elements were subjected to nondestructive testing (NDT) as outlined in Fig. B3. Then two elements from each extrusion lot in a given high-fire batch were selected to be cut up into a variety of evaluation samples.

Seven high-fire runs were made for the NF-1 experiment. The runs are described in Table BIV, which gives solidus temperatures for the elements as well as the maximum temperature (T_a) reported for each sight port in each run. The temperature control during a given high-fire run did not ensure that all stations of the fuel-element fixture reached the maximum temperature at the same time,

*The G-end of an element refers to low station numbers while the H-end refers to high station numbers.

TABLE BIV

TEMPERATURE DATA FOR HIGH-FIRE RUNS OF THE NF-1 EXPERIMENT

High-Fire No.	Lot No.	Filler Flour	Carbide Content, Vol%	U, Loading, kg/m^3	Solidus Temp, K	Reported Maximum Temp. (T_a), K SP 2 -114 mm	SP 3 254 mm	SP 4 622 mm	SP 5 991 mm	SP 6 1359 mm[a]
1	51	JM-15	30	424	2960	2910	2980	3020	3020	3040
	53	JM-15	35	308	3035					
	56	KX-88/JM-15	35	339	3025					
	58	GL-1076	30	382	2990					
2	50	KX-88	35	308	3035	2950	3030	3075	3045	3070
	60	KX-88	35	298	3040					
	62	KX-88	35	382	3005					
3	52	KX-88	30	435	2955	3020	3075	3025	3020	3015
	61	KX-88	30	343	3005					
4	62	KX-88	35	382	3005	2975	3025	3025	3020	3015
	63	POCO(L.F.)	30	435	2955					
5	51	JM-15	30	424	2960	3010	3070	3040	3030	3020
	52	KX-88	30	435	2955					
	58	GL-1076	30	382	2990					
	63	POCO(L.F.)	30	435	2955					
6	65	KX-88	30	435	2955	2950	2920	2965	----	2945
	66	KX-88	30	343	3005					
7	54	KX-88	35	725	2820	2695	2820	2790	2745	2795
	55	JM-15	35	725	2820					
	59	GL-1076	35	725	2820					

[a] SP = sight port; positions are relative to final 1320-mm-long element.

and the time at maximum temperature varied. Runs 3 and 5 resulted in excessive melting around the bores in portions of all elements.

2. Metallography

Metallographic examination of microstructures reveals the effects of heat-treatment. Microstructure changes that occur on heat-treatment at temperatures just below the solidus show coalescence of the carbide cross section (3 to 10 μm) and formation of Type-I graphite close to the carbide surfaces. At temperatures substantially above the solidus where perhaps 15 to 25% of the carbide is liquid, the carbide is coalesced into areas of 10 to 20 μm cross section, the smaller filler particles are approaching a Type-II graphite structure, and the larger filler particles are only slightly changed. However, at yet higher heat-treatment temperatures, massive carbide particles are found and all the graphite is in the form of large blocks of Type-II graphite.

Figures B8 and B9 show photomicrographs of metallographic sections from an element of one of the lots in each of four runs that did not result in excessive melting.

In High-Fire Run 1 the coarseness of the carbide increased toward the higher stations (H-end), which is consistent with the reported maximum temperatures. This is illustrated in Fig. B8 by an element from Lot 51. However, the coarseness of carbide of the target structure, shown in Fig. B2, was not attained and there was little, if any, reorganization of the large filler-flour particles at the H-end, despite the fact that Lot 51 had the lowest solidus temperature of the lots in High-Fire Run 1. The microstructures of the other lots in High-Fire Run 1 were little, if any, different from those of the Lot 51 elements.

Metallography of the Lot-62 elements from High-Fire Run 2 (see Fig. B8) indicated attainment of the target structure at all

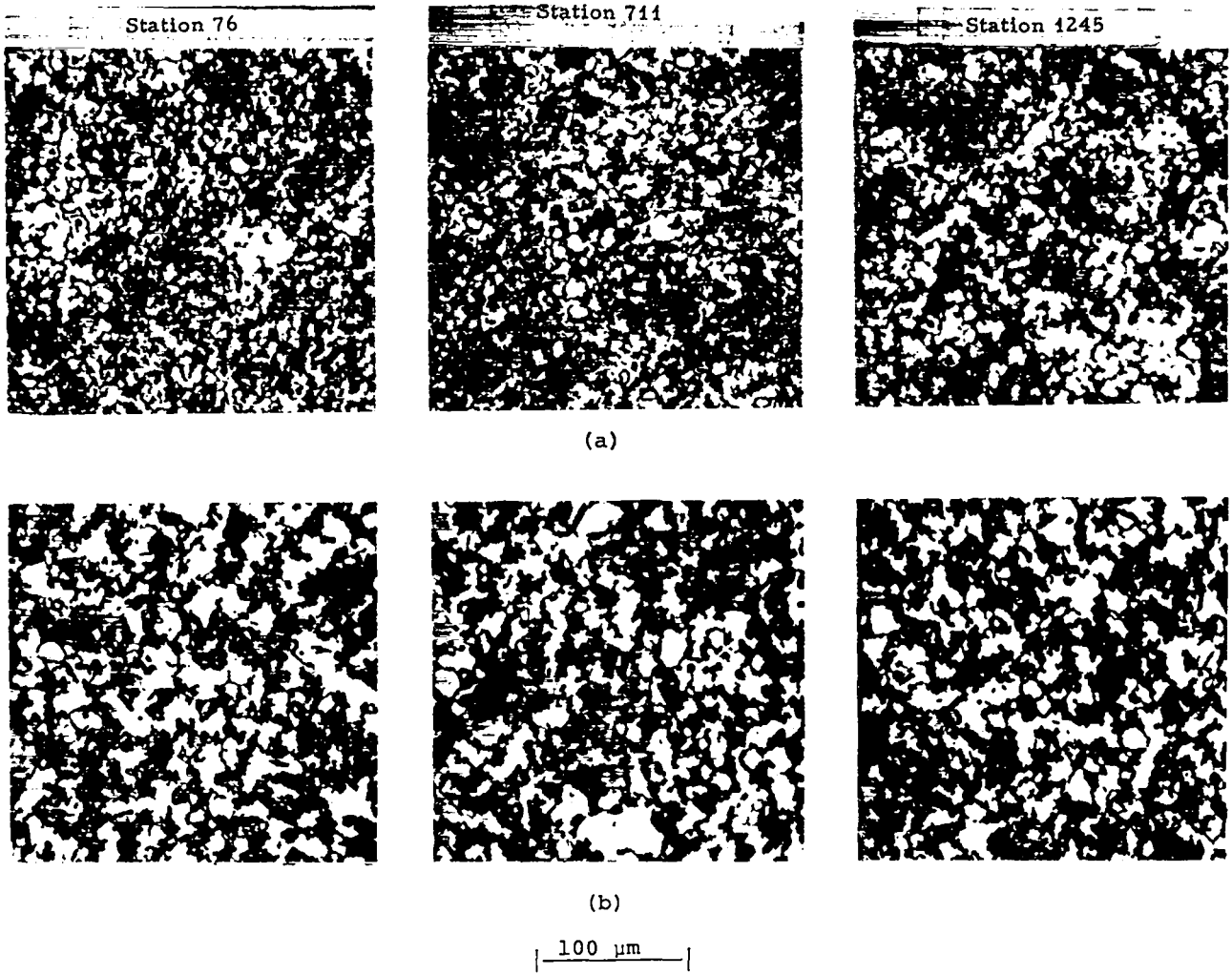

Fig. B8. Photomicrographs of high-fired elements. (a) Lot 51 (JM-15, 30 vol%, 424 kg U/m^3) from High-Fire Run 1; (b) Lot 62 (KX-88, 35 vol%, 382 kg U/m^3) from High-Fire Run 2.

stations. Variations of the extent of carbide consolidation and the degree of flour reorganization along the length of the element were small, but the MULE data as well as optical and electron microscopy showed that the first several inches of the G-end had been slightly cooler, and electron microscopy showed that the H-end had been the hottest. Lots 50 and 60 from the same high-fire run also had the target structure.

High-Fire Run 4 was conducted conservatively because excessive melting had been found in High-Fire Run 3. Metallography for an element from Lot 62 (Fig. B9) showed that the G-end was hotter than the H-end, but that the target structure was not attained at any station. Lot 63 from the same run, not shown in Fig. B9, did not attain the target structure at any station either, despite its lower solidus temperature.

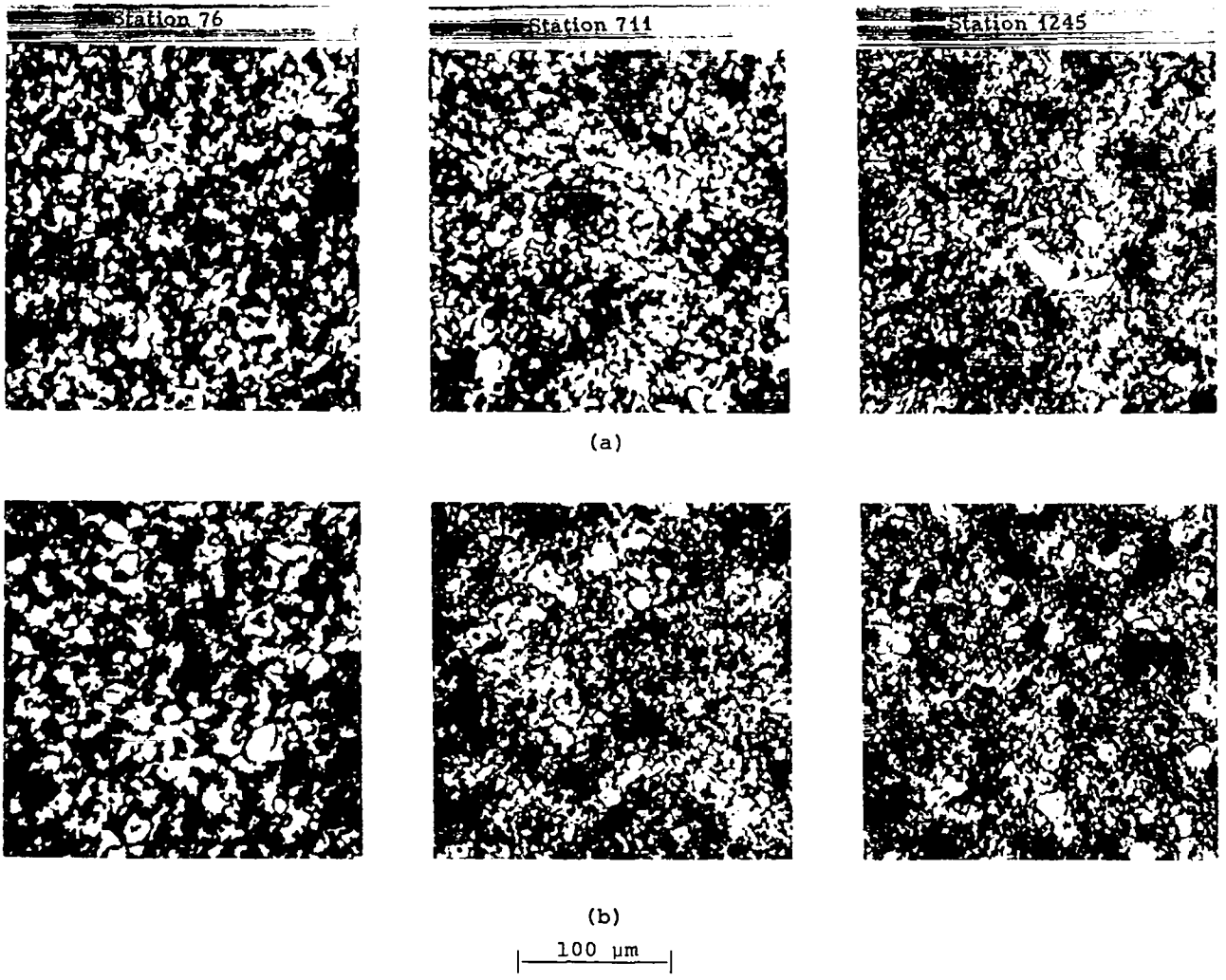

Fig. B9. Photomicrographs of high-fired elements. (a) Lot 62 (KX-88, 35 vol%, 382 kg U/m^3) from High-Fire Run 4; (b) Lot 65 (KX-88, 30 vol%, 435 kg U/m^3) from High-Fire Run 6.

High-Fire Run 6 was also conducted conservatively because excessive melting had been found in High-Fire Run 5. Metallography for an element from Lot 65 (Fig. B9) shows that the G-end was substantially hotter than the H-end. The target structure was attained only in the first few inches at the G-end.

Figures B10 and B11 show photomicrographs of a Lot-52 element that underwent excessive melting in High-Fire Run 5. At Station 76 (Fig. B10) there was evidence of excessive melting at the bore surface that resulted in formation of Type-II graphite (proeutectic graphite, i.e., graphite precipitated from a melt). The web consisted

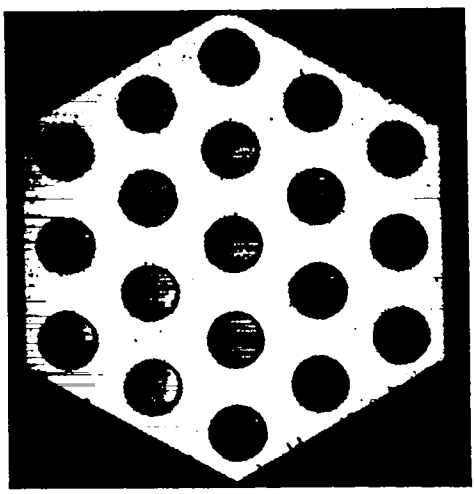

Complete cross section

10 mm

Web around center hole (upper right)

100 μm

Bore surface around center hole

100 μm

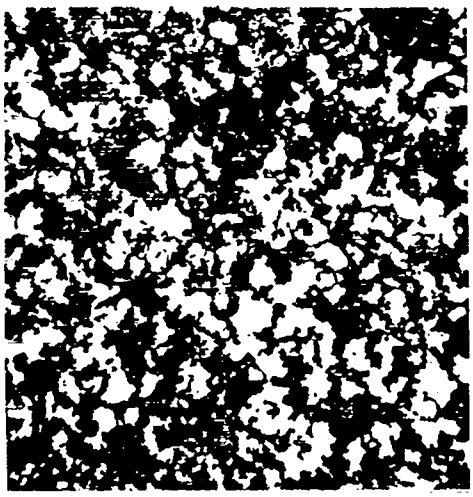

Interior of matrix around center hole

100 μm

Fig. B10. Photomicrographs of Lot 52 element(KX-88, 30 vol%, 435 kg/m^3) from High-Fire Run 5. Sample was from Station 76.

mainly of highly coarsened carbide and extensively reorganized large filler-flour particles. At Station 711 (Fig. B11) excessive melting extended almost 0.64 mm into the matrix around each hole, with the results that two-thirds of the ∿ 1.78-mm web between adjacent holes showed excessive melting. The excessively melted region contained large blocks of Type-II graphite and massively coarsened carbide, and was very porous. This region around each hole was highly symmetrical over the entire cross section of the element. The interior of the matrix contained coarsened carbide and highly reorganized large filler-flour particles. Metallography of the same element at Station 1245 showed microstructures essentially identical to those of Station 76. Chemical analysis of pieces of Lot-52 elements from High-Fire Run 3 that showed corresponding microstructures at corresponding axial stations indicated very little residual oxygen and nitrogen as follows: 270-ppm oxygen and 320-ppm nitrogen at Station 1; 140 ppm

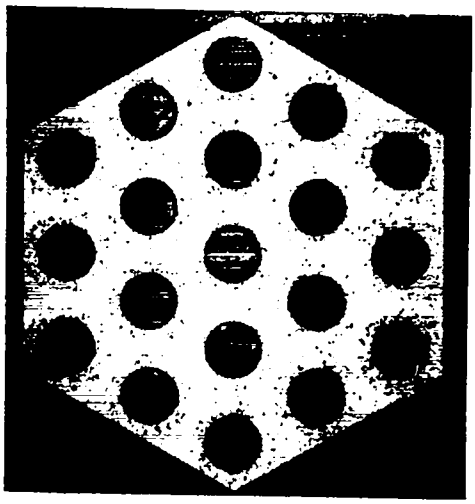

Complete cross section

10 mm

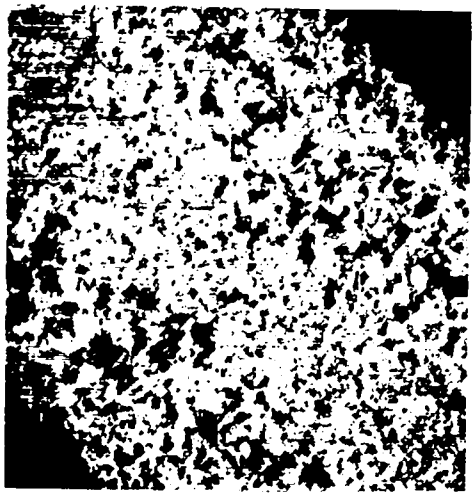

Web around center hole (upper right)

100 μm

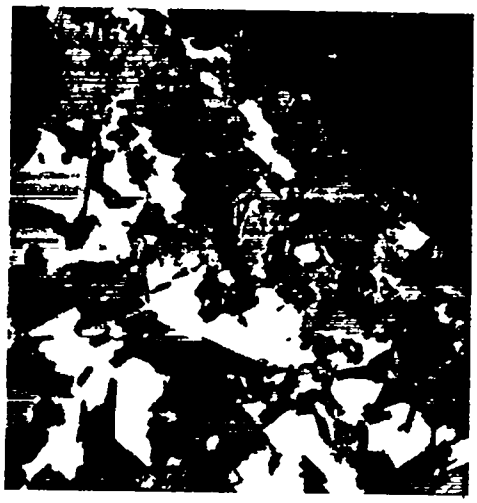

Bore surface around center hole

100 μm

Interior of matrix around center hole

100 μm

Fig. B11. Photomicrographs of Lot 52 element (KX-88, 30 vol%, 435 kg/m^3) from High-Fire Run 5. Sample was from Station 711.

oxygen and 280 ppm nitrogen at Station 23; and 240 ppm oxygen and 640 ppm nitrogen at Station 51.--A mechanism for the formation of the microstructure shown in Fig. B11 will be suggested after the MULE data have been presented.

Figure B12 shows photomicrographs for an element from Lot 54 both in the low-fired state, and after High-Fire Run 7. The microstructures of the low-fired pieces appear to be the same for all stations. The microstructures of the pieces from High-Fire Run 7 indicate that the G-end of the element was hottest, with coarsening of the carbide and substantial amounts of carbide in the interior of the large filler-flour particles. However, the microstructures of the high-fired pieces from Stations 711 and 1245 have essentially the same appearance as low-fired pieces from the same stations, indicating lower temperatures than at the

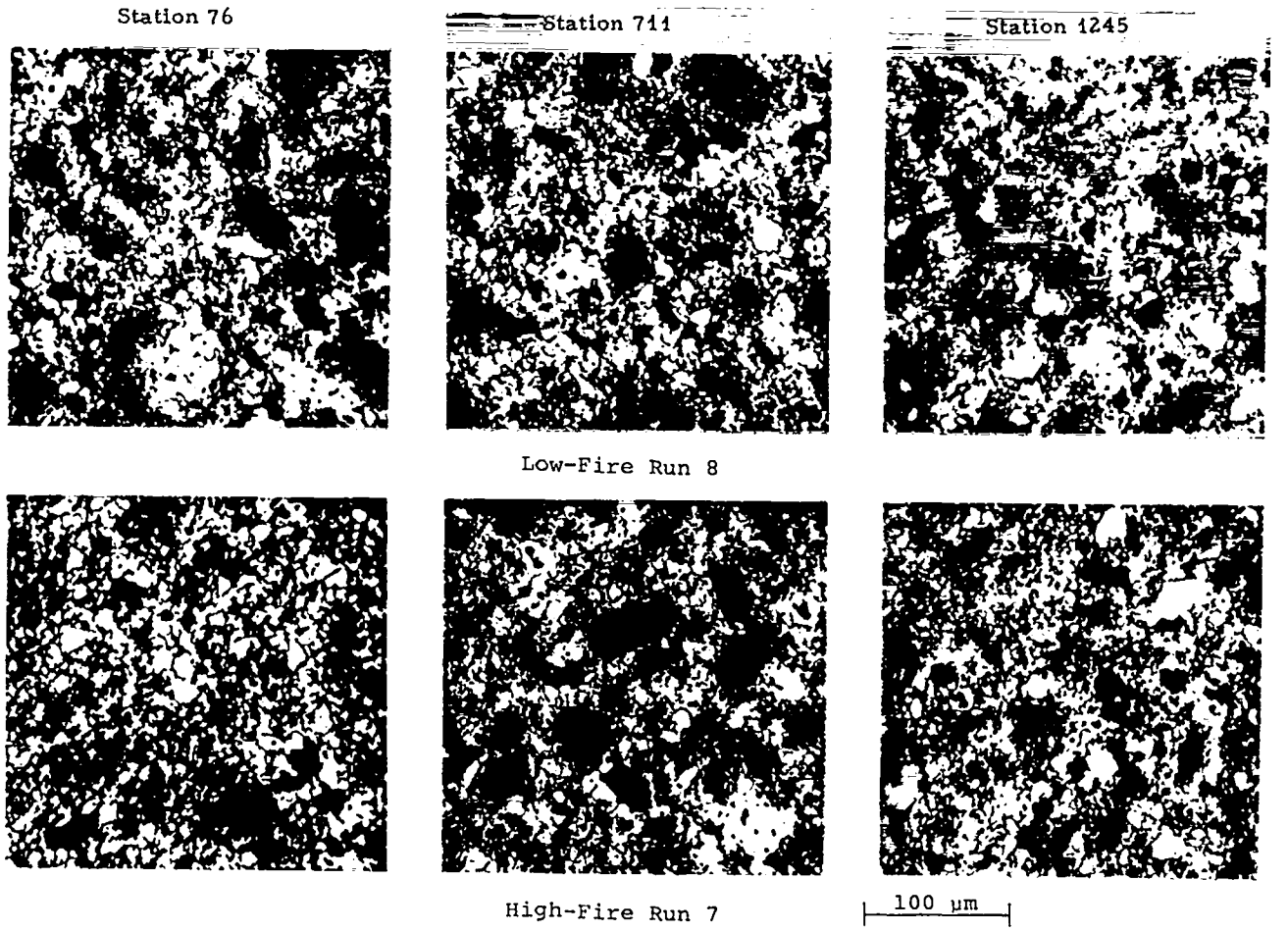

Fig. B12. Photomicrographs of Lot 54 elements (KX-88, 35 vol%, 725 kg/m^3)

G-end of the element. The IPDE data indicate the same trend of temperature along the elements from High-Fire Run 7. The resistances were 0.017 Ω/m at Station 76 and ∿ 0.019 Ω/m at Stations 711 and 1245. The characteristics of elements from High-Fire Run 7 are important for interpreting the CTE data for these elements.

3. IPDE Data

In general, resistance data for machined, high-fired elements that did not show excessive melting were consistent with metallographic observations. The resistance of the matrix decreased along the length of an element as the extent of coalescence of the carbide in the matrix increased. For these types of elements, the resistance data showed up the cold spots in the fixture adjacent to the line-of-sight ports and gave subtle indications that the elements in the outer ring of the fixture were slightly hotter than the elements in the inner ring. On the other hand, the resistance data for elements that had undergone excessive melting did not vary as much as the microstructure and the MULE data for such elements.

For elements that did not show excessive melting there appeared to be a sharp drop in resistance as the target structure was approached, i.e., when the solidus temperature was substantially exceeded. Previous LASL work indicates that the resistance of composite elements decreases linearly with increasing temperature from ∿ 2570 K to near the solidus temperature.

4. MULE Data

MULE plots have been used for some time as a sensitive indicator of the uniformity of fabrication of fuel elements, not only from element to element, but also along the length of a given element. After final heat-treatment of an element, the elements are machined to uniform external dimensions. MULE data collected on the machined elements are a measure of the density fluctuations in the elements. Interpretation of the MULE data in conjunction with metallographic and IPDE data has led to a detailed understanding of the fabrication variables that affect the properties of composite matrices. The following generalizations are used in the interpretations: (1) in elements in which no portion of the element has been heated above the solidus, MULE peaks occur in regions of higher temperature because these regions undergo more shrinkage (densification) than those in colder regions; and (2) in elements heated to temperatures considerably above the solidus the liquid carbide present moves to regions of lower temperature, resulting in MULE peaks in the colder regions and MULE valleys in the hotter regions.

5. X-ray Diffraction

X-ray diffraction investigations of the (U,Zr)C carbide in composite elements was of some help in interpreting the final heat-treatment temperatures and cooldown rates. In general, phases present in less than ∿ 5% quantities were not detected. Composite material heated above the solidus temperature will show (U,Zr)C solid solution of uniform composition if cooled slowly enough to reach equilibrium or may show solid solution of variable composition if cooled too rapidly to reach equilibrium. In the latter case, a solid-solution composition lower and higher than the nominal composition would be expected. (See Fig. 3, the pseudobinary phase diagram, in the main body of the report.) Some x-ray diffraction results were anomalous relative to the above discussion.

The x-ray diffraction data, Table BV, for the four elements in High-Fire Run 1 showed that the elements with the lower uranium atom ratios (solidus temperature, ∿ 3030 K) were single-phase while the two with higher uranium atom ratios (solidus temperature, ∿ 2970 K) had solid solutions of two different chemical compositions. The reported heat-treatment temperature was 3020 K. The elements with the lower uranium atom ratio had (U,Zr)C of only one chemical composition. The elements probably did not contain liquid carbide during heat-treatment and the cooling rate did not affect the solid-solution composition. However, the two elements with the higher uranium atom ratios probably contained liquid carbide during heat-treatment. On cooldown, equilibrium was not reached, and solid solutions of two different compositions were found by x-ray diffraction to be present at room temperature.

This type of explanation does not readily account for the presence of solid solutions of two different compositions in the elements from High-Fire Runs 4 and 5. All elements in High-Fire Run 2 were heat-treated at temperatures above the solidus and, on cooling, formed a solid solution essentially of one composition. The elements in High-Fire Run 7 were heated to a temperature below the solidus and they, too, contained solid solution of only one composition. Attempts to explain some of these results on the basis of different cooling rates that might be dependent upon location of the elements in the heat-treating fixture have not cleared up these apparent anomalies in the x-ray diffraction data.

6. Permeability

Table BVI presents the permeability data for machined, high-fired composite elements. GL-1076 filler flour gave a substantially less permeable matrix than did either KX-88 or JM-15, for all loadings. In High-Fire Run 7, GL-1076 gave the least permeable elements, JM-15 gave the most

TABLE BV

X-RAY DIFFRACTION DATA ON HIGH-FIRED ELEMENTS FROM THE NF-1 EXPERIMENT[a]

High-Fire No.	Element Lot Load No.	Filler Flour	Carbide Content, vol%	Atom Ratio U/(Zr+U) by Chem.	Lattice[b] Parameter (a_o), Å	Calculated Composition	Comments[d]
1	51- 424-93463	JM-15	30	0.091	4.7275(3)[c]	$U_{0.102}Zr_{0.898}C$	Major phase - doublets diffuse
					4.7150(3)	$U_{0.059}Zr_{0.941}C$	Minor phase
	53- 308-93520	JM-15	35	0.056	4.7138(5)	$U_{0.054}Zr_{0.946}C$	Single phase - doublets very broad but resolvable
	56- 339-93584	KX-88/ JM-15	35	0.061	4.7161(5)	$U_{0.062}Zr_{0.938}C$	Single phase - doublets diffuse and broad
	58- 382-93612	GL-1076	30	0.082	4.7247(2)	$U_{0.092}Zr_{0.908}C$	Major phase - doublets diffuse
					4.7108(4)	$U_{0.043}Zr_{0.957}C$	Minor phase
2	50- 308-93430	KX-88	35	0.057	4.7152(2)	$U_{0.059}Zr_{0.941}C$	Single phase - doublets resolved but diffuse
	60- 298-93640	KX-88	35	0.056	4.7151(4)	$U_{0.059}Zr_{0.941}C$	Single phase - doublets resolved but broad
	62- 382-93668	KX-88	35	0.070	4.7188(3)	$U_{0.071}Zr_{0.929}C$	Single phase - doublets a little broad
4	62- 382-93687	KX-88	35	0.070	4.7210(9)	$U_{0.079}Zr_{0.921}C$	Major phase[e]
					4.7185(8)	$U_{0.070}Zr_{0.930}C$	Minor phase[e]
	63- 435-93725	POCO (L.F.)	30	0.093	4.7287(9)	$U_{0.106}Zr_{0.894}C$	Major phase[e]
					4.7096(1)	$U_{0.039}Zr_{0.961}C$	Minor phase[e]
5	51- 424-93456	JM-15	30	∿ 0.091	4.7251(8)	$U_{0.093}Zr_{0.907}C$	Single phase - doublets resolvable but diffuse
	52- 435-93486	KX-88	30	---	4.7267(10)	$U_{0.099}Zr_{0.901}C$	Single phase - doublets resolvable but diffuse
	58- 382-93621	GL-1076	30	∿ 0.082	4.7216(12)	$U_{0.081}Zr_{0.919}C$	Single phase - but diffuse
	63- 435-93702	POCO (L.F.)	30	∿ 0.093	4.7398(2)	$U_{0.144}Zr_{0.856}C$	Major phase - diffuse
					4.7021(4)	$U_{0.012}Zr_{0.988}C$	Minor phase
6	65- 435-93782	KX-88	30	0.094	4.720(1)	$U_{0.076}Zr_{0.924}C$	Major phase - doublets diffuse
					4.7263(6)	$U_{0.098}Zr_{0.902}C$	Minor phase - doublets diffuse
7	54- 725-93557	KX-88	35	0.137	4.7376(4)	$U_{0.138}Zr_{0.862}C$	Single phase - doublets are resolved
	55- 725-93577	JM-15	35	0.137	4.7372(2)	$U_{0.138}Zr_{0.864}C$	Single phase - doublets are resolved
	59- 725-93637	GL-1076	35	0.137	4.7372(3)	$U_{0.136}Zr_{0.864}C$	Single phase - doublets are resolved

[a] Room temperature data.

[b] X-ray diffraction sample taken from Station 635.

[c] Standard deviation in parentheses of last place.

[d] If doublets are diffuse, there may be a gradation in composition.

[e] High angle lines broad and diffuse, doublets not resolved.

TABLE BVI

PERMEABILITY OF MACHINED, HIGH-FIRED ELEMENTS OF THE NF-1 EXPERIMENT

High-Fire No.	Lot No.	Filler Flour	Carbide Content, vol%	U, Loading, kg/m^3	Elements Measured	Permeability, m^3/s of air[a] Range	Average
1	51	JM-15	30	424	9	200-530 x 10^{-8}	300 x 10^{-8}
	53	JM-15	35	308	10	53-200	123
	56[d]	KX-88/JM-15	35	339	8	183-432	274
	58	GL-1076	30	382	8	36- 50	42
2	50[d]	KX-88	35	308	17	10- 70	33
	60	KX-88	35	298	7	42- 96	65
	62[d]	KX-88	35	382	12	10- 46	28
3	52	KX-88	30	435	17	10-7600	NA[b]
	61	KX-88	30	343	14	8- 40	20
4	62[d]	KX-88	35	382	7	216-365	304
	63	POCO(L.F.)	30	435	10	730-1230[c]	1020
5	51	JM-15	30	424	3	12000-16000	NA
	52	KX-88	30	435	7	1600-12000	NA
	58	GL-1076	30	382	5	365-1600	NA
	63	POCO(L.F.)	30	435	7	500-8300	NA
6	65	KX-88	30	435	17	330-813	455
	66	KX-88	30	343	14	450-580	495
7	54[e]	KX-88	35	725	18	2300-3100	2600
	55[e]	JM-15	35	725	6	3100-3800	3400
	59[e]	GL-1076	35	725	7	960-1400	1200

[a] Whole element permeability using 0.07-MPa differential air pressure.

[b] NA = not applicable because of excessive melting of portions of the matrix.

[c] The Lot 63 elements had fine matrix cracks.

[d] One element from each of Lots 50, 56, and 62 had permeability measured in the machined, low-fired condition. Permeability data were:

Lot No.	Low-Fire No.	Permeability, m^3/s of air
50	7	580
56	7	730
62	4	330

[e] Five elements from each of Lots 54, 55, and 59 were machined in the low-fired condition for coating. There were no abnormal permeability values. Permeability data were:

Lot No.	Low-Fire No.	Average Permeability, m^3/s of air
54	8	2100
55	9	2100
59	8	870

TABLE BVII

CHEMISTRY DATA FOR MACHINED, HIGH-FIRED ELEMENTS OF NF-1 EXPERIMENT[a]

Lot No.	Serial Number	Carbide Content, vol% Nominal	Carbide Content, vol% Actual	Nominal U Loading, kg/m³	Gross Density, Mg/m³	Zr Wt%	Zr Mg/m³	U Wt%	U kg/m³	C Wt%	C Mg/m³	Ta ppm
50	93430	35	35.2	308	3.561	53.9	1.92	8.43	300.2	37.5	1.34	130
51	93463	30	30.2	424	3.360	47.0	1.58	12.11	406.9	40.8	1.37	90
53	93520	35	35.2	308	3.564	54.0	1.92	8.21	292.6	37.6	1.34	150
54	93557	35	36.2	725	3.723	47.9	1.78	19.64	731.0	32.1	1.195	70
55	93577	35	36.3	725	3.754	47.7	1.79	19.48	731.0	32.6	1.224	60
56	93584	35	35.1	339	3.568	53.4	1.91	8.96	319.7	37.4	1.33	170
58	93612	30	30.1	382	3.351	47.5	1.59	10.90	365.3	41.5	1.39	130
59	93637	35	36.7	725	3.768	48.0	1.81	19.61	739.0	32.3	1.217	35
60	93640	35	34.6	298	3.518	53.8	1.89	8.22	289.2	37.5	1.32	100
62	93668[b]	35	35.1	382	3.561	52.9	1.88	10.20	363.2	36.7	1.31	100
62	93687[b]	35	35.0	382	3.557	52.8	1.88	10.31	366.7	36.9	1.31	90
63	93725	30	30.3	435	3.342	47.3	1.58	12.43	415.4	40.3	1.35	50
65	93782	30	30.1	435	3.362	46.6	1.56	12.50	420.0	40.5	1.362	55

[a]All samples taken from Station 1245.

[b]Element 93668 from High-Fire Run 2, maximum temp. 3075 K.
Element 93687 from High-Fire Run 4, maximum temp. 3025 K.

permeable elements, and KX-88 was in between. Note (see Footnote e of Table BVI) that machined elements of all lots were more permeable after High-Fire Run 7 than after the preceding low firing. Consolidation of the matrix of Lot 62 in High-Fire Run 2 led to much lower permeability values than were obtained in High-Fire Run 4 or in low firing (see Footnote d for the latter). The same was true for Lot 50 after High-Fire Run 2 relative to the low-fired condition (see Footnote d). The elements that showed excessive melting in High-Fire Runs 3 and 5 had either highly variable or consistently high permeability, depending on the lot.

7. Chemistry

The results of chemical analyses are given in Table BVII. In general, the intended carbide content was attained fairly closely. The actual uranium loadings were somewhat lower than the nominal (intended) loadings for all lots with medium loadings, whereas they were slightly higher for all lots with high loadings. Such variations are to be expected in initial work with new flours. The loading deviations did not change the expected solidus temperatures by more than ∿ 10 K, and the preceding discussions involving solidus temperatures based on nominal loadings are therefore still valid.

IV. MATRIX PROPERTIES

A. Microstructure

The matrix target structure is compared in Fig. B2 with that of Lot-62 elements that had been heated at various temperatures. The elements heated at ∿ 3070 K in High-Fire Run 2 attained the target structure, whereas the elements heated at ∿ 3020 K in High-Fire Run 4 did not. Metallographic examination of polished sections and electron microscopic examination of two-stage replicas of these sections revealed striking differences in the matrices resulting from these two high-fire runs. A Lot-62 element heated at ∿ 3020 K in

High-Fire Run 4 showed the following features at Station 25, 355, 735, and 1170: (a) no carbon-black particles or traces of binder residue were found; (b) Type-I reorganized graphite surrounded much of the carbide; (c) the carbide was coalesced but some small carbide particles were present; (d) original KX-88 filler was present, and small carbide particles that did not appear to be connected to the main body of coalesced carbide were found within the filler particles; and (e) voids generally had Type-I reorganized graphite at their peripheries. A Lot-62 element heated at ∿ 3070 K in High-Fire Run 2 showed the following features at Stations 25, 355, 735, and 1170: (a) no carbon-black particles or traces of binder residue were found; (b) Type-I reorganized graphite was present adjacent to some carbides at all stations, whereas some blocky Type-II reorganized graphite may have been present at Station 1170; (c) the carbide was well coalesced, to the greatest extent at Station 1170; (d) none of the structure of the small random domains of KX-88 filler was found, the reorganized filler became more blocky as the station increased, small carbide particles that did not appear to be connected to the main body of coalesced carbide were within the reorganized filler, and blocky reorganized filler contained angular voids; and (e) voids, excluding the above-mentioned angular ones, had scalloped edges and were generally bounded by Type-I graphite for specimens up to Station 735, but many of the voids at Station 1170 were very angular and had straighter edges than the voids at lower stations. Microscopy of the latter element illustrates the variations in the microstructure that can be seen in an element having the target structure.

B. Carbide Network Structure

A piece of a Lot-62 element heated at ∿ 3020 K in High-Fire Run 4 and a piece of another Lot-62 element heated at ∿ 3070 K in High-Fire Run 2 (elements from the lot for which metallography is shown in Fig. B2) were leached in 1-atm H_2 for 240 h at ∿ 1800 K. Comparison of mass losses with chemistry data for the starting material showed that 99% of the free carbon was leached from both pieces. The leached pieces did not change their shape or dimensions as a result of the leaching. Figure B2 shows scanning-electron-microscope (SEM) pictures of the residual interconnected network of carbide (carbide cage structure). Heating the matrix to a nominally 50-K higher temperature drastically increased the coarseness of the carbide particles in the network and doubled the room-temperature axial crushing strength of the carbide cage structure, from 5.5 to 11.7 MPa.

C. Coefficient of Thermal Expansion

Table BVIII lists CTE data for composite elements with medium loadings and, below the broken line, with high loadings.

For medium loadings the following conclusions can be drawn from the CTE data:

- The coefficients of thermal expansion of matrices from the NF-1 experiment were substantially higher than those of matrices containing S-97 filler flour.
- The CTE increased with carbide content for comparable heat-treatment.
- The CTE of a matrix containing KX-88 filler flour appears to be insensitive to heat-treatment temperature (see Lots 50 and 62).
- The CTE of a matrix containing JM-15 filler flour, and perhaps POCO (L.F.) filler flour, was sensitive to heat-treatment temperature.
- The CTE of matrices from the NF-1 experiment were more isotropic than the CTE of matrices containing S-97 filler flour, with the matrix containing POCO (L.F.) filler flour being virtually isotropic.
- Most important, coefficients in the longitudinal orientation above 6.8 μm/m·K

TABLE BVIII

COEFFICIENT OF THERMAL EXPANSION OF UNCOATED COMPOSITE ELEMENTS FROM THE NF-1 EXPERIMENT

Filler Flour	Carbide Content, vol%	Element Lot Load No.	Heat-Treatment Temp., K	CTE (293-2300 K), μm/m·K Long.	Trans.	CTE Ratio Trans./Long.
S-97	30	100-500 load	2970	6.1	6.8	1.10
KX-88	30	65-435-93782	2945	6.5	6.8	1.04
	35	60-298-93640	3050	6.6	6.9	1.03
		50-308-93452	2635	6.7	6.9	1.03
		50-308-93430	3050	6.7	6.9	1.03
		62 382-93701	2635	6.8	7.2	1.05
		62-382-93687	3025	6.6	6.9	1.05
		62-382-93668	3050	6.8	7.0	1.03
JM-15	30	51-424-93463	3010	6.5	6.6	1.03
	35	53-308-93514	2570	7.1	7.2	1.01
		53-308-93520	3010	6.7	6.8	1.02
KX-88/JM-15	35	56-339-93584	3010	6.7	7.0	1.05
GL-1076	30	58-382-93612	3010	6.5	6.8	1.05
POCO (L.F.)	30	63-435-93728	2635	7.0	7.0	1.00
		63-435-93725	3025	6.7	6.7	1.00
KX-88	35	54-725-93529	2610	7.0	7.0	1.00
		54-725-93557	2785	7.0	---	----
JM-15	35	55-725-93572	2610	7.1	7.3	1.02
		55-725-93577	2785	7.1	---	----
GL-1076	35	59-725-93631	2610	7.1	7.1	1.00
		59-725-93637	2785	7.2	---	----

were not obtained for medium loadings with any flour used in the NF-1 experiment for heat-treatment temperatures above 2970 K.

The coefficients in the longitudinal direction for all low-fired elements with uranium loadings of 725 kg/m^3 were 7.0 to 7.1 μm/m·K. The same elements heated to ∿ 2790 K had coefficients of 7.0 to 7.2 μm/m·K. This heat-treatment temperature over most of the length of the elements was too low to substantially alter the low-fired structure and the expansion properties. It is not known whether the CTE would remain at these high values if the entire element had been heated high enough to produce the target structure.

CTE measurements were made of three samples from an excessively melted element from High-Fire Run 3. The longitudinal expansion values were 6.6, 6.6, and 6.3 μm/m·K for samples from Stations 380, 810, and 1170, respectively (the amount of melting decreased with increasing station). The CTE for elements of this type heated close to the solidus temperature is ∿ 6.5 μm/m·K. Thus, no large differences in expansion were encountered in the excessively heated material.

D. Thermal Conductivity

Table BIX shows room-temperature thermal conductivity data, derived from thermal diffusivity, for elements from High-Fire Runs 1, 2, 4, 6, and 7. The measurements were made by the flash-diffusivity technique; a helical xenon flash lamp surrounding the nominal 6.1-mm-o.d. by 2.6-mm-i.d. by 100-mm-long specimen was used with a detector thermocouple probing the interior of the specimen. The specimens had been

TABLE BIX

ROOM-TEMPERATURE THERMAL CONDUCTIVITY FOR NF-1 EXPERIMENT AND COMPARISON ELEMENTS

High-Fire No.	Element Lot Load No.	Filler Flour	Carbide Content, vol%	Sample Location[a]	Heat-Treatment Temp., K	Thermal Conductivity, W/m·K
1	51-424-93466	JM-15	30	M & H	3030	87
	53-308-93528	JM-15	35	M & H	3030	75
	56-339-93591	KX-88/JM-15	35	M & H	3030	76
	58-382-93618	GL-1076	30	M & H	3030	78
2	50-308-93436	KX-88	35	M & H	3060	81
	60-298-93645	KX-88	35	M & H	3060	85
	62-382-93674	KX-88	35	M & H	3060	87
4	62-382-93683	KX-88	35	M & H	3020	71
	63-435-93718	POCO(L.F.)	30	M & H	3020	69
6	65-435-93781	KX-88	30	M & H	2955	62
	-93790	KX-88	30	G	> 2945	93
				H	2945	68
7	54-725-93558	KX-88	35	M & H	2780	49
---	---	---	---	---	---	---
9	69-424-93903	KX-88	30	G	> 2890	80
				H	2940	72
	-93904	KX-88	30	G	> 2890	81
				H	2940	69
WANL	8-413-203205	GL-1074	30	M	3020	∿ 80
				H	3020	∿ 80
-	68-500-92025	S-97	30	H	< 2970	61
-	68-500-92011	S-97	30	G	< 2970	54
				M	∿ 2970	76
				H	< 2970	59
-	713-339-62155	S-97	30	Sta. 50	< 2970	47
				Sta. 330	< 2970	51
				Sta. 500	∿ 2970	54
				Sta. 790	∿ 2970	53
				Sta. 965	< 2970	49
				Sta. 1270	< 2970	41

[a]G-sample from Station 0, M-sample from Station 810, and H-sample from Station 1270.

trepanned from around the central hole (Hole 10) of the fuel elements. In all elements except one, the samples were from Stations 760 to 860 and 1220 to 1320. The diffusivity data for each element were the average of at least two determinations at points 180 deg apart, 38 mm from the end of the tube. The data agreed within experimental precision and were averaged for calculating thermal conductivity. Also included in Table BIX are data for several materials for comparison (below broken line). For those elements, which were not uniform along their lengths, values for individual samples are listed.

Figure B13 depicts the extraordinarily high thermal conductivities of a Lot-52 element that showed excessive melting in High-Fire Run 5 (see Figs. B10 and B11). Several values are higher than the room-temperature thermal conductivity of ATJ-S graphite and must be attributed to the crystalline character of the graphite in the composite matrix.

The thermal conductivity of a composite matrix clearly is determined primarily by the thermal conductivity of the carbon phase.

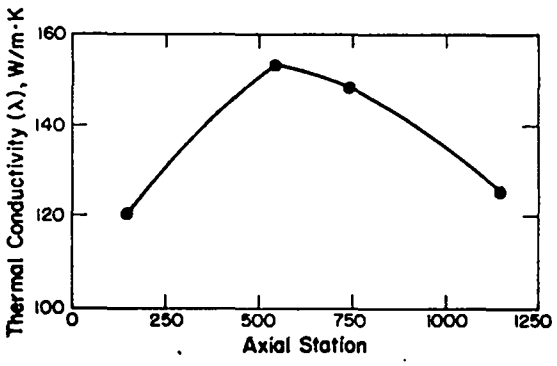

Fig. B13. Room-temperature thermal conductivity of Element 52-435-93486 that showed excessive melting in High-Fire Run 5.

The contribution of the carbide cage structure would be expected to be substantially less than the ∿ 25 W/m·K for dense ZrC. The degree of reorganization of polygonization of the filler flour that occurs at temperatures near and above the solidus temperature of the composite matrix clearly is the important factor because the carbon blacks and binder residues have earlier been converted to Type-I graphite.

E. Thermal-Shock Resistance (ZAP Test)

Thermal-shock data for 13 lots of uncoated, machined composite elements were obtained by using the thermal-shock apparatus previously developed for circular disk specimens. The measurements were made on 1.6-mm-thick cross-sectional wafers cut from the G-end, middle, and H-end of the elements.

The results of these measurements, summarized in Table BX, were very reproducible for most materials; however, in some sections of a few elements the data were widely scattered. These anomalous results were traced to the presence of extrusion flaws.

Some specimens from elements heated in High-Fire Run 5, for which MULE data indicated excessive melting in portions of each element, showed spectacular increases in thermal-shock resistance. The specimens from the middle of elements from Lots 51, 52, and 63 heated in High-Fire Run 5 showed the greatest resistance to thermal shock. For the Lot-52 element, this corresponded to room-temperature thermal conductivities of ∿ 150 W/m·K (see Fig. B13). Metallography indicated that this high resistance also corresponded to excessive melting of the bore surfaces (see Figs. B10 and B11). The element from Lot 58 heated in High-Fire Run 5 showed only a moderate improvement of thermal-shock resistance. This was not consistent with the MULE data, which indicated excessive melting comparable in extent and location to that of elements from the other three lots. The ZAP test results on these three lots led to further work on Lot-52 elements, i.e., to thermal-conductivity measurements and metallography.

The elements that did not show excessive melting had very typical thermal-shock indices of ∿ 130 to 170, except for the highly loaded elements of Lots 54, 55, 59. All samples of the latter elements from High-Fire Run 7, except the G-end samples, had very low thermal-shock resistances. (See Fig. B12 for correlation with metallography.)

The general trend was that 30-vol%-carbide materials were more resistant to thermal shock than 35-vol%-carbide materials. No correlation with flour type was found. For elements with medium loadings that did not show excessive melting, it did not seem to make much difference whether the elements from a given lot had been high-fired or low-fired (see elements in Lots 50, 53, and 62). Thus, for these elements, thermal conductivity did not appear to affect the ZAP test results. The situation appears to be different, however, for elements with high loadings (see Lots 54, 55, and 59).

TABLE BX

SUMMARY OF THERMAL-SHOCK RESULTS FOR COMPOSITE ELEMENTS OF THE NF-1 EXPERIMENT

Lot No.	U Loading, kg/m^3	Carbide Content, vol%	Filler Flour	Heat-Treatment Temp., K	Heat-Treatment[a] Batch Number	Thermal-Shock Index[b] G-end	Middle	H-end
50	308	35	KX-88	3050	H.F. 2	137.5/145	130/137.5	135/145
		35	KX-88	2635	L.F. 7	137.5/142.5	135/137.5	145/152.5
51	424	30	JM-15	Melting[c]	H.F. 5	200/202.5	300	Flaws
		30	JM-15	3010	H.F. 1	165/170	167.5/170	162.5/190
52	435	30	KX-88	Melting[c]	H.F. 5	157.5/160	380	162.5/165
53	308	35	JM-15	3010	H.F. 1	129/132.5	125/137.5	127.5/131
		35	JM-15	2570	L.F. 11	125/130	132.5/135	Flaws
54	725	35	KX-88	2785	H.F. 7	130/142.5	107.5/112.5	117.5/120
		35	KX-88	2610	L.F. 8	112.5/115	112.5/115	105/112.5
55	725	35	JM-15	2785	H.F. 7	130/132.5	115/117.5	112.5/115
		35	JM-15	2610	L.F. 8	110/122.5	110/112.5	117.5/120
56	339	35	KX-88/JM-15	3010	H.F. 1	130/132.5	137.5/145	137.5/145
58	382	30	GL-1076	Melting[c]	H.F. 5	170/182.5	177.5/182.5	162.5/165
		30	GL-1076	3010	H.F. 1	162.5/165	165/167.5	164/169
59	725	35	GL-1076	2785	H.F. 7	130/132.5	105/107.5	107.5/115
		35	GL-1076	2610	L.F. 8	107.5/110	--	122.5/125
60	298	35	KX-88	3050	H.F. 2	--	145/147.5	137.5/140
62	382	35	KX-88	3050	H.F. 2	Flaws	137.5/150	135/142.5
		35	KX-88	3025	H.F. 4	132.5/142.5	135/137.5	135/137.5
		35	KX-88	2635	L.F. 7	127.5/132.5	127.5/130	Flaws
63	435	30	POCO	Melting[c]	H.F. 5	$\sim$ 250	$\sim$ 350	$\sim$ 300
		30	POCO	3025	H.F. 4	Flaws	150/152.5	127.5/140
		30	POCO	2635	L.F. 7	127.5/130	Flaws	Flaws
65	435	30	KX-88	2945	H.F. 6	165/167.5	145/152.5	140/142.5

[a] H.F. = High Fire; L.F. = Low Fire.

[b] The first number gives a relative power setting at or below which all specimens survive, and the second gives a relative power setting at or above which all specimens fail. The differences between the two settings may be considered to be the overlap or scatter.

[c] Excessive melting in portions of the element was indicated by MULE data.

F. Thermal-Stress Resistance (Peak-Power Density Test)

A number of uncoated composite elements in the machined, high-fired condition were tested for thermal-stress resistance by means of a modified peak-power density test.* This test attempts to match the thermal stress, calculated for a specimen tested in the thermal-stress apparatus, to the axial peak-power density of a nuclear propulsion-reactor fuel element. This was achieved by reducing the diameter of the sonic-flow nozzles in the six corner holes of a 356-mm-long fuel-element specimen, which makes it possible to duplicate (at a single point in the experimental power ramp) the power density, temperature, and thermal stress of a reactor element at full-power steady-state operating condition. The test procedure was designed to permit the evaluation of relative thermal-stress resistances of single elements from individual development and reactor production extrusion lots. The various uncoated specimens were compared on the basis of the relative power density attained at failure. The performance relative to reactor operating conditions was measured with respect to the peak reactor axial power density of $\sim$ 4100 MW/m^3.

*See Ref. A4 of Appendix A.

For assigned values of thermal conductivity* and a test flow rate of 0.0177 kg/s H_2, this power density corresponds to a test temperature of 1795 K and to a $\Delta T = \bar{T} - T_{min} = 80$ K, where $\bar{T}$ is the calculated mean matrix cross-section temperature and T_{min} is the minimum temperature at the surface of the corner coolant hole. For material of higher thermal conductivity, higher power densities and test temperatures are reached before this ΔT is exceeded.

Table BXI shows performances of composite matrices and of various comparison materials in the above test. Most important, the results show that 35-vol%-carbide matrices with good thermal stress resistance ($q''' > 4100$ MW/m in this test) in the uncoated condition were made from KX-88 or JM-15 filler flours, provided that the thermal conductivity was high enough. All composite elements except the Lot-54 element from High-Fire Run 7 showed generally better thermal-stress resistance than the LASL-produced AXM graphite element containing pyrocarbon-coated UC_2 particles.

The S-97, 30-vol%-carbide element from Lot 68 gave extremely uniform, high values of q''' ($\sim$6200 MW/m^3) at fracture. The thermal conductivity at the H-end was 61 W/m·K. The GL-1074, 30-vol%-carbide element from WANL Lot 8 had a high thermal-stress resistance. This element essentially had the matrix target structure at all stations.

The KX-88, 30-vol%-carbide elements of Lot 65 gave variable results. The values of q''' at fracture from this lot were consistent with the fact that the G-end of the element had been hotter than the rest of the element and had a thermal conductivity of 93 W/m.K. However, another element from this lot had a low value of q''' at fracture at the G-end.

The KX-88, 35-vol%-carbide elements showed increasing thermal-stress resistance that correlated well with the degree to which the target structure was approached and the thermal conductivity increased. The low values of q''' at fracture for the pieces of the Lot-54 element were consistent with inadequate firing in High-Fire Run 7 ($\lambda \approx 49$ W/m·K at the H-end), and the order of the q''' values were consistent with the fact that the G-end was the hottest. The q'''-values for the pieces of the Lot-62 element from High-Fire Run 4 were consistent with the fact that the G-end was the hottest. The performances of the pieces from the elements of Lots 50 and 60 from High-Fire Run 2 were very similar, except for the middle piece of the Lot-60 element that had not fractured when the test was taken off line at $q''' > 6900$ MW/m^3. The order of the values of q''' at fracture for the pieces of the Lot-62 element from High-Fire Run 2 was inverted from that expected on the basis of MULE-data evidence that the H-end was hottest.

Both the JM-15, 35-vol%-carbide element of Lot 53 and the JM-15/KX-88, 35-vol%-carbide element of Lot 56 generally showed q'''-values similar to those for the KX-88, 35-vol%-carbide element of Lot 62 from High-Fire Run 4, which likewise had not been heated above the solidus temperature. The G-end piece showing the lowest value for the Lot-53 element is consistent with the fact that the G-end was coldest in High-Fire 1, but the G-end piece showing the highest value for the Lot-56 element from the same high firing is anomalous.

Elements showing thermal-stress performance for the three pieces that were neither consistent with their IPDE and MULE data nor with metallographic data on sister elements, were examined further. Metallographic examinations were made on each of these thermal-stress pieces to complement the metallographic data obtained on sister elements.

*A value of 74 W/m·K for room-temperature thermal conductivity was used in the analysis. A standard temperature dependence of conductivity was used which reduced this value to 39 W/m·K at 1795 K.

TABLE BXI

THERMAL-STRESS RESISTANCE TEST RESULTS ON UNCOATED COMPOSITE ELEMENTS

Extrusion Lot	Filler Flour	Carbide Content, vol%	CTE (293-2300 K), μm/m·K	Room-Temperature Thermal Cond.,[a] W/m·K	Fracture Power Density,[a] MW/m³
17	AXM	Graphite[b]	5.6	-----	4050G, 4500M, 4500
8[c]	GL-1074	30	6.6	75H	6200G, 5500M, >6300H
68	S-97	30	6.1	61H	6600G,M,H
65	KX-88	30	6.5	62M,H	4300G, 4700M, 5500H
65	KX-88	30	6.5	93G, 68H	>6700G, 5100M, 5300H
713	S-97	35	6.3	50G,M,H	4700G, >6200M, >5300H
54	KX-88	35	7.0	49M,H	4000G, 3700M, 3500H
62	KX-88	35	6.6	71M,H	5200G, 5100M, 4400H
60	KX-88	35	6.6	85M,H	5000G, >6900M, 5300H
50	KX-88	35	6.8	81M,H	5400G, 5300M, 5200H
62	KX-88	35	6.8	87M,H	6800G, 6000M, 5800H
53	JM-15	35	6.7	75M,H	3700G, 5200M, 5000H
56	JM-15/KX-88	35	6.7	76M,H	5100G, 4600M, 4800H

[a] G,M,H refer to low, middle, and high stations.

[b] A graphite matrix element containing pyrocarbon coated UC_2 particles.

[c] Composite elements fabricated by WANL.

Again, the metallographic data offered no explanation for the anomalous q'''-values. Flaws in the matrix, not revealed in inspection, could have been present leading to the anomalous results.

V. APPLICATION OF ZrC COATINGS*

The surfaces of the coolant channels and all external surfaces of the composite elements were protected with a ZrC carbide coating deposited by a chemical-vapor-deposition (CVD) process. This coating was expected to prevent or limit the chemical reaction of hot hydrogen with the carbon of the fuel-element matrix. In preparation for the application of the carbide coating the external surfaces of the fuel elements were machined to the specified dimensions (∿ 19.1 mm across flats). The coolant channels were not machined but were extruded to ∿ 2.59 mm-diam.

*This section presents a general discussion of the ZrC coating conditions used for NF-1 elements.

The overall CVD reaction may be represented by the equation

$$ZrCl_4(g) + CH_4(g) = ZrC(s) + 4HCl(g).$$

This thermodynamic relation not only establishes the lower bound for the coating-gas composition, but also serves as the basis for mass-balance calculations along the axial length of the fuel elements. It also suggests that the partial pressure of HCl(g) will have a strong effect on the deposition rate. Consequently, the reduction of $ZrCl_4(g)$ in the system must be considered:

$$ZrCl_4(g) + 1/2\ H_2(g) = ZrCl_3(g) + HCl(g)$$

and

$$ZrCl_3(g) + 1/2\ H_2(g) = ZrCl_2(g) + HCl(g).$$

The reduction reaction is important near the coating-gas inlet end of the elements

because it determines the quantity of HCl formed, which strongly affects the initial deposition rate. The quantities affecting the deposition, which can be calculated from the above thermodynamic relations, and appropriate mass-balance equations as function of axial position along the element are: P_{Salt}--sum of partial pressures of $ZrCl_4(g)$, $ZrCl_3(g)$, and $ZrCl_2(g)$; P_{CH_4}--partial pressure of methane; P_{HCl}--partial pressure of hydrogen chloride; and P_{H_2}--partial pressure of hydrogen. An analytical calculational program was used to understand the variables affecting the deposition conditions.

The general deposition conditions used in coating the composite elements are listed in Table BXII. Inspection and evaluation procedures for evaluating the coatings included: high-resolution-eddy-current examination for the detection of cracks, MULE examination for mass of coating deposited vs length of fuel element, x-ray diffraction analysis for the determination of lattice parameter, chemical analysis for impurities such as Cl_2 and O_2, microstructure determination by optical and scanning-electron microscope, determination of coefficient of thermal expansion, and determination of the effectiveness of the coating as a protective layer in a component test that simulated conditions in a nuclear propulsion reactor.

TABLE BXII

PROCESS CONDITIONS FOR DEPOSITION OF ZrC COATING IN THE COOLANT CHANNELS OF A COMPOSITE FUEL ELEMENT

(A) Initial Composition of Coating Gas

Constituents	Flow/Element,[a] m^3/s (STP)
$ZrCl_4$	1.2×10^{-6}
CH_4	0.9
H_2	66
Ar	66
HCl (first 20 h)	2.6
HCl (last 5 h)	0

(B) Deposition Temperature and Coating Thickness

Station from Inlet End, mm	Deposition Temp., K	ZrC Coating Thickness, μm
127	1525	60
254	1540	89
508	1580	119
762	1615	132
1012	1640	135
1270	1660	132

[a]Coating time was 25 h at ∿ 0.9 atm. This flow of gas was coating the channel surfaces of one element (0.235 m^2 of surface area).

ACKNOWLEDGMENTS

R. Bard and A. Driesner deserve recognition for their efforts in organizing and managing the complex details of the NF-1 composite element experiment.

APPENDIX C

PROPERTIES OF (U,Zr)C-GRAPHITE (COMPOSITE) FUEL ELEMENTS

I. INTRODUCTION

This appendix presents the available property data for (U,Zr)C-graphite fuel elements. The data are presented in a series of tables and figures; comments are made in the text, only where required.

II. CHEMICAL CONTENT AND DENSITY

Table CI presents chemical-composition and density data for composite fuel elements of ∿ 70 kg/m^3 uranium loading at 15, 20, and 30-vol% carbide contents. Table CII presents similar data for elements of ∿ 435 kg/m^3 uranium loading at 30-, 35-, 40- and 45-vol% carbide contents.

III. MECHANICAL PROPERTIES

Table CIII presents room-temperature flexural, compressive, and tensile-strength data for composite fuel elements of 10- to 50-vol% carbide content.

Table CIV gives room-temperature elastic-modulus data, longitudinal and transverse to the extrusion direction, for composite materials of 10-to 50-vol% carbide content. Table CV presents the temperature dependence of elastic modulus for 30- and 35-vol% carbide-content composite materials.

Stress-strain properties of composite materials are given in Table CVI and Fig. C1.

Compressive-deformation information, for the longitudinal orientation, is given in Table CVII for composites of 10- to 50-vol% carbide content at temperatures from 2773 to 2973 K.

TABLE CI

CHEMICAL CONTENT AND DENSITY OF (U,Zr)C-GRAPHITE (COMPOSITE) FUEL ELEMENTS (URANIUM LOADING, ∿ 70 kg/m^3)

	Nominal Carbide Content, vol%		
Parameter	15[a]	20	30
Gross density, Mg/m^3	2.62	2.82	3.26
Zirconium, wt%	34.0	40.7	52.9
Mg/m^3	0.89	1.15	1.72
Uranium, wt%	2.7	2.58	2.22
Mg/m^3	70.0	72.8	72.4
Carbon, wt%	63.3	56.4	44.8
Mg/m^3	1.66	1.59	1.46
Carbide, vol%[b]	15.0	20.2	30.1
Carbon, vol%[b]	73.3	68.4	58.6
Voids, vol%[b]	11.7	11.4	11.3
ZrC, wt%	38.4	46.1	59.7
UC, wt%	2.8	2.7	2.4
Free C, wt%	58.8	59.9	37.7

[a] Estimated.

[b] The density of carbon in a composite was assumed to be 2.1 Mg/m^3 rather than the value of 2.26 for crystalline graphite. The densities of $ZrC_{0.97}$ and $UC_{0.97}$ were assumed to be 6.59 and 13.60 Mg/m^3, respectively. The density of $(U,Zr)C_{0.97}$ was assumed to be proportional to the mole fraction of the carbide constituents.

IV. THERMAL PROPERTIES

Table CVIII presents thermal-conductivity data for ATJ-S graphite, ZrC carbide, and two (U,Zr)C-graphite composites. The data for Composite A in Table CVIII represent the thermal conductivity-vs-temperature relationship for a 30- or 35-vol% carbide-content composite that had been heat-treated at temperatures below the solidus line (see Fig. 3 of main body of report). The data

TABLE CII

CHEMICAL CONTENT AND DENSITY OF (U,Zr)C-GRAPHITE (COMPOSITE) FUEL ELEMENTS (URANIUM LOADING, ∿ 435 kg/m³)

Parameter	Nominal Carbide Content, vol% 30	35	40	45
Gross density, Mg/m³	3.36	3.59	3.87	4.09
Zirconium, wt%	46.6	51.0	56.0	59.7
Mg/m³	1.56	1.83	2.17	2.44
Uranium, wt%	12.50	12.02	11.22	10.65
kg/m³	420	431	435	436
Carbon, wt%	40.5	36.5	32.6	29.2
Mg/m³	1.36	1.31	1.26	1.20
Carbide, vol%[a]	30.5	35.2	41.0	45.5
Carbon, vol%[a]	54.0	49.8	45.5	40.5
Voids, vol%[a]	15.5	15.0	13.5	14.0
ZrC, wt%	52.7	57.7	63.4	67.6
UC, wt%	13.1	12.6	11.8	11.2
Free C, wt%	33.7	29.2	24.7	20.8

[a]The density of carbon in a composite was assumed to be 2.1 Mg/m³ rather than the value of 2.26 for crystalline graphite. The densities of $ZrC_{0.97}$ and $UC_{0.97}$ were assumed to be 6.59 and 13.60 Mg/m³, respectively. The density of $(U,Zr)C_{0.97}$ was assumed to be proportional to the mole fraction of the carbide constituents.

TABLE CIII

ROOM TEMPERATURE FLEXURAL, COMPRESSIVE, AND TENSILE FRACTURE STRENGTHS OF (U,Zr)C-GRAPHITE FUEL ELEMENTS

Carbide Content, vol%	Strength,[a] MPa Flexural	Compressive	Tensile
10	44.8 ± 2.7	74.5 ± 0.7	35
20	47.9 ± 1.4	97.6 ± 1.8	43
25	63.4 ± 5.1	109.5 ± 12.4	49
30	53.0 ± 1.6	118.1 ± 10.3	39
50	65.6 ± 2.3	> 290	68
Pewee-1 graphite elements	35.0 ± 3.4	85.3 ± 4.3	--

[a]Average of at least three samples. Samples were of full cross section, ∿ 19 mm across flats. The flexural and tensile strengths were transverse to the extrusion direction and the compressive strengths were parallel to the extrusion direction.

TABLE CIV

ROOM-TEMPERATURE ELASTIC MODULUS OF (U,Zr)C-GRAPHITE COMPOSITES

Carbide Content, vol%	Longitudinal Elastic Modulus,[a] GPa	Transverse Effective Elastic Modulus,[b] GPa	Modulus Ratio Long./Trans.
10	17.6	5.9	3.0
20	25.4	7.9	3.2
25	30.3	9.6	3.2
30	42.0	11.8	3.6
50	108.0	44.0	2.5

[a]Dynamic method.

[b]Load-deflection method.

TABLE CV

TEMPERATURE DEPENDENCE OF ELASTIC MODULUS OF (U,Zr)C-GRAPHITE FUEL ELEMENTS

Temperature, K	Reduced Modulus[a] 30-vol% Carbide	35-vol% Carbide
300	1.0(35 GPa)	1.0(44 GPa)
500	1.0	1.0
1000	1.05	1.03
1250	1.11	1.08
1500	1.18	1.14
2000	1.29	1.26
2250	1.28	1.23
2500	1.18	1.08
2750	1.03	0.81

[a]Uranium loading, 166 kg/m³.

for Composite B in Table CVIII represent about the highest thermal conductivity that can be achieved (optimum heat-treatment conditions) for a 30- or 35-vol% carbide-content composite that still retains desirable mechanical properties.

Table CIX presents typical thermal-expansion data for a 35-vol% carbide-content composite having a CTE of 6.7 μm/m·K for the 293 to 2300 temperature range.

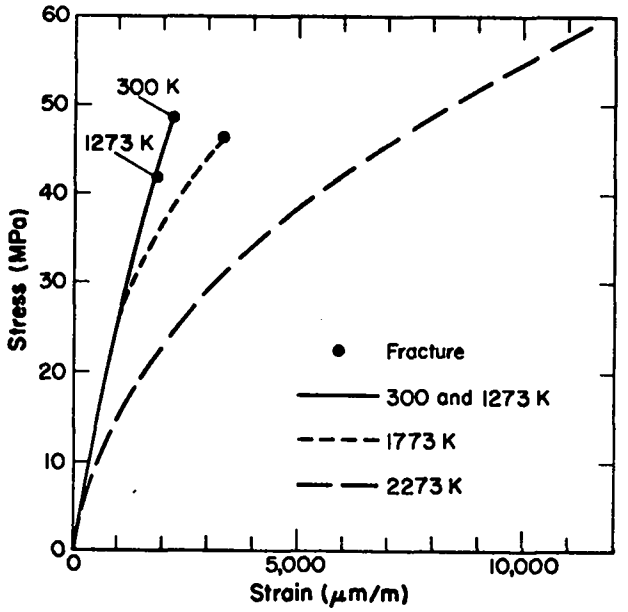

Fig. C1. Stress-strain data from room temperature to 2273 K for a (U,Zr)C-graphite composite of 30-vol% carbide content and 630 kg/m^3 uranium loading.

TABLE CVI

ROOM-TEMPERATURE STRESS-STRAIN PROPERTIES FOR (U,Zr)C-GRAPHITE COMPOSITES

Carbide Content, vol%	Zero Stress Modulus, GPa	Failure Strain, m/m	Failure Stress, MPa
10	20	3900	38
20	27	3000	40
25	31	1600	35
30	37	1800	44
30	37	1500	42
35	44	1500	39
35	40	1000	26
40	68	500	32
40	54	1100	48
50	57	1500	61
50	100	1000	84

Table CX presents C_p data for ZrC, UC, and carbon. To obtain C_p for a composite, multiply the appropriate component by the corresponding mass fraction (obtain chemical-analysis data from Tables CI and CII). To obtain $\rho.C_p$, use the $\Delta L/L$ data from Table CIX to calculate the dependence of ρ on temperature, i.e.,

$$\rho_T = \rho_A \, (1 + \Delta L/L)^{-3}$$

where ρ_T is the density at temperature T; ρ_A is the density at ambient temperature from Tables CI and CII; and $\Delta L/L$ is the fractional change in linear thermal expansion from ambient to temperature T from Table CIX.

TABLE CVII

COMPRESSIVE DEFORMATION OF (U,Zr)C-GRAPHITE (COMPOSITE) ELEMENTS SUBJECTED TO 3.45 MPa FOR ONE HOUR

Carbide Content, vol%	Uranium Loading, kg/m^3	Compressive Deformation, % 2773 K	2873 K	2923 K	2973 K
10	300	0.22	0.21	0.26	0.20
20	300	0.43	1.02	1.08	1.10
25	300	0.37	0.50	0.59	0.61
30	300	0.72	0.98	1.45	2.35
30	500	0.41	0.43	----	----
40	500	0.76	0.87	----	----
50	300	0.8	3.1	5.1	11.1
50	500	2.5	2.6	----	----

TABLE CVIII

THERMAL CONDUCTIVITY OF ATJ-S GRAPHITE, ZrC CARBIDE AND TWO (U,Zr)C-GRAPHITE COMPOSITES

Temperature, K	Thermal Conductivity, W/m·K Composite A	Composite B	ATJ-S	ZrC
300	52	90	125	19
400	49	71	110	20
500	46	60	97	20.5
600	43	53	86	21
700	40	48	78	21.5
800	38	44	72	22
1000	34	38	60	23.5
1200	32	36	52	25
1400	30	30	45	27
1600	30	30	41	29
1800	30	30	38	31
2000	30	30	35	33
2200	30	30	33	35
2400	30	30	32	36
2600	30	30	30	38

TABLE CIX

THERMAL EXPANSION PROPERTIES OF A HIGH EXPANSION (U,Zr)C-GRAPHITE (COMPOSITE) FUEL ELEMENT

Temperature, K	% ΔL/L	μm/m·K	Inst. CTE, μm/m·K
293	0.000	4.26	4.26
300	0.003	4.28	4.31
500	0.101	4.88	5.42
750	0.249	5.44	6.28
1000	0.412	5.83	6.70
1250	0.583	6.09	6.85
1500	0.756	6.26	6.88
1750	0.930	6.38	6.96
2000	1.109	6.50	7.25
2200	1.260	6.61	7.74
2300	1.340	6.68	8.10

TABLE CX

CALCULATION OF C_p FOR (U,Zr)C-GRAPHITE COMPOSITES

Temperature, K	C_p, W·s/g·K		
	ZrC[a]	UC[b]	Carbon[c]
300	0.368	0.201	0.721
400	0.430	0.219	1.03
500	0.454	0.227	1.27
600	0.468	0.233	1.42
700	0.476	0.237	1.55
800	0.482	0.242	1.65
900	0.484	0.245	1.71
1000	0.486	0.249	1.76
1200	0.493	0.257	1.85
1400	0.498	0.265	1.93
1600	0.507	0.275	1.98
1800	0.520	0.286	2.03
2000	0.540	0.299	2.07
2200	0.564	0.313	2.11
2400	0.592	0.328	2.14
2600	0.623	0.345	2.16
2800	0.656	0.363	2.18

[a] E. K. Storms, The Refractory Carbides, 1967.

[b] Ibid.

[c] C. B. Spence, "Research and Development on Advanced Graphite Materials -- Analytical presentation of the Measurement of the Specific Heat of Graphite," WADD-TR-61-72, Vol XLI, Nat. Carbon Co., Parma, OH, July 1963.

APPENDIX D

STABILITY OF (U,Zr)C-GRAPHITE FUEL ELEMENTS

I. INTRODUCTION

An experiment was conducted at LASL to ascertain the effect of storage for periods of time up to two years on (U,Zr)C-graphite (composite) fuel elements. Depending upon process conditions and uranium loading, small quantities of both UC_2 and (U,Zr)C solid solution of relatively high uranium mole percent could be present in some composite elements. The hydrolysis of UC_2 with moisture in air is rapid, but little is known about the stability of (U,Zr)C solid solutions. Two storage conditions were used in these studies: (1) in air of 90% relative humidity and 310 K temperature, and (2) in nitrogen of very low relative humidity at ambient temperature. The elements were evaluated before and after storage for changes in electrical resistance, dimensions, number of cracks in ZrC coolant-channel coating, mass, carbide microstructure,and performance in a hydrogen corrosion test.

II. RESULTS OF STORAGE EXPERIMENT

The (U,Zr)C-graphite elements used in the experiments had a carbide content of 30 vol% and uranium loadings of 125 and 500 kg/m^3,--2.8 and 11 mole percent UC in the solid solution, respectively.

After 77 days of storage, no significant changes were observed in the elements stored in either the wet or dry condition.

The results of the evaluation of elements stored for 6 and 12 months are given in Table DI. Because there were no significant differences between the results obtained with elements of different uranium loading, the data given are averages of those for all elements. A very slight increase in the number of coating cracks was observed after six months for both the dry and wet storage conditions. No additional increase in the number of coating cracks was observed after 12 months storage. The slight increase observed in the number of coating cracks probably was due to handling operations rather than to changes during storage.

TABLE DI

CHANGES IN (U,Zr)C-GRAPHITE FUEL ELEMENTS AFTER STORAGE FOR 6 AND 12 MONTHS

Parameter	Dry Storage[a]		Wet Storage[b]	
	6 Mos.	12 Mos.	6 Mos.	12 Mos.
Electrical resistance, %	-0.6	-0.2	+1.9	+2.4
Mass change, %	0.0	0.0	+0.4	+0.5
Dimensional change across flats, %	+0.0012	+0.0011	+0.0012	+0.0016

[a] Storage at ambient temperature in nitrogen containing Linde Molecular Sieve 4A desiccant.

[b] Storage in air at 310 K and 90% relative humidity.

Fuel elements from the various storage conditions were evaluated for their hydrogen corrosion resistance in a component test consisting of 30 cycles of 10 min duration at maximum matrix temperatures of ∿ 2250 K. The mass loss was determined after completion of the 5-h test. The mass losses were: 3.4 g for the control element, 4.2 g for the element in wet storage for six months, 2.5 g for the element in wet storage for 12 months, and 2.1 g for the element in dry storage for 12 months.

The results of these experiments indicated that the composite elements were stable over a relatively wide range of storage conditions.

APPENDIX E

(U,Zr)C (CARBIDE) FUEL ELEMENTS

I. INTRODUCTION

The major difference between a (U,Zr)C all-carbide fuel element and a (U,Zr)C-graphite (composite) element is the absence of free carbon in the all-carbide element. As shown elsewhere (see Fig. 16 of main body of this report) a matrix temperature of ∿ 3200 K has been proposed as a possible operating condition in a nuclear propulsion reactor if the combined carbon-to-metal ratio in (U,Zr)C is maintained between ∿ 0.88 and ∿ 0.95.

The all-carbide element, substoichiometric in carbon, may be able to achieve a very high operating temperature, but this advantage is offset, to some degree, by high density and very poor resistance to thermal stress. The density of a graphite-matrix fuel element containing pyrolytic-carbon-coated UC_2 spheres is ∿ 2.3 Mg/m^3, that of a (U,Zr)C-graphite (composite) element is ∿ 3.5 Mg/m^3, and that of a (U,Zr)C-all-carbide element is ∿ 5.5 Mg/m^3 (all elements at ∿ 300 kg/m^3 uranium loading).

The carbide elements were fabricated by an extrusion process. Most of the extrusion work on carbide elements was done by using an extrusion mixture consisting of ZrC, UO_2, ZrO_2, graphite flour, and a thermosetting binder. The amount of carbon added in the form of ZrC, graphite, and binder was enough to react with all the oxygen in the UO_2 and ZrO_2, and still to leave 1 to 3 wt% of free carbon in the element after high-temperature heat treatment. This amount of carbon in the fuel element was of help in the extrusion process, prevented the elements from sticking to the graphite fixtures used to support the elements during high-temperature heat treatment, aided in densification during heat treatment, and facilitated the machining of elements into a hexagonal cross section. After machining, the free carbon was removed by leaching the elements with hot, flowing hydrogen gas. The elements were then impregnated with zirconium using a modified chemical-vapor-deposition process. The fuel elements were then given a final heat-treatment at $\geq$ 2800 K.

II. FABRICATION OF (U,Zr)C FUEL ELEMENTS

The following is a description of the materials and procedures used to fabricate the carbide fuel elements. Most of the raw materials and equipment were those used in making composite fuel elements.

A. Materials

The ZrC powder used in the manufacture of fuel elements was reactor-grade (< 200 ppm Hf) and had a Fisher average particle size of 3.5 μm. A typical analysis was 88.0% zirconium and 11.5% total carbon, ∿ 0.3%, of which was free carbon. Impurities included 0.2% N_2, 0.2% O_2, and 90 ppm of sulfur. Metallic impurities were low, the major ones being 200 ppm of titanium, 150 ppm of tantalum, and 100 ppm of iron. The carbide particles were very dense and relatively equiaxed.

The enriched UO_2 powder used in the fuel-element extrusion mix was produced at LASL. The powder had a Fisher average particle size of ∿ 5 μm. The particles were

dense and discrete. Total metallic impurities were limited to 500 ppm, with a maximum 1 ppm of boron and 0.5 ppm of cadmium.

The ZrO_2 powder used was reactor-grade (< 200 ppm Hf) and had a Fisher average particle size of ∿ 1 μm. The powder contained ∿ 1500 ppm metallic impurities (mostly silicon and iron), from 0.1 to 0.5% sulfur, and had a surface area of ∿ 10 m^2/g.

The carbon addition to the carbide extrusion mix was in the form of a fine graphite flour having a Fisher average particle size of 0.6 μm. This flour was obtained by grinding and classifying -200 mesh reactor-grade graphite powder. The maximum particle size was ∿ 10 μm. This flour contained 500-ppm ash, most of which was iron.

Varcum* 8251 thermosetting resin was used as the binder. Varcum is a partially polymerized furfuryl alcohol with a viscosity of ∿ 300 cP at room temperature. The Varcum was catalyzed with 4 g of maleic anhydride per 100 cm^3 of resin used.

B. Extrusion Formulation

The extrusion mixture was calculated to provide 1 to 3% free carbon in the fuel elements after the first high-temperature treatment. This free carbon added strength to the elements, making them easier to process and machine. Most extrusion mixes consisted largely of ZrC powder with smaller amounts of UO_2, ZrO_2, and carbon powder bonded together with Varcum binder.

The carbon powder and the carbon residue from the Varcum binder, ∿ 45% of the Varcum by weight, were used by the UO_2 and ZrO_2 in converting to the carbide, except for the free carbon left in the heat-treated element. The amount of ZrO_2 added to the extrusion mix depended upon the amount of UO_2 added to the mix. As the uranium loading decreased, the ZrO_2 content increased. No ZrO_2 was required at high uranium loadings. The extrusion mixes contained a constant oxygen content regardless of loading. The zirconium content of the extrusion mix remained constant.

Production batches, enough for 500 to 2500 cm^3 of final product, were mixed in Patterson-Kelly (P-K) twin-shell blenders. Just before being extruded, the larger batches were mixed intensively by passing them through a Hobart Model-4532 2-hp meat chopper. This operation was used to homogenize, densify, and heat the extrusion mix. The mix was usually passed through the chopper twice before extrusion and once between each extrusion.

The carbide and oxide particles in the mix --especially the ZrC particles -- tend to be angular, are hard, and make the mix very abrasive. Die wear is particularly severe where the flow of extrudate impinges on a die surface and changes direction, as on the upstream face of the plenum and at the base of the pin. However, surfaces over which the mix only slides are also worn, but to a lesser degree. These surfaces include the extrusion cylinder, ram head, feed holes, pin diameter, and the plenum near the exit end. After much experimentation, Ferro-TiC, a steel-bonded carbide manufactured by Sintercast, West Nyack, NY, was chosen for its ease of fabrication and very high wear resistance.

Because of bowing and twisting, it was impractical to fabricate the hexagonal fuel-element shapes. Therefore, cylindrical extrusions with an axial hole were extruded and processed, and this stock was then machined into the hexagonal fuel-element shape. The extrusions were first centerless-ground and then diamond-milled into shape. Figure E1 shows the type of die used for extruding the one-hole cylindrical carbide fuel-element stock. The 40-ton press was also equipped with a run-out table and cut-off arrangement that allowed the continuous extrusion from a chamber full of mix, usually

*Varcum Chemical Division of Reichhold Chemicals, Inc.

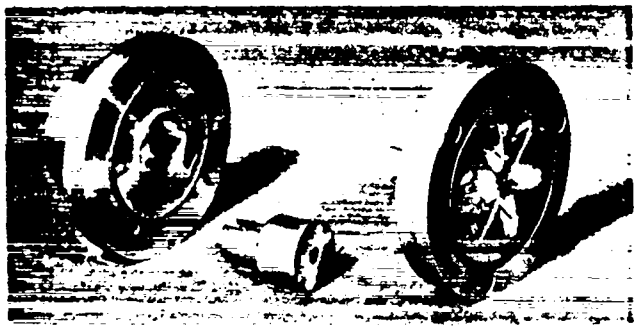

Fig. E1. Extrusion die used for fabricating (U,Zr)C fuel elements.

enough for ∿ 16 elements. The run-out table, curing fixture, and cut-off device are shown in Fig. E2.

The elements were heat-treated in electrically heated circulated-air ovens to polymerize the thermosetting resin. The heating rate for the 90-h cycle was 1°/h from 325 to 385 K, 2°/h from 385 to 405 K, and a gradual increase to a maximum of 8°/h from 405 to 525 K. The carbide extrusions were then heat-treated over a period of 54 h to 1125 K at a pressure of ∿ 10 Torr, using an argon flush through the furnace. The products of decomposition of the Varcum binder, especially the water vapor, were sufficiently corrosive to the ZrC at the baking temperature to produce considerable amounts of loose ZrO_2 powder on the surfaces of the extrusions. An adequate supply of argon flowing through the holes and around the outside of the extrusions diluted and swept these products away, thus considerably reducing surface oxidation.

The carbide elements were given a high-temperature heat treatment in induction-heated vertical furnaces capable of reaching temperatures up to ∿ 3000 K. The cylindrical stock for the carbide fuel elements was held in seven-hole cassettes that were placed in holes in graphite fixtures, which, in turn, were placed in the vertical heat-treating furnaces. Two furnaces were used to heat-treat all elements both for low firing (2625 K) and high firing up to 2875 K; an argon atmosphere was used.

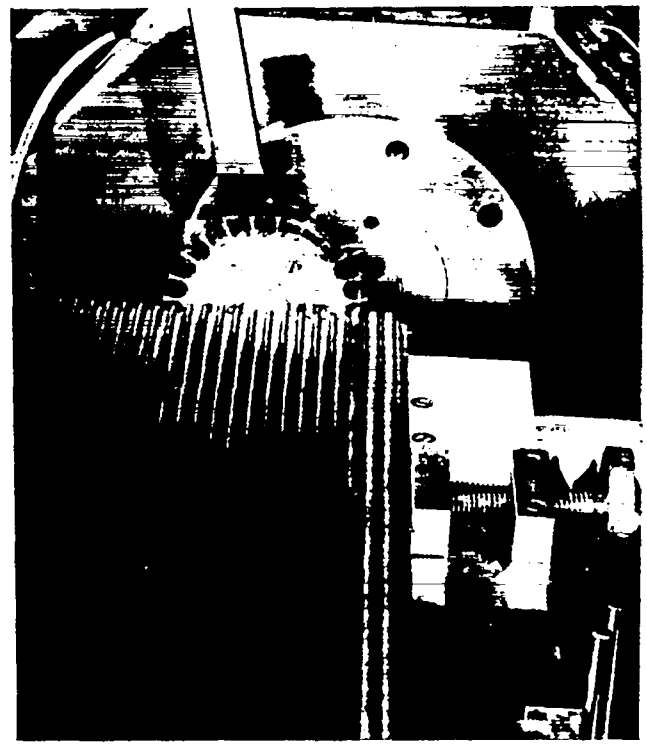

Fig. E2. Photograph of extrusion of carbide elements showing run-out table, fixture to support elements, and cut-off wheel.

The heating rate for the first high-temperature heat treatment to 2625 K was as follows: 2.5 h to 1875 K, a 3-h drift upward to 2625 K at reduced power, and a 0.5-h hold at 2625 K.

During heating at the slower rate, the UO_2 and ZrO_2 in the extrusions reacted with the carbon surrounding the particle and were converted to carbide with the evolution of CO gas. Heating at the slower rate was intended to release this gas without injuring the element.

The cassettes holding the carbide elements during the second, high-temperature, heat treatment had insertion holes that were smaller than those in the low-fire cassettes, to compensate for fuel-element shrinkage during low-fire heat treatment.

The heating rate for the second, high-temperature, treatment was 3 h to 2625 K with a 3.5-h hold at temperature. The hold at 2625 K was to allow complete solid-

solution formation below the UC_2-C eutectic melting temperature of ∿ 2725 K. The temperature was then increased to between 2775 and 2875 K and was held for 2 h.

C. Development of Substoichiometric (U,Zr)C

The carbide fuel elements should contain no free carbon and the carbon-to-metal ratio should range from 0.88 to 0.95, to achieve the highest melting point, to minimize creep, to obtain usable strength properties at matrix temperatures $\geq$ 3000 K, and to minimize uranium and carbon losses in flowing hot hydrogen gas.

Because of the several processing considerations described previously, the extruded carbide elements contained ∿ 3 wt% free carbon. Three alternative methods of removing the free carbon and rendering the resulting fuel-element matrix substoichiometric in carbon were explored. The simplest process in principle was to leach out the excess carbon with hot hydrogen. After all the free carbon was removed, a portion of the chemically bound carbon could be removed by continuing the leaching process, viz.,

$$C + H_2 \longrightarrow \text{hydrocarbons}$$

$$(U,Zr)C_{0.97} + H_2 \longrightarrow (U,Zr)C_{\sim 0.9} + \text{hydrocarbons.}$$

A second method of obtaining substoichiometric (U,Zr)C was to subject the fuel elements containing the free carbon to a gas mixture similar to that used in the chemical vapor deposition of ZrC coatings. In effect, the free carbon in the fuel element reacted to form ZrC and then, under suitable conditions, the reaction would continue after the free carbon was exhausted, with zirconium being added to the (U,Zr)C to produce a fuel substoichiometric in carbon. The overall reactions can be represented as follows:

$$(U,Zr)C + C_{free} \xrightarrow[H_2,\ HCL,A]{ZrCl_4} (U,Zr)C_{\sim 0.9}$$

+ some hydrocarbons.

A third method, a combination of the first two, was the most practical. The free carbon was removed by flowing hydrogen at a temperature of 2200 to 2300 K for 40 to 60 h. The elements were then impregnated with zirconium in a gas mixture of the following composition (vol%): $ZrCl_4$, 1.8%; H_2, 8.2%; CH_2, 0.02%; HCl, 0.10%; and Ar, 89.9%. The temperature of impregnation was ∿ 1900 K.

The elements were given a final heat treatment at ∿ 2800 K for 2 h. The properties of elements made by this process are described in Table VI of the main body of the report.

ACKNOWLEDGMENTS

The following people should be given credit for the development of the (U,Zr)C all-carbide fuel element: F. Criss, K. Davidson, A. Driesner, D. MacMillan, D. Schell and T. Wallace.